STABILITY OF A FLEXIBLE CYLINDER IN AXISYMMETRICALLY CONFINED FLOW

by

Woo-Gun Sim

Department of Mechanical Engineering
McGill University
Montreal, Quebec, Canada

July 1987

A Thesis submitted to the Faculty of Gradute Studies and Research
in partial fulfillment of requirements for degree of
Master of Engineering

ABSTRACT

This thesis investigates the stability of a flexible centre-body, considered as a clamped-clamped beam, in narrow annular flow. The equations of motion are derived, considering inviscid and viscous fluid-dynamic coupling for small amplitude oscillations of the beam.

For the fluid-dynamic problem, two theoretical models have been developed. In the first theoretical model, the unsteady inviscid fluid-dynamic forces acting on the flexible centre-body are derived by means of potential flow theory. In the second model, the viscous components of the fluid-dynamic forces acting on the body have been determined for evaluating the unsteady and steady viscous effects based on simplified forms of the Navier-Stokes and continuity equations.

A five-mode Galerkin discretization of the continuous system is employed in the solution of equations of motion to yield a set of ordinary differential equations, from which the eigenfrequencies are obtained.

It is noted that the viscous effects on the system are important for annular flow, as opposed for unconfined flow; moreover, the difference between the instabilities given by potential and viscous flow theories becomes larger as the viscosity of fluid is increased or the annulus decreased.

It was found that the system subjected to inviscid flow becomes unstable by first-mode buckling and is monotonically destabilized as the annular gap becomes smaller; however, the stabilizing influence of the viscous effects increases with diminishing annular gap, overcoming the destabilizing influence of the gap decrease in inviscid case.

SOMMAIRE

Cette thèse présente une étude sur la stabilité d'un cylindre central flexible, consideré comme une poutre encastrée, dans un écoulement annulaire étroit. Les équations de mouvement sont dérivées, en prenant en considération les interactions dynamiques de fluide visqueux et non-visqueux pour des oscillations de la poutre de petite amplitude.

Pour le problème de la dynamique du fluide, deux modèles théoriques ont été dévelopés. Dans le premier modèle théorique, les forces dynamiques due à un écoulement non-stationnaire et non-visqueux agissant sur le cylindre central flexible sont dérivées à l'aide de la théorie de l'écoulement potentiel. Dans le second modèle, les composantes visqueuses des forces dynamiques du fluide agissant sur le corps ont été déeterminées pour évaluer les effets stationnaires et non-stationnaires de la viscosité en utilisant des formes simplifiées des équations de Navier-Stokes et de continuité.

Une discrétisation de type Galerkin de cinq modes du système continu est employée dans la solution des équations de mouvement dans le but d'obtenir un système d'équations différentielles ordinaires, desquelles sont obtenues les fréquences propres.

Il est à noter que les effets visqueux sur le système sont importants dans le cas d'un écoulement annulaire, par opposition à l'écoulement non-confiné; de plus, la difference entre les instabilités obtenues par les théories d'écoulement potentiel et visqueux deviennent plus importantes lorsque la viscosité du fluide est augmentée ou que l'espace annulaire est diminué.

Les résultats démontrent que le système sujet à un ecoulement non-visqueux devient instable au niveau du flambage du prémier mode, et est déstabilisé de façon monotone lorsque l'espace annulaire est réduit; cependant, l'influence stabilisatrice des effets visqueux augmente avec la reduction de l'espace annulaire, surmontant l'influence déstabilisatrice de la réduction de l'espace annulaire dans le cas non-visqueux.

ACKNOWLEDGEMENTS

The author wishes to express his sincere appreciation and thanks to his research directors, professors M. P. Paidoussis and D. Mateescu, for their continuous encouragement and valuable guidance shown to overcome the inherent many difficulties during the course of this research work. The suggestions, offered with great insight and experience in the field of flow-induced vibration, play the most valuable roles in this work, and are clearly acknowledged.

The author is grateful to his research directors for awarding him a research assistantship.

The author also gratefully acknowledges the one year fellowship and award with David Steward Memorial.

Latest but not at least, the author offers his heartfelt thanks to his family having given the constant encouragement and support.

TABLE OF CONTENTS

* total number of pages.

NOMENCLATURE+

Space symbols

x^*, r^*, θ	Cylindrical coordinates
$\vec{I}_{x^*}, \vec{I}_{r^*}, \vec{I}_\theta$	Unit vectors associated with the coordinate system

Ordinary symbols

a	Radius of the centre-body
A_s	Cross-sectional area of the centre-body
D_H	Hydraulic diameter
E	Young's modulus of elasticity of the flexible centre-body
$E_\kappa(X)$	Comparison functions
e_o^*	Lateral displacement of the centre-boby axis
F	Fluid-dynamic forces
H^*	Annular clearance
I	Moment of inertia of the centre-body
I_P, I_T, I_H	Integrals of the corresponding comparison function products defined by equation (4-7d)
ℓ^*	Length of the oscillating flexible centre-body
M	Mass of fluid contained in the annular passage per unit length
m	Mass of the centre-body per unit length
Re	Reynolds number
P	Amplitude of the nondimensional counterpart of fluid-dynamic forces
p	Static pressure of fluid flow
r_d^*	Duct-wall radius
T	Tension acting on the centre-body
t^*	Time
U^*	Mean flow velocity
U_{ref}, U_{refl}	Reference velocities defined by equation (2-3b)
$z=\frac{r^*}{a}-1$	Nondimensional radial coordinate

+ These are the principal notations only; the nondimensional counterpart of some of these parameters are shown in section 2.3, equations (2-3a).

Greek letters

β_κ	Eigenvalues
μ	Viscosity of fluid
ρ_f	Density of fluid
ρ_s	Density of the flexible centre-body
σ	Mass ratio defined by equation (2-12)
τ	Shear stress acting on the wall
$\hat{\phi}$	Reduced-motion potential
Φ	Velocity potential
ω	Complex eigenfrequency
Ω	Circular frequency of the flexible centre-body

Matrix symbols

[M], [C], [K]	Mass, damping and stiffness matrices
$m_{j\kappa}, c_{j\kappa}, k_{j\kappa}$	Elements of the corresponding matrix

CHAPTER I

INTRODUCTION

1.1 REVIEW OF PREVIOUS STUDIES

The flow of fluid around structures, although sometimes generated for useful purposes (e.g., in promoting heat transfer), can cause destructive vibrations. Flow-induced vibration problems are of great technical and financial importance and safety concern, in many practical structures; e.g., heat exchangers, nuclear reactors and skyscrapers. These flow-induced vibration problems have become increasingly important in recent years because designers are using materials to their limit, causing structures to become progressively lighter and more flexible.

The structures immersed in fluid flow are subjected to forces generated by the fluid flow; as a result, the fluid-dynamic forces cause the structures to deform. When the structures deform, they change their orientations to the fluid, and the fluid-dynamic forces may change, so that there is generally fluid-structure coupling and interaction. All these structures are subjected to flow-induced vibration and to fluidelastic instabilities of different types, depending on the characteristics of the structure and the fluid field — where the term "fluidelastic instability" generally implies a self-excited divergence or oscillation, an instability in the linear sense.

For the motions of the structures and for the fluid flow, mathematical models may be generated. In some cases, structural motions are near-linear and the structure may thus be modeled as one or more linear oscillators; however, a general model for the fluid-dynamic forces acting on an arbitrary bluff structure does not exist. In many cases, the fluid models rely on extrapolation of test measurements of lift, drag, or surface pressure, which generally vary

nonlinearly with motion of the structure. Therefore, the dynamic interaction of structures and fluid is generally described by nonlinear equations. As a result, few general solutions are available.

Broadly grouped according to flow configuration, the vibration problems are classified as being associated with (i) cross-flow, (ii) internal axial flow, (iii) external axial flow and (iv) annular (to be discussed here) and leakage flow. The distinction between confined axial flow and annular flow is rather artificial. In general, "annular" is used in its hydraulically generic sense, to include not only cylindrical geometries, but also flat plates in narrow rectangular conduits. This paper is concerned with a special case: that of a flexible centre-body in an axisymmetrically narrow annular flow.

A brief review of the state of the art in axial-flow-induced vibrations, either internal or external, and in annular-flow-induced vibrations may be summarized as follows: (i) the mechanism of instabilities induced by axial flow is well understood; (ii) this is also true for the mechanism of the small, turbulence induced vibrations, but means of prediction of the excitation field are not yet adequate; (iii) the fundamental mechanism of annular-flow-induced instabilities is fairly well understood, but, generally, complexities of geometry and fluid field make prediction of the instabilities difficult.

A considerable amount of work has been done on the dynamics of a cylinder immersed in stationary confined fluid. The system was modeled as a cylindrical beam within a rigid cylindrical container [1], as a cylindrical beam within a cylindrical shell [2] and as two coaxial shells [3]. The common factor in all these studies is that motions of the fluid were described by means of potential flow. In most of these studies, in which, it is reiterated, there was no steady state annular flow, the main distinguishing feature of the dynamics of the systems is associated with the large added

mass effect, which results from the large accelerations suffered by the fluid in the narrow annular passage when the structure vibrates As a result, the natural frequencies of the coupled system in stationary confined fluid are much lower than those of the system without fluid.

The concept of the added or hydrodynamic mass has been described by Stokes [4], Lamb [5], Fritz [1] and others These investigators have generally considered the motion of a single body in fluid The fluid-dynamic motion and associated steady pressures and forces acting on the annulus inner and/or outer wall was described by means of ideal flow theory (normally potential flow theory) Nowadays, the added mass and damping of a structural component with a simple geometry in a viscous confined flow, in which mean flow effect is not considered, can be calculated rather easily [6] Recent investigation of the influence of viscosity [7] indicates that its effect on the natural frequencies of the system is small; however, the modal damping ratio is noticeably increased, especially, for low frequency oscillations

To the author's knowledge, the dynamics of flexible cylinders immersed in steady axial flow was first studied by Paidoussis [8-10], both theoretically and experimentally, based on elementary beam theory for the flexural motions of the cylinder, slender body theory for the coupled inviscid fluid-dynamic forces, and fairly simple linearized relationships for the corresponding viscous forces, earlier proposed by Taylor [11].

This system was studied further, and more completely, by Paidoussis [12] The theory was extended to the case where the flow is confined by adjacent structures, so that the virtual mass of fluid becomes larger, and the instabilities occur at lower flow velocities, but, the fundamental nature of the stability behaviour is not altered. In this respect, the similarity in dynamical behaviour between this system and that of a pipe conveying fluid [13] should be remarked.

An interesting aspect of the dynamics and stability of cylinders in axial flow is that cylinders generally lose stability by divergence (in fact, the stability of a cantilevered cylinder is fundamentally dependent on the shape of the free end). The post-divergence behaviour involves coupled-mode flutter for cylinders supported at both ends, or single-mode flutter for cantilevered ones. The experiments with a flexible cylinder in confined flow [14] have shown that the theoretical model is in qualitative agreement with the essential features of the observed dynamical behaviour, and the cylinders are greatly destabilized by confinement. It is of interest that friction forces, whether the flow is confined or unconfined, do not greatly alter the fundamental behaviour of the system as determined by the inviscid forces.

On the effect of slenderness of the cylinder in confined axial flow and compressibility of the fluid, a mathematical formulation and numerical solution for the problem were presented by Paidoussis and Ostoja-Starzewski [15], utilizing the generalized-force Fourier Transform techniques developed earlier by Dowell and Widnall [16]. Interestingly, the effect of compressibility on the stability of the system is surprisingly small in the subsonic region and once again the fundamentals of the stability of the system are almost the same as those described in the foregoing.

The dynamics and stability of clustered cylinders within a confined flow was studied by Chen [17] and by Paidoussis and Suss [18]. It was found that the dynamics of a system of N cylinders is subject to 2N coupled modes for each flexural deflection mode, and is considerably more complex than that of a solitary one.

The analytical models developed in most of the above studies for a confined flow are not particularly suitable for very narrow annuli. Although the inviscid part of the model is clearly applicable, irrespective of the degree of confinement, the viscous effects in very narrow passages cannot reliably be adapted from the formulations for less severely confined

geometries. Thus, the applicablity of these models to very narrow passages, especially with regard to the viscous effect, may be considered to be questionable.

In recent years, the dynamics of this system, by means of formulations specially applicable to narrow annuli, which is the case frequently associated with real problems, has received considerable attention [20-23].

The initial motivation in the study of dynamics and instability of a cylindrical centre-body in a narrow annular flow springs from a desire to understand the mechanism underlying flow-induced vibrations in a number of engineering applications; e g , control rods in guide tubes of PWR-type nuclear reactors, fuel-cluster stringers in coolant channels in AGR-type reactors, and feedwater spargers in BWR-type reactors Flexible bodies, such as these, in narrowly confined annular flow have been shown to be particularly prone to a host of vibration-induced problems [19].

An attempt to generate a comprehensive analytical model for these problems was perhaps first made by Hobson [20]. In that study, neglecting the radial variation of fluid velocity and based on the assumption of a very narrow annular clearance, the dynamics of a rigid cylindrical body, coaxially positioned in an annular passage of generally nonuniform cross-sectional area and hinged at one point, was considered. Hobson in effect attempts to solve a problem similar to that in this Thesis, and his work is therefore of direct interest; however, the approach and method of solution adopted by Hobson are completely different -

A more rigorous inviscid analytical model, but more limited in its applicability to real engineering problems at the same time (because it did not take viscous effects into account, nor discontinuities in the shape of the annulus), was developed by Mateescu and Paidoussis [21]. In this study, radial variations in the unsteady annular flow were taken into account, despite the assumption of small annular clearance with respect to the centre-body radius. The system, consisted

of an axisymmetric rigid body pinned at one point and coaxially mounted in a cylindrical duct; free motion was constrained by a rotational spring and a rotational dashpot at the hinge point. In order to determine the generalized unsteady fluid-dynamic forces, potential flow theory, which is applicable for an incompressible irrotational flow, was used in the analytical model. In a subsequent paper [22], the effect of fluid viscosity on the flow-induced vibration of the rigid centre-body was taken into account, using a simplified form of the Navier-Stokes equation for the three dimensional incompressible fluid motion.

In the present analysis, the analytical model developed in the two papers [21,22] for the dynamics of a rigid centre-body in narrow annular passage, which may be considered as a one-degree of freedom system, is extended to deal with the case of a continuously flexible system; i e., for the study of the dynamics of a flexible centre-body in a narrow annular passage.

1.2 OUTLINE OF THE THESIS

In order to investigate the flow-induced instabilities of the system, a theoretical analysis will be developed for both potential and viscous flows past the flexible centre-body oscillating in a narrow annular passage. The main feature of the dynamical behaviour of such a system is that the flexible centre-body may be subject to divergence (buckling) or to oscillatory instability (flutter) in the first and/or higher flexural modes at sufficiently high flow velocities Normally, the determination of the lowest critical flow velocity is the main aim, in the dynamical analysis of such a system.

The problem is formulated as being made up of a cylindrical beam with clamped ends, subjected to fluid forces generated in the annular flow passage, initially considered to be inviscid. In this Thesis, a rigorous method for inviscid

flow and an approximate method for viscous flow have been developed for obtaining the corresponding fluid-dynamic forces acting on the flexible centre-body.

In chapter II, the equation of the small lateral motion of the flexible centre-body, modeled as an Euler-Bernoulli beam, is derived, subjected to external forces, such as the fluid-dynamic distributed forces. These fluid-dynamic forces, coupled with the motion of the flexible centre-body, are separated into two parts; i.e., inviscid and viscous fluid-dynamic forces, which are obtained in chapters III and V, respectively. The problem is redefined in terms of dimensionless parameters. An approximate solution subject to the boundary conditions is obtained, using Galerkin's method.

In chapter III, neglecting the viscous effects, the inviscid fluid-dynamic forces acting on the flexible centre-body are developed by means of potential flow theory. The Laplace equation and the Bernoulli-Lagrange equation are expressed in terms of a potential Φ, adapted for the problem at hand from the earlier work on a rigid body pinned at one point, as mentioned before.

In chapter IV, the fluid-dynamic coupling terms (the fluid-dynamic damping and stiffness and virtual mass matrices) are determined from the results obtained in chapters II and III, based on Galerkin's method. Then, typical results, illustrating the general dynamical behaviour of system due to the inviscid fluid-dynamic force, are obtained and discussed.

In chapter V, using the linearized Navier-Stokes equations governing the viscous fluid motion and considering the results obtained in chapter III (inviscid flow), the normal and axial frictional forces are obtained.

In chapter VI, the steady and unsteady effects, arising from the viscous forces, are considered by means of Galerkin's method. Here, the normal frictional force, which is due to the normal shear stress and viscous perturbation pressure, and comprises the unsteady viscous effects and the steady viscous effects, are derived from the axial viscous force according to

the axial constraints on the flexible centre-body, which is clamped at both ends. The general dynamical behaviour of the system, as influenced by the unsteady and steady viscous effects, is illustrated and is compared with that in which only inviscid effects have been taken into account.

Finally, chapter VII is devoted to discussions on the obtained results and conclusions, as well as suggestions for future work.

CHAPTER II

PROBLEM FORMULATION

2.1 GENERAL CONSIDERATIONS

The system considered in the present analysis consists of a flexible cylindrical centre-body coaxially mounted in a narrow cylindrical duct conveying fluid. The flexible part of the centre-body has a length ℓ^* and is continued, upstream and downstream, by two semi-infinite rigid cylinders of the same radius, a; both ends of the flexible part of the centre-body are supposed to be clamped, as shown in Fig. 1.

The flexible centre-body is free to oscillate in flexure inside the duct. Although the duct cross-section is considered constant in the present analysis, it is convenient to assume that the duct has a specified axial variation in its cross-sectional area for further work. This system is coupled, by the fluid-dynamic distributed force acting on the flexible centre-body, due to the annular flow, which is obviously unsteady.

In the present analysis, it is assumed that the length of the oscillating flexible centre-body is reasonably large and the overall annular clearance is reasonably small, both with respect to the centre-body radius a. It is also supposed that the rigid cylinders and the duct have no oscillatory motion.

Far upstream, the annular flow is assumed to be steady and is characterized by the mean flow velocity U_o^*, the static pressure p_o and the density ρ_f, which is considered constant.

Several combinations of fluid and centre-body material will be considered in the examples to be presented, such as air, water or oil for the fluid and rubber or steel for the centre-body material.

The time-dependent lateral displacement $e_o^*(x^*,t^*)$ of the centre-body axis is assumed to be small with respect to its radius, which permits to use linear theory for the flexural

oscillations of the centre-body; hence, i) no separation occurs in the annular flow, and ii) the fluid-dynamic forces acting on each element of the flexible centre-body may be determined using a convenient linearization of the aerodynamic boundary conditions on the oscillating centre-body. This also means that the assumption of small amplitude oscillations can be utilized in simplifying the inviscid and the viscous analysis of the unsteady fluid-dynamic problem, in chapter III and chapter V.

The following notation will be used in formulating the analytical model (see also Fig. 1):

ℓ^*	length of oscillating flexible centre-body
a	radius of the centre-body
x^*, r^*, θ^*	cylindrical co-ordinate system
H_o^*	annular clearance at upstream end
$H^*(x^*)$	annular clearance at location x^*
$e_o^*(x^*, t^*)$	lateral displacement of centre-body axis
$r_d^*(x^*)=a+H^*$	duct-wall radius at location x^*
U_o^*	mean flow velocity at upstream end
$U^*(x^*)$	mean flow velocity at location x^*.

The dimensionless quantities corresponding to the above, which are more widely used, will be defined in section 2.3 without superscript; e.g. $x=x^*/a$ or $X=x^*/\ell^*$.

2.2 EQUATION OF MOTION OF THE FLEXIBLE CENTRE-BODY

The oscillating flexible centre-body is considered as an Euler-Bernoulli beam characterized by flexural rigidity EI, length ℓ^*, cross-sectional area A_s, and density ρ_s.

The derivation of the equation of small lateral motions, is obtained by considering the equilibrium of forces acting on a differential segment of the flexible centre-body, taken as an Euler-Bernoulli beam, subjected to distributed external forces; it is shown in Appendix A, based on Hamilton's principle. The distributed force is due to the fluid motion of

this system which, as discussed before, is coupled to the flexible centre-body motion. Therefore, the equation of motion of the flexible centre-body is expressed, as follows:

$$EI \frac{\partial^4 e_o^*}{\partial x^{*4}} + \rho_s A_s \frac{\partial^2 e_o^*}{\partial t^2} = F(x^*, t^*), \qquad (2\text{-}1)$$

where $F(x^*, t^*)$ is the fluid-dynamic distributed force acting on the centre-body per unit length. The first term and the second term of the left-hand side of equation (2-1) may be interpreted physically as the flexural restoring force and the beam inertia force, respectively.

This unsteady fluid-dynamic force, $F(x^*, t^*)$, represents the resultant of the pressure forces and of the viscous shear stresses acting on the centre-body surface. The analysis developed in chapter III and chapter V has as its main aim the determination of this unsteady fluid-dynamic force, firstly assuming the case of an unsteady potential(inviscid) flow in chapter III and then, in chapter V, considering also the main effects of fluid viscosity.

In this analysis, the flexible cylindrical centre-body is considered to be a clamped-clamped beam, for which the boundary conditions are

$$e_o^*(0, t^*) = 0, \qquad e_o^*(\ell^*, t^*) = 0,$$
$$\frac{\partial e_o^*(0, t^*)}{\partial x^*} = 0, \qquad \frac{\partial e_o^*(\ell^*, t^*)}{\partial x^*} = 0. \qquad (2\text{-}2)$$

These boundary conditions determine uniquely the form of the solution, leaving the amplitude arbitrary, and yield a characteristic equation from which the eigenfrequencies of the system may be determined.

It is noted that the differential equation of motion of the flexible centre-body together with these boundary conditions constitutes a boundary-value problem. Moreover, these boundary conditions are used to derive a typical eigenvalue problem, as shown in Appendix A.

The transition between the boundary value problem and the eigenvalue problem is effected by means of the separation of variables method. The expansion theorem plays a major role in the field of vibrations and will be used here also to obtain a solution of the system by normal mode analysis. This underscores the importance of solving the eigenvalue problem and obtaining a set of eigenfrequencies and the corresponding eigenmodes.

The solution of the eigenvalue problem is not as straightforward as for discrete systems. By using Galerkin's method, however, the system is discretized, leading eventually to the determination of the mass, damping and stiffness matrices of the system. The discretized problem is then easy to solve.

2.3 GENERAL METHOD OF APPROACH

In order to generalize the equation of motion of the system, it is convenient to define the following dimensionless parameters:

$$X = \frac{x^*}{\ell^*}, \quad \ell = \frac{\ell^*}{a}, \quad x = \frac{x^*}{a} = \frac{\ell^*}{a} X = \ell X,$$

$$r = \frac{r^*}{a}, \quad r_d = \frac{r_d^*}{a}, \quad h = \frac{H^*(x^*)}{a}, \quad h_o = \frac{H_o^*}{a},$$

$$e_o = \frac{e_o^*}{a}, \quad e_r = \frac{e_r^*}{a}, \quad t = \frac{U_{ref}}{\ell^*} t^*, \quad \omega = \frac{\Omega \ell^*}{U_{ref}}, \tag{2-3a}$$

$$U_o = \frac{U_o^*}{U_{ref}}, \quad U_{o1} = \frac{U_o^*}{U_{ref1}}, \quad U(X) = \frac{U^*(x^*)}{U_{ref}}, \quad \bar{U}(X) = \frac{U^*(x^*)}{U_o^*},$$

where

$$U_{ref} = \left(\frac{EI}{\rho_s A_s \ell^{*2}}\right)^{1/2}, \quad U_{ref1} = \left(\frac{EI}{\rho_f \pi a^2 \ell^{*2}}\right)^{1/2}, \tag{2-3b}$$

and where the fluid velocity $U^*(x^*)$ is the mean fluid velocity at location x^* (or X) and the circular frequency of the flexible centre-body is expressed by Ω. For hollow cylinders, $\rho_s A_s$ appears to be more general. Here it should be explained that the dual nondimensional X and x, inter-related by $x=\ell X$, are introduced for convenience; X is most useful in the overall analysis, whereas x is most useful in analysis of the fluid flow. Some of these variables have been introduced in refs. [13,21].

Substituting equations (2-3a) into equation (2-1), the equation of motion is expressed in dimensionless form, as follows:

$$\frac{\partial^4 e_o}{\partial X^4} + \frac{\partial^2 e_o}{\partial t^2} = \frac{\ell^{*4}}{aEI} F(X,t), \qquad (2\text{-}4)$$

where

$$e_o^* = a e_o .$$

In order to solve this equation with the boundary conditions, equations (2-2), various methods of approach have been used. In some cases it might be possible to obtain a solution by means of an integral transform method, such as the Laplace or Fourier transform method. However, in the method adopted in the present analysis, it is assumed that the solution has the form of an infinite series. This approach is possible if the separation of variables method can be used to obtain an eigenvalue problem and, furthermore, if the eigenvalue problem is easily soluble.

The series referred to above is, more specifically, a normal mode expansion, which reduces the complex partial differential equation describing the motion of the continuous structure to a set of much simpler, ordinary differential equations. Thus, solutions to equation (2-4) are sought in terms of the eigenfunctions of the associated equation,

$$EI \frac{\partial^4 e_o^*}{\partial x^{*4}} + \rho_s A_s \frac{\partial^2 e_o^*}{\partial t^{*2}} = 0, \qquad (2\text{-}5)$$

i.e., the equation of free vibration of the beam.

Hence, it is assumed that an approximate solution of equation (2-1), which also satisfies the boundary conditions of equation (2-2), has the form of an infinite series,

$$e_o^* = aE(x^*)e^{i\Omega t^*} = aE(X)e^{i\omega t} = ae^{i\omega t}\sum_{\kappa}' a_\kappa E_\kappa(X), \qquad (2\text{-}6)$$

where the comparison functions $E_\kappa(X)$ are taken to be the eigenfunctions of a clamped-clamped beam and it is recalled that $e_o = E(x)e^{i\omega t}$ as a solution of the equation (2-4). From Appendix A, the normal-mode expression for E(X) is given by

$$E(X) = \sum_{\kappa} a_\kappa E_\kappa(X) = \sum_{\kappa} a_\kappa [E_{T\kappa}(X) + E_{H\kappa}(X)], \qquad (2\text{-}7)$$

where

$$E_{T\kappa}(X) = -\cos(\beta_\kappa X) + \sigma_\kappa \sin(\beta_\kappa X),$$

$$E_{H\kappa}(X) = \cosh(\beta_\kappa X) - \sigma_\kappa \sinh(\beta_\kappa X),$$

are the trigonometric and hyperbolic components of $E_\kappa(X)$,

$$\sigma_\kappa = \frac{\cosh(\beta_\kappa) - \cos(\beta_\kappa)}{\sinh(\beta_\kappa) - \sin(\beta_\kappa)},$$

and

$$\cosh(\beta_\kappa)\cos(\beta_\kappa) = 1, \qquad (2\text{-}8)$$

is the characteristic equation for a clamped-clamped beam. Solving equation (2-8) numerically, e.g., by the secant method, it is possible to obtain the infinite set of eigenvalues β_κ, the first five being given below:

$$\begin{aligned} \beta_1 &= 4.7300407, \\ \beta_2 &= 7.8532046, \\ \beta_3 &= 10.9956078, \\ \beta_4 &= 14.1371655, \\ \beta_5 &= 17.2787597. \end{aligned} \qquad (2\text{-}9)$$

Considering equation (2-7), the fluid-dynamic force per unit length F(X,t) can be conveniently expressed as

$$F(X,t) = -\rho_f U_{ref}^2 a\pi P(X) e^{i\omega t}, \qquad (2\text{-}10a)$$

where the amplitude of its nondimensional counterpart may be

expressed as

$$P(X) = \sum_{\kappa} a_{\kappa} [- \omega^2 P_{2\kappa}(X) + i\omega P_{1\kappa}(X) + P_{0\kappa}(X)]; \quad (2\text{-}10b)$$

the distributed force $F(X,t)$ and hence $P(X)$ and its components are obtained in chapter III (for inviscid fluid flow) and VI (for viscous fluid flow).

Because $e_o(X,t)$ is only an approximate solution, it will not satisfy equation (2-4) exactly. Nevertheless, it is assumed that the difference between the approximate and the exact solution is small, and that difference is denoted by ϵ, such that subsequent substitution of equation (2-6) and equation (2-10) into equation (2-4) yields

$$\epsilon = \frac{d^4 E(X)}{dX^4} - \omega^2 E(X) + \sigma P(X), \quad (2\text{-}11)$$

where

$$\sigma = \frac{\rho_f}{\rho_s} \frac{\pi \ell^{*2}}{A_s}. \quad (2\text{-}12)$$

According to Galerkin's method, it is required that the weighted error integrated over the domain be zero. The weighted functions are the comparison functions $E_\kappa(X)$, such that

$$\int_0^1 \epsilon \, E_j(X) dX = 0, \qquad j = 1, 2, 3, \ldots, n, \quad (2\text{-}13)$$

where j is a dummy index.

Since $E_\kappa(X)$ are the eigenfunctions of a clamped-clamped beam, they satisfy the equation,

$$\frac{d^4 E_\kappa(X)}{dX^4} = \frac{\beta_\kappa^4}{\ell^{*4}} E_\kappa(X). \quad (2\text{-}14)$$

Thus, equation (2-11) through equation (2-13) leads to

$$\sum_{\kappa} a_{\kappa} \int_0^1 \{ - \omega^2 [E_\kappa(X) + \sigma P_{2\kappa}(X)] + i\omega\sigma P_{1\kappa}(X) + [\beta_\kappa^4 E_\kappa(X) + \sigma P_{0\kappa}(X)] \} E_j(X) \, dX = 0. \quad (2\text{-}15)$$

Accordingly, it is possible to express the equation of motion in the form

$$-\omega^2[M]\{A\}e^{i\omega t} + i\omega[C]\{A\}e^{i\omega t} + [K]\{A\}e^{i\omega t} = 0, \qquad (2\text{-}16)$$

where the elements of [M], [C] and [K] are given by

$$m_{j\kappa} = \int_0^1 [E_\kappa(X) + \sigma P_{2\kappa}(X)]\, E_j(X)\, dX, \qquad (2\text{-}17a)$$

$$c_{j\kappa} = \int_0^1 \sigma P_{1\kappa}(X)\, E_j(X)\, dX, \qquad (2\text{-}17b)$$

$$k_{j\kappa} = \int_0^1 [\beta_\kappa^4 E_\kappa(X) + \sigma P_{0\kappa}(X)]\, E_j(X)\, dX, \qquad (2\text{-}17c)$$

and {A} is the vector of the a_κ of equation (2-6). Once equation (2-16) has been obtained by Galerkin's method, all the matrix techiques of a discrete system become available to the solution of the continuous system.

CHAPTER III

THE UNSTEADY POTENTIAL FLOW IN THE ANNULAR PASSAGE AROUND AN OSCILLATING CYLINDRICAL CENTRE-BODY

3.1 BASIC EQUATIONS OF UNSTEADY FLOW

In general, the principle of conservation of mass and momentum is applied to the analysis of the fluid flow. In this chapter, the flow is presumed to be irrotational and incompressible, in addition to being inviscid, so that Laplace equation is derived from the continuity equation Without the complication of viscosity, the momentum equation is reduced to Bernoulli-Langrange equation. Considering the flexible centre-body to be executing small motions, these two equations are subject to boundary conditions, which imply that the normal velocities of the bodies are equal to those of the fluid at the boundary surface between the fluid and the body.

Ideally, the hydrodynamic force should be calculated through the use of the three-dimensional Navier-Stoke's equation and the continuity equation. However, the effects of fluid viscosity and compressibility on the hydrodynamic force may be of secondary importance in some cases and may be neglected in a first attempt to study the behaviour of the system.

As discussed in the Introduction (chapter I), the fluid-dynamic force acting on an oscillating rigid body in a narrow annular passage has been developed by means of potential flow theory [21], thus, the stability of flow-induced vibration of the flexibly mounted centre-body has been studied with the aid of this inviscid fluid-dynamic force. Recently, the viscous effects for the flow in the narrow passage were taken into account [22], as will be discussed in chapter V.

The equations of the unsteady potential flow will be discussed here, and then adapted to the problem at hand, namely to the case of a flexible cylindrical centre-body.

At the upstream end of the system shown in Fig. 1, the fluid flow is assumed to be uniform and steady, with velocity U_o^*, as mentioned in chapter II. The unsteady potential flow is of course irrotational, and may be expressed in terms of the potential $\Phi(x^*, r^*, \theta, t^*)$. Assuming an incompressible and irrotational flow, the equation of continuity in this case reduces to the Laplace equation in terms of the potential $\Phi(x^*, r^*, \theta, t^*)$, as follows

$$\nabla^{*2}\Phi = \frac{\partial^2\Phi}{\partial x^{*2}} + \frac{\partial^2\Phi}{\partial r^{*2}} + \frac{1}{r^*}\frac{\partial\Phi}{\partial r^*} + \frac{1}{r^{*2}}\frac{\partial^2\Phi}{\partial\theta^2} = 0, \qquad (3\text{-}1)$$

subject to boundary conditions

$$\left.\frac{\partial\Phi}{\partial r^*}\right|_{r^*=r_d^*} = \left[\frac{\partial\Phi}{\partial x^*}\right]_{r^*=r_d^*} \frac{dH^*}{dx^*}, \qquad (3\text{-}2a)$$

$$\left.\frac{\partial\Phi}{\partial r^*}\right|_{r^*=a} = \frac{\partial e_r^*}{\partial t^*} + \left[\frac{\partial\Phi}{\partial x^*}\right]_{r^*=a} \frac{\partial e_r^*}{\partial x^*} + \left[\frac{1}{r^*}\frac{\partial\Phi}{\partial\theta}\right]_{r^*=a} \frac{1}{r^*}\frac{\partial e_r^*}{\partial\theta}, \qquad (3\text{-}2b)$$

$$\left.\frac{\partial\Phi}{\partial x^*}\right|_{x^*\to-\infty} = U_o^*, \qquad (3\text{-}2c)$$

where $e_r^*(x^*, \theta, t^*)$ represents the radial displacement of the oscillating center-body surface, i.e.

$$e_r^*(x^*, \theta, t^*) = e_o^*(x^*, t^*)\cos\theta = aE(x^*)e^{i\Omega t^*}\cos\theta. \qquad (3\text{-}3)$$

The function $E(x^*)$ can be expanded in terms of the beam eigenfunctions, depending on the type of end conditions of the beam, as discussed in chapter II. Based on the assumption of small amplitude oscillations, the last term of the right-hand-side of equation (3-2b) can be neglected.

The unsteady perturbation potential is determined by integrating the partial differential equation of the potential subject to the boundary conditions on the oscillating centre-body and on the fixed duct walls, in cylindrical coordinates;

in this respect, the method developed in ref. [21] is here extended to the case of oscillating flexible centre-body.

In order to obtain the inviscid fluid-dynamic force acting on the flexible centre-body, the momentum equation may be used, i.e.,

$$\frac{D^*V}{D^*t^*} = -\frac{1}{\rho_f}\nabla^* p + f, \tag{3-4}$$

where the last term of the right-hand side is often called the body force and would here be caused by gravity. In the present analysis, it may be neglected.

The vector equation (3-4) can be put into several different forms by making use of some well-known properties of vectors. First it is convenient to make use of the conventional "del" operator to write equation (3-4) as

$$\frac{D^*V}{D^*t^*} = \frac{\partial V}{\partial t^*} + (V\cdot\nabla^*)V = -\frac{1}{\rho_f}\nabla^* p. \tag{3-5}$$

An alternative expression of equation (3-5), which is of great usefulness, follows from the vector identity

$$\frac{1}{2}\nabla^*(V\cdot V) = \nabla^*(\tfrac{1}{2}V^2) - (V\cdot\nabla^*)V + V\wedge(\nabla^*\wedge V), \tag{3-6}$$

where $\wedge$ represents the cross-product of vectors. Substituting this equation into equation (3-5) leads to

$$\frac{\partial V}{\partial t^*} + \nabla^*(\tfrac{1}{2}V^2) + \frac{1}{\rho_f}\nabla^* p = V\wedge(\nabla^*\wedge V). \tag{3-7}$$

For irrotational motions ($\nabla\wedge V=0$), the fluid velocity V is derived from the potential $\Phi(x^*, r^*, \theta, t^*)$,

$$V = \nabla^*\Phi. \tag{3-8}$$

Therefore, equation (3-7) may be expressed in terms of the potential $\Phi(x^*, r^*, \theta, t^*)$, as follows:

$$\nabla^*\left(\frac{\partial\Phi}{\partial t^*} + \frac{1}{2}|\nabla^*\Phi|^2 + \frac{1}{\rho_f}p\right) = 0. \tag{3-9}$$

This equation can also be written in the following form, usually known as Bernoulli-Lagrange equation,

$$\frac{\partial \Phi}{\partial t^*} + \frac{1}{2} |\nabla^* \Phi|^2 + \frac{1}{\rho_f} p = \text{constant}. \qquad (3\text{-}10)$$

To get the pressure force acting on the centre-body, it is convenient to reformulate equation (3-10) into the following form:

$$p - p_o = \frac{1}{2} \rho_f U_o^{*2} - \frac{1}{2} \rho_f |\nabla^* \Phi|^2 - \rho_f \frac{\partial \Phi}{\partial t^*}, \qquad (3\text{-}11)$$

where p_o is the static pressure at the upstream end, and $\nabla^* \Phi = U_o^*$. Thus, the inviscid or potential fluid-dynamic force (denoted with the subscript "p") acting on the centre-body per unit length is given by integrating equation (3-11), i.e.,

$$F_p(X,t) = - \int_0^{2\pi} a \left[p - p_o \right]_{r^*=a} \cos\theta \, d\theta. \qquad (3\text{-}12)$$

3.2 METHOD OF SOLUTION FOR THE UNSTEADY ANNULAR FLOW

3.2.1 The Reduced-Motion Potentials

Introducing the dimensionless quantities defined in chapter II and separating the fluid flow into a steady axisymmetric component (denoted with the subscript "s") and an unsteady one (without subscript), the potential $\Phi(x^*, r^*, \theta, t^*)$ becomes

$$\Phi(x^*, r^*, \theta, t^*) = U_o^* a [\phi_s(x,r) + \phi(x,r,\theta,t)]. \qquad (3\text{-}13)$$

Substituting this equation into equation (3-1) and then separating into two parts, corresponding to the axisymmetric component and unsteady one, respectively, the potential flow equation, in nondimensional form, becomes

$$\frac{1}{\ell^2} \frac{\partial^2 \phi_s}{\partial X^2} + \frac{\partial^2 \phi_s}{\partial r^2} + \frac{1}{r} \frac{\partial \phi_s}{\partial r} = 0, \qquad (3\text{-}14a)$$

$$\frac{1}{\ell^2}\frac{\partial^2\phi}{\partial X^2} + \frac{\partial^2\phi}{\partial r^2} + \frac{1}{r}\frac{\partial\phi}{\partial r} + \frac{1}{r^2}\frac{\partial^2\phi}{\partial\theta^2} = 0, \qquad (3\text{-}14b)$$

subject to the boundary conditions

$$\left.\frac{\partial\phi_s}{\partial r}\right|_{r=1} = 0, \qquad (3\text{-}15a)$$

$$\left.\frac{\partial\phi_s}{\partial r}\right|_{r=r_d} = \left[\frac{\partial\phi_s}{\partial x} + \frac{\partial\phi}{\partial x}\right]_{r=r_d}\frac{\partial h}{\partial x}, \qquad (3\text{-}15b)$$

$$\left.\frac{\partial\phi_s}{\partial x}\right|_{x=-\infty} = 1, \qquad (3\text{-}15c)$$

and

$$\left.\frac{\partial\phi}{\partial r}\right|_{r=1} = \left[\frac{1}{\ell U_o}\frac{\partial e_r}{\partial t} + \left[\frac{\partial\phi_s}{\partial x} + \frac{\partial\phi}{\partial x}\right]\frac{\partial e_r}{\partial x}\right]_{r=1} e^{i\omega t}\cos\theta, \qquad (3\text{-}16a)$$

$$\left.\frac{\partial\phi}{\partial r}\right|_{r=r_d} = 0, \qquad \left.\frac{\partial\phi}{\partial x}\right|_{x=-\infty} = 0, \qquad (3\text{-}16b)$$

where the last term of right-hand side of equation (3-2b) has been neglected and it is recalled that $\ell=\ell^*/a$.

Taking into consideration these boundary conditions, it is convenient to define the reduced-motion potentials $\hat{\phi}_{T\kappa}(X,r)$, and $\hat{\phi}_{H\kappa}(X,r)$, as follows:

$$\phi(X,r,\theta,t) = \sum_{\kappa}\frac{a_\kappa}{\ell U_o}\left[\hat{\phi}_{T\kappa}(X,r) + \hat{\phi}_{H\kappa}(X,r)\right] e^{i\omega t}\cos\theta, \qquad (3\text{-}17)$$

where the subscripts "T" and "H" represent the trigonometric and hyperbolic components of $\phi(X,r,\theta,t)$, respectively. In this manner, equations (3-14b) may be reformulated into the following reduced-potential equations:

$$\frac{1}{\ell^2}\frac{\partial^2\hat{\phi}_{T\kappa}}{\partial X^2} + \frac{\partial^2\hat{\phi}_{T\kappa}}{\partial r^2} + \frac{1}{r}\frac{\partial\hat{\phi}_{T\kappa}}{\partial r} - \frac{1}{r^2}\hat{\phi}_{T\kappa} = 0, \qquad (3\text{-}18a)$$

$$\frac{1}{\ell^2}\frac{\partial^2\hat{\phi}_{H\kappa}}{\partial X^2} + \frac{\partial^2\hat{\phi}_{H\kappa}}{\partial r^2} + \frac{1}{r}\frac{\partial\hat{\phi}_{H\kappa}}{\partial r} - \frac{1}{r^2}\hat{\phi}_{H\kappa} = 0, \qquad (3\text{-}18b)$$

subject to the boundary conditions

$$\left.\frac{\partial \hat{\phi}_{T\kappa}}{\partial r}\right|_{r=1} = i\omega E_{T\kappa}(X) + U(X)E'_{T\kappa}(X), \qquad (3\text{-}19a)$$

$$\left.\frac{\partial \hat{\phi}_{H\kappa}}{\partial r}\right|_{r=1} = i\omega E_{H\kappa}(X) + U(X)E'_{H\kappa}(X), \qquad (3\text{-}19b)$$

$$\left.\frac{\partial \hat{\phi}_{T\kappa}}{\partial r}\right|_{r=r_d} = 0, \qquad \left.\frac{\partial \hat{\phi}_{Hk}}{\partial r}\right|_{r=r_d} = 0, \qquad (3\text{-}19c)$$

where $E_{H\kappa}(X)$ and $E_{T\kappa}(X)$ are the hyperbolic and trigonometric parts of the beam eigenfunctions introduced in chaper II.

3.2.2 Linearization Procedure

Based on the small disturbance assumption, equations (3-18 a,b) are linearized in order to obtain an analytical solution of the problem.

For the case where the duct has specified axial variations in its cross-section, it is noted that the usual procedure of linearization, with respect to the undisturbed velocity U_o^*, is not sufficiently accurate, since the mean axial flow velocity $U^*(x^*)$ at location x^* could be substantially different from U_o^*.

Therefore, a procedure of local linearization will be used in order to obtain the local mean flow velocity, $U^*(x^*)$. The local dimensionless mean flow velocity, $\bar{U}(X)=U^*(x^*)/U_o^*$, may be obtained by applying the equation of continuity in integral form; thus, the local dimensionless mean flow velocity can be expressed in terms of the rate of annular clearance

$$\bar{U}(X) = \frac{\pi[(a+H_o^*)^2 - a^2]}{\pi[(a+H^*) - a^2]} \approx \frac{h_o}{h}, \qquad (3\text{-}20)$$

where $h_o = h(0) = h^*(0)/a$ is the dimensionless width of the annular passage at the upstream end.

Taking advantage of the assumption of a narrow annular flow, one can define the following nondimensional variable:

$$z = \frac{r^* - a}{a} = r - 1, \tag{3-20}$$

where the approximation, $r \simeq 1$, could be used. Consequently, the potential flow equations (3-18 a,b) may be expressed as the following linearized equations in terms of the reduced-motion potentials:

$$\frac{1}{\ell^2}\frac{\partial^2 \hat{\phi}_{T\kappa}}{\partial X^2} + \frac{\partial^2 \hat{\phi}_{T\kappa}}{\partial z^2} + \frac{\partial \hat{\phi}_{T\kappa}}{\partial z} - \hat{\phi}_{T\kappa} = 0, \tag{3-21a}$$

$$\frac{1}{\ell^2}\frac{\partial^2 \hat{\phi}_{H\kappa}}{\partial X^2} + \frac{\partial^2 \hat{\phi}_{H\kappa}}{\partial z^2} + \frac{\partial \hat{\phi}_{H\kappa}}{\partial z} - \hat{\phi}_{H\kappa} = 0, \tag{3-21b}$$

subject to the boundary conditions given by equations (3-19 a,b,c).

3.3 SOLUTION FOR THE REDUCED-MOTION POTENTIALS

According to slender body theory [24], the first term of equations (3-21 a,b) may be neglected. However, the slender body approximation is not sufficiently accurate for higher frequency oscillations; this is because the virtual mass coefficient and the coefficient of fluid dynamic damping, which depend on the reduced-motion potentials $\hat{\phi}_{T\kappa}$, $\hat{\phi}_{H\kappa}$, cannot be accurately reproduced if the slender body approximation were adopted. Hence, the slender body approximation will not be used in this analysis.

Considering the complete form of partial differential equations (3-21 a,b), expansions of the reduced-potentials could be assumed in the form

$$\hat{\phi}_{T\kappa} = f_{T\kappa}(X)\, F_{T\kappa}(z), \tag{3-22a}$$

$$\hat{\phi}_{H\kappa} = f_{H\kappa}(X)\, F_{H\kappa}(z). \tag{3-22b}$$

Thus, the linearized equations (3-21 a,b) become

$$-\frac{1}{\ell^2}\frac{f_{T\kappa}''(X)}{f_{T\kappa}(X)} = \frac{1}{F_{T\kappa}(z)}\left[F_{T\kappa}''(z)+F_{T\kappa}'(z)-F_{T\kappa}(z)\right] = \frac{1}{\ell^2}\beta_\kappa^2, \tag{3-23a}$$

$$-\frac{1}{\ell^2}\frac{f_{H\kappa}''(X)}{f_{H\kappa}(X)} = \frac{1}{F_{H\kappa}(z)}\left[F_{H\kappa}''(z)+F_{H\kappa}'(z)-F_{H\kappa}(z)\right] = -\frac{1}{\ell^2}\beta_\kappa^2, \tag{3-23b}$$

which reduce to two sets of separate ordinary differential equations

$$f_{T\kappa}''(X) + \beta_\kappa^2 f_{T\kappa}(X) = 0, \tag{3-24a}$$

$$F_{T\kappa}''(z) + F_{T\kappa}'(z) - \left(1 + \frac{1}{\ell^2}\beta_\kappa^2\right) F_{T\kappa}(z) = 0,$$

$$f_{H\kappa}''(X) - \beta_\kappa^2 f_{H\kappa}(X) = 0, \tag{3-24b}$$

$$F_{H\kappa}''(z) + F_{H\kappa}'(z) - \left(1 - \frac{1}{\ell^2}\beta_\kappa^2\right) F_{H\kappa}(z) = 0.$$

These admit the following general solutions:

(i) for equations (3-24a),

$$f_{T\kappa} = A_1 \cos(\beta_\kappa X) + A_2 \sin(\beta_\kappa X), \tag{3-25a}$$

$$F_{T\kappa} = \left[\cosh(q_\kappa z) + R_1 \sinh(q_\kappa z)\right] e^{-\frac{1}{2}z}, \tag{3-25b}$$

where

$$q_\kappa = \left[\frac{5}{4} + \left(\frac{\beta_\kappa}{\ell}\right)^2\right]^{1/2};$$

(ii) for equations (3-24b),

$$f_{H\kappa} = B_1 \cosh(\beta_\kappa X) + B_2 \sinh(\beta_\kappa X), \tag{3-26a}$$

$$F_{H\kappa} = \left[\cos(c_\kappa^* z) + R_2 \sin(c_\kappa^* z)\right] e^{-\frac{1}{2}z} \quad \text{for } \left(\frac{\beta_\kappa}{\ell}\right)^2 > \frac{5}{4},$$

$$F_{H\kappa} = \left[\cosh(c_\kappa z) + R_2 \sinh(c_\kappa z)\right] e^{-\frac{1}{2}z} \quad \text{for } \left(\frac{\beta_\kappa}{\ell}\right)^2 < \frac{5}{4}, \tag{3-26b}$$

where

$$c_\kappa^* = \left[\left(\frac{\beta_\kappa}{\ell}\right)^2 - \frac{5}{4}\right]^{1/2},$$

$$c_\kappa = \left[\frac{5}{4} - \left(\frac{\beta_\kappa}{\ell} \right)^2 \right]^{1/2}$$

Using the boundary conditions (3-19 a-c) expressed in terms of z rather than r (see equation (3-20)), the solutions above must satisfy

$$\left. \frac{\partial \hat{\phi}_{T\kappa}}{\partial z} \right|_{z=0} - f_{T\kappa}(X)\, F'_{T\kappa}(z) = i\omega E_{T\kappa}(X) + U(X) E'_{T\kappa}(X), \qquad (3\text{-}27a)$$

$$\left. \frac{\partial \hat{\phi}_{H\kappa}}{\partial z} \right|_{z=0} - f_{H\kappa}(X)\, F'_{H\kappa}(z) = i\omega E_{H\kappa}(X) + U(X) E'_{H\kappa}(X), \qquad (3\text{-}27b)$$

$$\left. \frac{\partial \hat{\phi}_{T\kappa}}{\partial z} \right|_{z=h} - f_{T\kappa}(X)\, F'_{T\kappa}(z) = 0, \qquad (3\text{-}27c)$$

$$\left. \frac{\partial \hat{\phi}_{H\kappa}}{\partial z} \right|_{z=h} - f_{H\kappa}(X)\, F'_{H\kappa}(z) = 0. \qquad (3\text{-}27d)$$

In order to determine the unknown solution parameters (A_1, A_2, B_1, B_2, R_1, R_2), it is necessary to have six equations, whereas apparently only four are available, equations (3-27 a-d). However, examining equations (3-27 a,b) more carefully, it is realized that each of the left(middle) and right-hand sides may be separated into two parts, each including $\sin(\beta_\kappa X)$ or $\cos(\beta_\kappa X)$ and $\sinh(\beta_\kappa X)$ or $\cosh(\beta_\kappa X)$, thus giving rise to six independent equations. Hence, solving this closed problem, the unknown variables are found to be

(i) for the "trigonometric" equation, i.e., the part of the solution with subscript T,

$$A_1 = G_{T\kappa}\left(-i\omega + U(X)\sigma_\kappa\beta_\kappa \right),$$

$$A_2 = G_{T\kappa}\left(i\omega\sigma_\kappa + U(X)\beta_\kappa \right), \qquad (3\text{-}28a)$$

$$R_1 = \frac{q_\kappa \sinh(q_\kappa h) - \frac{1}{2}\cosh(q_\kappa h)}{-q_\kappa \cosh(q_\kappa h) + \frac{1}{2}\sinh(q_\kappa h)}$$

where

$$G_{T\kappa} = \frac{-q_\kappa + \frac{1}{2}\tanh(q_\kappa h)}{(q_\kappa^2 - \frac{1}{4})\tanh(q_\kappa h)}, \qquad (3\text{-}28b)$$

(ii) for the "hyperbolic" equation, i.e., the part of the solution with subscript H,

$$B_1 = G_{H\kappa}(i\omega - U(X)\sigma_\kappa\beta_\kappa),$$

$$B_2 = G_{H\kappa}(-i\omega\sigma_\kappa + U(X)\beta_\kappa), \qquad (3\text{-}28c)$$

$$R_2 = \frac{c_\kappa^* \sin(c_\kappa h) + \frac{1}{2}\cos(c_\kappa^* h)}{c_\kappa^* \cos(c_\kappa h) - \frac{1}{2}\sin(c_\kappa^* h)} \quad \text{for } \left(\frac{\beta_\kappa}{\ell}\right)^2 > \frac{5}{4},$$

$$R_2 = \frac{-c_\kappa \sinh(c_\kappa h) + \frac{1}{2}\cosh(c_\kappa h)}{c_\kappa \cosh(c_\kappa h) - \frac{1}{2}\sinh(c_\kappa h)} \quad \text{for } \left(\frac{\beta_\kappa}{\ell}\right)^2 < \frac{5}{4},$$

where

$$G_{H\kappa} = \frac{c_\kappa^* - \frac{1}{2}\tan(c_\kappa^* h)}{(c_\kappa^{*2} + \frac{1}{4})\tan(c_\kappa^* h)} \quad \text{for } \left(\frac{\beta_\kappa}{\ell}\right)^2 > \frac{5}{4},$$

$$G_{H\kappa} = \frac{-c_\kappa + \frac{1}{2}\tanh(c_\kappa h)}{(c_\kappa^2 - \frac{1}{4})\tanh(c_\kappa h)} \quad \text{for } \left(\frac{\beta_\kappa}{\ell}\right)^2 < \frac{5}{4}. \qquad (3\text{-}28d)$$

Hence, the reduced-motion potentials, $\hat{\phi}_{T\kappa}$ and $\hat{\phi}_{H\kappa}$, on the flexible centre-body surface at location X may be obtained as

$$\hat{\phi}_{T\kappa}(X, z=0) = G_{T\kappa}[\, i\omega E_{T\kappa}(X) + U(X)E'_{T\kappa}(X)\,],$$
$$\hat{\phi}_{H\kappa}(X, z=0) = G_{H\kappa}[\, i\omega E_{H\kappa}(X) + U(X)E'_{H\kappa}(X)\,]. \qquad (3\text{-}29)$$

3.4 DETERMINATION OF THE UNSTEADY PRESSURE DISTRIBUTION AND THE RESULTANT FORCE ON THE CENTRE-BODY

The unsteady perturbation pressure, associated with body motion, is obtained from the perturbation velocity potential via the Bernoulli-Lagrange equation, given as equation (3-11) in section 3.1. This perturbation pressure may be divided into

$p_s(X,r)$ and $p_p(X,r,\theta,t)$, corresponding to the axisymmetric steady component and unsteady component, respectively. Thus,

$$p - p_o = p_s + p_p. \tag{3-30}$$

The fluid-dynamic pressure force exerted on the flexible centre-body will be obtained by means of the potential flow theory [21], developed in section 3.2 and 3.3. Substituting equation (3-13) into equation (3-11), the unsteady pressure is expressed as the following nondimensional equation in terms of the steady axisymmetric component and the unsteady one of the velocity potential Φ:

$$-\frac{1}{\rho_f U_o^{*2}}(p_s + p_p) = \frac{1}{U_o \ell}\frac{\partial \phi}{\partial t} + \frac{1}{2}\left|\nabla\phi_s + \nabla\phi\right|^2 - \frac{1}{2}, \tag{3-31}$$

where ∇^* operator from equation (3-11) has been replaced by

$$\nabla^* = \vec{i}_x{}^* \frac{\partial}{\partial x^*} + \vec{i}_r{}^* \frac{\partial}{\partial r^*} = \frac{1}{a}\left(\vec{i}_x \frac{\partial}{\partial x} + \vec{i}_r \frac{\partial}{\partial r}\right) = \frac{1}{a}\nabla .$$

In the above equation, the circumferential component is neglected.

Introducing the linearization procedure into the second term of the right-hand side of equation (3-31) and then considering the assumption of small amplitude motion of the centre-body yields

$$\nabla\phi_s \simeq \bar{U}(X)\vec{i}_x, \quad (\nabla\phi)^2 << (\nabla\phi_s)^2 \tag{3-32}$$

where $\bar{U}(X)$ is defined in equation (2-3). Therefore, it is possible to rewrite the second term of the right hand-side of equation (3-31) as

$$\left|\nabla\phi_s + \nabla\phi\right|^2 \simeq \bar{U}^2(X) + 2\bar{U}(X)\frac{1}{\ell}\frac{\partial\phi}{\partial X}; \tag{3-33}$$

since, the radial and circumferential component of the flow velocity is negligible as compared with the axial one. Thus,

equation (3-31) may be written in terms of the nondimensional fluid velocity, U(X), at location X:

$$-\frac{1}{\rho_f U_o^{*2}}(p_s + p_p) = \frac{1}{U_o \ell}\frac{\partial \phi}{\partial t} + \frac{1}{2}\left[\bar{U}^2(X) + 2\bar{U}(X)\frac{1}{\ell}\frac{\partial \phi}{\partial X}\right] - \frac{1}{2}. \quad (3\text{-}34)$$

Taking into account the forms of the inviscid fluid-dynamic force and reduced-motion potentials, it is convenient to rewrite these equations, with respect to the set of reduced-motion potentials defined in equation (3-17), i.e.,

$$-\frac{1}{\rho_f U_o^{*2}}(p_s + p_p) = \sum_\kappa a_\kappa \left(\left(\frac{1}{\ell U_o}\right)^2 [\hat{\phi}_{T\kappa} + \hat{\phi}_{H\kappa}] i\omega e^{i\omega t}\cos\theta - \frac{1}{2} + \frac{1}{2}\bar{U}^2(X) + \bar{U}(X)\frac{1}{\ell^2}\frac{1}{U_o}\left[\frac{\partial \hat{\phi}_{T\kappa}}{\partial X} + \frac{\partial \hat{\phi}_{H\kappa}}{\partial X}\right] e^{i\omega t}\cos\theta \right). \quad (3\text{-}35)$$

The unsteady fluid-dynamic force acting on the unit length of the flexible centre-body is then determined by integrating circumferentially the pressure distribution, by means of equation (3-12). Thus, substituting equation (3-35) into equation (3-12), the inviscid fluid-dynamic force, acting on the oscillating centre-body, in the dimensionless form, is

$$F_p(X,t) = \sum_\kappa a_\kappa \rho_f U_{ref}^2 a\pi e^{i\omega t}\left(\frac{i\omega}{\ell^2}\left[\hat{\phi}_{T\kappa} + \hat{\phi}_{H\kappa}\right]_{z=0} + U(X)\frac{1}{\ell^2}\left[\frac{\partial \hat{\phi}_{T\kappa}}{\partial X} + \frac{\partial \hat{\phi}_{H\kappa}}{\partial X}\right]_{z=0} \right). \quad (3\text{-}36)$$

Hence, the above equation, in terms of $P_{j\kappa p}$ (j=0,1,2) which are the inviscid components of $P_{j\kappa}$ (j= 0, 1, 2) defined in section 2.3, equations (2-10 a,b), may be written as

$$F_p(X,t) = -\rho_f U_{ref}^2 a\pi e^{i\omega t}\sum_\kappa a_\kappa \left(-\omega^2 P_{2\kappa p} + i\omega P_{1\kappa p} + P_{0\kappa p} \right), \quad (3\text{-}37)$$

where

$$P_{2\kappa p}(X) = -\left[G_{T\kappa}E_{T\kappa}(X) + G_{H\kappa}E_{H\kappa}(X) \right]/\ell^2, \quad (3\text{-}38a)$$

$$P_{1\kappa p}(X) = -2\,U(X)\,[\,G_{T\kappa}E_{T\kappa}'(X) + G_{H\kappa}E_{H\kappa}'(X)\,]/\ell^2, \qquad (3\text{-}38b)$$

$$P_{0\kappa p}(X) = -U^2(X)\,\beta_\kappa^2\,[\,-G_{T\kappa}E_{T\kappa}(X) + G_{H\kappa}E_{H\kappa}(X)\,]/\ell^2 \qquad (3\text{-}38c)$$

It is obvious that these terms, which in fact are related to the inertial, damping and stiffness components, respectively, of the generalized nondimensional fluid-dynamic force due to inviscid flow, do not depend on the steady-motion potential ϕ_s because of the axisymmetric shape of the flow passage.

CHAPTER IV

DYNAMICS AND STABILITY OF THE FLEXIBLE CENTRE-BODY BASED ON POTENTIAL FLOW THEORY

4.1 FORMULATION OF THE EIGENVALUE PROBLEM USING GALERKIN'S METHOD

This part of the Thesis is devoted to the determination of the fluid-dynamic coupling terms, fluid-dynamic stiffness, damping and virtual mass, of the system generated by inviscid flow, by means of Galerkin's method.

Introducing the terms associated with the inviscid fluid-dynamic force, as determined in the previous section, into the equation of motion of the flexible centre-body, the following equation may be obtained

$$EI \frac{\partial^4 e_o^*}{\partial x^{*4}} + \rho_s A_s \frac{\partial^2 e_o^*}{\partial t^{*2}} = F_p(x^*, t^*). \qquad (4\text{-}1)$$

According to equation (3-35), the inviscid fluid-dynamic force may be expressed nondimensionally as

$$F_p = - \rho_f U_{ref}^2 \, a\pi \, P_p(X) \, e^{i\omega t}, \qquad (4\text{-}2)$$

where

$$P_p(X) = \sum_{\kappa} a_\kappa \left[- \omega^2 P_{2\kappa p}(X) + i\omega P_{1\kappa p}(X) + P_{0\kappa p} \right].$$

Recalling the approach to be used to obtain an approximate solution, which was introduced in chapter II, and combining equations (2-11) and (4-1) yields

$$\epsilon_p = \frac{d^4 E(X)}{dX^4} - \omega^2 E(X) + \sigma \, P_p(X), \qquad (4\text{-}3)$$

where the form of the complex eigenfrequencies ω, which depend on flow velocity, indicates the stability or instability of the system. In order to investigate the dynamics and stability

of the system, Galerkin's method is applied to this system. In this respect, ϵ_p multiplied by the weighting functions and integrated over the domain must satisfy.

$$\sum_{\kappa} a_{\kappa} \int_0^1 \{ -\omega^2 [E_{\kappa}(X) + \sigma P_{2\kappa p}(X)] + i\omega \sigma P_{1\kappa p}(X) + [\beta_{\kappa}^4 E_{\kappa}(X) + \sigma P_{0\kappa p}(X)] \} E_j(X)\, dX = 0, \quad (4\text{-}4)$$

where each of the functions $E_{\kappa}(X)$ is a suitable comparison function satisfying all the boundary conditions of a clamped-clamped beam, in fact, a beam eigenfunction, as shown in Appendix A.

Introducing equations (3-38) in the above equation yields

$$-\omega^2 [M_p]\ (A)\ e^{i\omega t} + i\omega\ [C_p]\ (A)\ e^{i\omega t} + [K_p]\ (A)\ e^{i\omega t} = 0, \quad (4\text{-}5)$$

where

$$m_{pj\kappa} = \int_0^1 (E_{T\kappa}E_{Tj} + E_{T\kappa}E_{Hj} + E_{H\kappa}E_{Tj} + E_{H\kappa}E_{Hj})\, dX - \sigma \frac{1}{\ell^2} \{ \int_0^1 [G_{T\kappa} (E_{T\kappa}E_{Tj} + E_{Tk}E_{Hj}) + G_{H\kappa} (E_{H\kappa}E_{Tj} + E_{H\kappa}E_{Hj})]\, dX = 0, \quad (4\text{-}6a)$$

$$c_{pj\kappa} = -2 U_o \sigma \frac{1}{\ell^2} \{ \int_0^1 \frac{h_o}{h} [G_{Tk} (E_{T\kappa}'E_{Tj} + E_{T\kappa}'E_{Hj}) + G_{H\kappa} (E_{H\kappa}'E_{Tj} + E_{H\kappa}'E_{Hj})]\, dX \}, \quad (4\text{-}6b)$$

$$k_{pj\kappa} = \beta_{\kappa}^4 \int_0^1 (E_{T\kappa}E_{Tj} + E_{T\kappa}E_{Hj} + E_{H\kappa}E_{Tj} + E_{H\kappa}E_{Hj})\, dX + \sigma \frac{1}{\ell^2} \beta_{\kappa}^2 U_o^2 \{ \int_0^1 (\frac{h_o}{h})^2 [G_{T\kappa} (E_{T\kappa}E_{Tj} + E_{T\kappa}E_{Hj}) - G_{H\kappa} (E_{H\kappa}E_{Tj} + E_{H\kappa}E_{Hj})]\, dx \}, \quad (4\text{-}6c)$$

where the subscript p is used to indicate that these terms are associated with the potential solution of the problem, and the quantities $E_{T\kappa}$, $E_{H\kappa}$ are defined in equation (2-7) with $G_{T\kappa}$, $G_{H\kappa}$ having been determined in equations (3-27) and (3-28).

Alternative expressions of equations (4-6 a-c) in the case of a constant annular flow passage ($h=h_o$=constant) may be obtained, based on the small disturbance assumption. In this

case, the fluid dynamic stiffness and damping coefficients may be linearized to give

$$m_{pj\kappa} = I_p - \frac{A}{A_f}\frac{M}{m}\left[G_{T\kappa} I_T + G_{H\kappa} I_H \right], \tag{4-7a}$$

$$c_{pj\kappa} = -2 U_{o1} \left(\frac{M}{m}\right)^{1/2} \left(\frac{A}{A_f}\right)^{1/2} \left[G_{T\kappa} I_T' + G_{H\kappa} I_H' \right], \tag{4-7b}$$

$$k_{pj\kappa} = \beta_\kappa^4 I_p + \beta_\kappa^2 U_{o1}^2 \left[G_{T\kappa} I_T - G_{H\kappa} I_H \right], \tag{4-7c}$$

where

$$I_T = \int_0^1 \left(E_{T\kappa} E_{Tj} + E_{T\kappa} E_{Hj} \right) dX,$$

$$I_H = \int_0^1 \left(E_{H\kappa} E_{Tj} + E_{H\kappa} E_{Hj} \right) dX,$$

$$I_p = I_T + I_H = \int_0^1 \left(E_{T\kappa} E_{Tj} + E_{T\kappa} E_{Hj} + E_{H\kappa} E_{Tj} + E_{H\kappa} E_{Hj} \right) dX, \tag{4-7d}$$

$$I_T' = \int_0^1 \left(E_{T\kappa}' E_{Tj} + E_{T\kappa}' E_{Hj} \right) dX,$$

$$I_H' = \int_0^1 \left(E_{H\kappa}' E_{Tj} + E_{H\kappa}' E_{Hj} \right) dX,$$

$$A_f = \pi \left((a + H^*)^2 - a^2 \right), \qquad A = \pi a^2,$$

$$m = \rho_s A_s, \qquad M = \rho_f A_f$$

The integrals in the above equations could be evaluated by using an analytical method or a numerical method. The numerical solutions are shown in Appendix C, where they are compared with the analytical ones. From the above equations, it is obvious that the virtual mass coefficient does not depend on the flow velocity, as expected; the fluid-dynamic stiffness and damping coefficients, however, are affected by the fluid velocity.

The problem has now been rendered discrete and, upon truncating the summation at $\kappa = n$, equation (4-4) may be written in matrix form, as follows;

$$[M_p] (\ddot{q}) + [C_p] (\dot{q}) + [K_p] (q) = 0, \tag{4-8}$$

where

$$\{q\} = \{A\} e^{i\omega t}.$$

Here, it is assumed that the order of this matrix equation is sufficiently high to allow the determination of the response within the desired accuracy. In the present analysis this is achieved with n=5.

In this case, the asymmetry in the matrices, $[C_p]$ and $[K_p]$, is entirely due to the presence of inviscid fluid-dynamic forces; e.g. in the case of $[C_p]$, the asymmetry is due to the Coriolis force, which corresponds to equation (4-7b). Accordingly, equation (4-8) can not be decoupled easily. A quite general method of decoupling this equation is shown in Appendix B.

In order to obtain the eigenvalues of this system, equation (4-8) may be manipulated further, yielding finally

$$\det \left[-\omega^2 m_{pj\kappa} + i\omega c_{pj\kappa} + k_{pj\kappa} \right] = 0. \qquad (4\text{-}9)$$

This method is much easier to apply and more efficient than the general method shown in Appendix B. The method used to find the roots of equation (4-9) is based on a quadratic fit called "ZANLYT". The general computer program for dynamic stability of the system is given in Appendix D.

Because of the numerous parameters characterizing the system, no attempt has been made to investigate the effect of each one; e.g. length/radius ratio, gap width/radius ratio, physical properties of the fluid and of the materials, etc. [see the principal nondimensional parameters affecting the system, introduced in chapter II, equations (2-3)]. Here, the effects of varying the fluid velocity and the fluid properties are investigated, by conducting calculations with air, water and oil flow; the annular-gap/radius ratio is taken to be 1.5/10, 1/10 and 1/20, and ℓ^*/a=20 throughout; the material of cylinder is taken to be rubber, so that U_{ref}=1.198 m/s and U_{ref1}=36.77 m/s (for air), 1.287 m/s (for water) or 1.332 m/s (for oil).

4.2 ANALYSIS OF DYNAMICS AND STABILITY OF THE FLEXIBLE CENTRE-BODY.

Typical results, illustrating the general dynamical behaviour of the system under consideration, subject to inviscid flow, are presented in this section. As discussed in the previous section, the dynamical behaviour of this system is modified (as compared to the basic beam in vacuum) by the fluid-dynamic force acting on it, which is a function of the flow velocity. For convenience the results will be presented in terms of the nondimensional flow velocity U_{o1}, rather than U_o - see equations (2-3).

At zero flow velocity, it is obvious that the natural frequencies depend on $(A/A_s)\cdot(M/m)$, considering the added mass; fluid-dynamic stiffness and damping coefficients are, of course, equal to zero at zero flow velocity, but the corresponding virtual mass is not. With increasing flow velocity, the frequencies of most of the modes are diminished. Because the system under the consideration here is conservative (clamped ends), the eigenfrequencies remain real with increasing U_{o1}, at least up to the point of loss of the stability, when the equivalent generalized centrifugal force overcomes the flexural restoring force.

At this point, one may note that the lowest critical flow velocity indicating the onset of buckling may be found easily, taking into consideration Euler's method of equilibrium (see Appendix E). At the buckling onset, the time derivatives in the equation of motion of the centre-body could be eliminated; i.e., the determinant of $[K_p]$ should be zero. Thus, from equation (4-7c), it is obvious that at divergence instability the nondimensional critical flow velocity, with respect to U_{refl}, does not depend on the properties of the fluid but only on the geometry of the system (gap ratio and length ratio).

The dimensionless complex eigenfrequencies, ω_n, of the system are calculated using the computer program given in Appendix D.

Typical variations of the real and imaginary parts of the complex eigenfrequencies, ω_n, with the nondimensional fluid velocity U_{01} are presented, for the lowest four modes (out of five modes) in Figures 2, 3 and 4, for the 1/10 gap systems rubber-air, rubber-water and rubber-oil, respectively. The fifth mode, also obtained, is not shown because the results are considered unreliable with a five-mode Galerkin approximation (n=5).

In Figure 2, it is noted that the frequencies of all modes vanish in turn, indicating the onset of buckling in the corresponding modes of the system with increasing flow velocity. The frequency of the first mode vanishes at $U_{01} = \sqrt{3}$ (point A in the diagram), which is the first critical velocity for buckling, being associated with the point where ω changes from purely real to purely imaginary, and one branch of the bifurcated locus on the Im(ω)-axis is negative. Similarly, the frequencies of the other modes vanish at U_{01} = 3.21 (point B), 4.85, and 7.13.

However, at slightly higher flow velocities than necessary for buckling in the first and second modes, the loci of these two modes, and similarly those of the third and fourth modes, coalesce on the Im(ω)-axis and leave the axis at symmetrical points, indicating the onset of coupled-mode flutter (for example, point C in Figure 2a), in the pair of modes concerned. This behaviour does not appear in the case of higher mass ratio, M/m as shown Figures 3 and 4.

At this point, it is of interest to note that the main interest in the practical engineering applications, for design considerations, is the determination of the critical flow velocity for which the system loses stability. The dynamical behaviour of the system at high velocities than the this critical threshold is more of an academic interest; on the other hand, the amplitude of the oscillations after the loss of the stability may increase beyond the assumed limits of the this theory, although it was shown that, in some cases, a linear theory is also capable of predicting the post-critical

behaviour of the system (see, for example refs. 8 and 12). A similar capability will be presumed to exist here also.

In Figures 3 and 4, it is noted that even though the first mode frequency also vanishes at A (U_{o1}=2.13), the loci of the other modes do not reach the Im(ω)-axis directly. But the system regains stability in its first mode at B (U_{o1}=3.21), the corresponding buckling point of the second mode in the previous case. At slightly higher flow velocity, the loci of the first and second modes coalesce on the Re(ω)-axis and become complex, indicating the onset of the coupled-mode flutter at C. Interestingly, this behaviour was suggested to be related to the well-known destabilizing effect of gyroscopic forces, e.g. in connection with the whirling of shafts [26]. According to this relation, the Coriolis forces being proportional to $(M/m)^{\frac{1}{2}}$ stabilize the system prior to the onset of coupled-mode flutter; therefore, oscillatory instabilities connected to the presence of Coriolis forces could exist whenever $(M/m)^{\frac{1}{2}} \neq 0$ - which is always true for the present system. These symmetric coupled-modes, with respect to Re(ω)-axis, bifurcate on the Re(ω)-axis at D, where the system regains stability. At slightly higher flow velocity, one of these bifucating modes has pure imaginary value, indicating the re-occurrence of buckling, at E (U_{o1} = 4.85). Then, by a similar process, coupled-flutter re-occurs at F, involving the loci of the other bifurcated modes and the third mode. The regions associated with higher flow velocity are quite complex.

The effect of varying the relative gap $h-H^*/a$ for given length to radius ratio $\ell-\ell^*/a$ is illustrated in Figures 5 and 6 for the case of rubber-air and rubber-oil systems, respectively. Here, the first and second modes appear to buckle at A and B in Figure 5, but in Figure 6 these points are seen to correspond, respectively, to the onset of buckling and re-stabilization therefrom (for the first mode), as discussed before.

Table 1 Values of U_{o1} for instabilities obtained with potential flow theory (ℓ=20, σ=0.4246 and U_{ref1}=36.77m/s)

annular gap ratio, h	1st mode buckling, A	2nd mode buckling, B	coupled mode (1st & 2nd modes) flutter, C
0.05	1.49	2.24	2.34
0.10	2.13	3.21	3.40
0.15	2.64	3.97	4.25

Table 2 Values of U_{o1} for instabilities obtained with potential flow theory (ℓ=20, σ=346.62 and U_{ref1}=1.287m/s)

annular gap ratio, h	1st mode buckling, A	1st mode re-stabilization, B	coupled mode (1st & 2nd modes) flutter, C
0.05	1.49	2.24	2.47
0.10	2.13	3.21	3.51
0.15	2.64	3.97	4.31

It is of interest to see in Table 1 and 2 that the nondimensional critical flow velocities for divergence and for coupled-mode flutter of the 1/20-gap system are lower than those corresponding to systems with lager relative gap. It is also shown that the lowest nondimensional flow velocity for divergence does not depend on σ, for any considered relative gap, while the coupled-mode flutter critical velocity depend slightly on σ. This is because $U_{o1}=U_o/\sigma^{\frac{1}{2}}$, and hence the lowest nondimensional critical flow velocity for divergence, U_{oldiv}, is dependent on h and ℓ, but not on σ, as it can be seen from equations (3-28) and (4-7); one may note in the same sense that flutter is affected by the damping matrix, while the buckling is not affected by it. The destabilizing effect on oscillatory instabilities of narrowing the annular gap was well documented for a similar system [21].

It is also of interest to compare these critical velocities with those obtained by approximate method proposed by Paidoussis [14] for confined flow; this comparison is shown in detail in Appendix E. Satisfaction, in quantitative agreement of critical flow velocity, is found to be adequate for the narrow inviscid flow analyzed; however, the approximate method for the critical flow velocity based on the virtual mass is suitable for a slender body. Moreover, it is noted that the dynamical behaviour of the system, based on inviscid flow theory for the narrow flow analyzed is similar to that of system with confined flow [25] or with internal flow [13]: the system loses stability by the divergence in its first mode, is restabilized according to the Coriolis force and then becomes subject to coupled-mode flutter through coalescence of the first- and second-mode loci.

Finally, from the above results, it is noted that the system with the lowest density fluid requires a much higher dimensional flow velocity to cause instability - which is reasonable; however, the lowest nondimensional critical flow velocity is kept the same, as discussed above.

It is worth noting the difference in behaviour between systems of low and high mass ratio. In summary, the following way be said. (i) The lowest nondimensional critical flow velocity with respect to U_{refl}, which is of course for divergence, is not dependent on the properties of fluid but on the geometry of the system. (ii) For small values of mass ratio, the system buckles in the second mode before the onset of flutter; for large values of mass ratio, the system does not buckle in the second mode prior to the onset of flutter, but the loss of stability in the second mode is preceded by regaining of stability in the first mode; moreover, at higher flow, the regaining of stability of this coupled-mode occurs at a slightly lower U_{01} than necessary for the onset of third-mode flutter. It is well known [13] that these effects could be even more pronounced at higher mass ratio. (iii) As the annular gap is diminished, U_{01} is reduced. (iv) The lowest

density fluid requires a much higher dimensional flow velocity, U_o^*, to cause instability.

CHAPTER V

STUDY OF VISCOUS FLOW IN THE ANNULAR PASSAGE AROUND AN OSCILLATING FLEXIBLE CENTRE-BODY

5.1 GENERAL CONSIDERATIONS

The analytical model developed by Mateescu and Paidoussis [22] for considering the viscous effects in the case of oscillating rigid cylinder will be extended here to evaluate the viscous effects of real fluid flow in the case of flexible cylinders. The fluid-dynamic forces acting on the centre-body were obtained previously by means of potential flow theory, neglecting viscous effect; however, it is well known that viscous effects in real flows are enhanced in narrow passages, and therefore it is even more important to take them into account for the problem at hand.

In a viscous flow, the fluid-dynamic forces are considerably more complicated than for inviscid flow and in general the Navier-Stokes equations are used to obtain them.

The principal purpose of this work is to evaluate the viscous effects on the dynamics of the flexible centre-body in the annular flow. Actually, only the case of the system consisting of constant cross-sections of both the flexible centre-body and the cylindrical coaxial duct, will be considered.

Based on the assumption of small amplitude oscillations of the flexible centre-body in a narrow annular flow, the following two flow fields are considered, in order to simplify the approach of this problem:

a) a potential flow, which represents the perturbation flow field according to inviscid flow theory,

b) a viscous flow field, which includes the steady and unsteady viscous effects.

In the present analysis, the annular flow is considered as a laminar flow. However, the approach taken here could be

adopted in the case of turbulent flow also, if desired. As assumed in chapter II, an incompressible fluid of density ρ_f and viscosity μ flows in the annulus with mean flow velocity U_o^*. Assuming the fluid to be Newtonian, the shear stress between fluid layers is proportional to the velocity gradient across the layer.

The viscous forces acting on the flexible centre-body may be separable into two parts according to their respective orders of magnitude. The "zero-order" viscous forces are derived from the longitudial(axial) frictional force and from pressurization of the flow - necessary to overcome the frictional pressure drop. They are known as the time-independent viscous steady forces, and they may be quite important in dealing with flexible bodies in annular flow; however, they nearly have no effect on the dynamics of rigid bodies [22]. The "first-order" viscous forces arise from normal friction forces containing the effect of the viscous pressure distribution along the circumference. These forces comprise the unsteady viscous effects.

Thus, free oscillations of the flexible centre-body under consideration are influenced by both steady and unsteady viscous forces.

It is necessary to get the normal and tangential friction forces acting on the flexible centre-body, and for this purpose the viscous tangential stress acting on the centre-body surface and viscous pressure distribution must be obtained first. From these results, the analysis is adapted to determine the viscous steady and unsteady forces, as shown in section 5.3. Here, the basic equations of the viscous flow, adopted from the problem of a rigid cylindrical body in a narrow annular duct [22], will be extended to deal with this case (i.e., a flexible centre-body).

5.2 THE BASIC EQUATIONS OF FLUID MOTION AND FORMULATION OF THE UNSTEADY VISCOUS PROBLEM

In order to get a complete and fundamental understanding of fluid dynamic problems of viscous incompressible flow, it is believed that the most general governing equations of continuity and momentum should be first derived and explained. The complete solution for the governing equations of viscous incompressible flow is still not possible because of insurmountable mathematical difficulties. However, many fluid mechanics problems can be treated via these governing equations, which may be greatly simplified in special cases.

In the study of viscous incompressible flow, it is necessary to obtain the three components of velocity and pressure P, as a function of space and time. These four unknowns can be determined in principle from governing equations: i) the continuity equation and ii) Navier-Stokes equations.

For our purposes, it is convenient to use the nondimensional components of flow velocity in cylindrical coordinates and nondimensional pressure perturbation associated with the motion of the flexible centre-body, i.e.,

$$V(x^*, r^*, \theta, t^*) = U_o^*[u(X, r, \theta, t)\vec{i}_x + v(X, r, \theta, t)\vec{i}_r + w(X, r, \theta, t)\vec{i}_\theta], \tag{5-1}$$

$$p(x^*, r^*, \theta, t^*) = \frac{(P - P_o)}{\rho_f U_o^{*2}} = \frac{(p_v + p_p)}{\rho_f U_o^{*2}},$$

where the subscripts v and p stand for the viscous and potential components, respectively.

Now, in terms of the dimensionless cylindrical coordinates defined in equations (2-3), continuity and Navier-Stokes equations may be written, as follows:

$$\frac{\partial u}{\partial X} + \ell \frac{1}{r}\frac{\partial}{\partial r}(rv) + \ell \frac{1}{r}\frac{\partial w}{\partial \theta} = 0. \tag{5-2}$$

$$\frac{1}{U_o}\frac{\partial u}{\partial t} + u\frac{\partial u}{\partial X} + v\,\ell\,\frac{\partial u}{\partial r} + w\,\ell\,\frac{1}{r}\frac{\partial u}{\partial \theta} = -\frac{\partial p}{\partial X}$$

$$+ \frac{2h}{Re}\frac{1}{\ell}\left(\frac{\partial^2 u}{\partial X^2} + \ell^2\,\frac{1}{r}\frac{\partial}{\partial r}\left(r\frac{\partial u}{\partial r}\right) + \ell^2\,\frac{1}{r^2}\frac{\partial^2 u}{\partial \theta^2}\right),$$

$$\frac{1}{U_o}\frac{\partial v}{\partial t} + u\frac{\partial v}{\partial X} + v\,\ell\,\frac{\partial v}{\partial r} + w\,\ell\,\frac{1}{r}\frac{\partial v}{\partial \theta} - \ell\,\frac{w^2}{r} = -\ell\,\frac{\partial p}{\partial r}$$

$$+ \frac{2h}{Re}\frac{1}{\ell}\left(\frac{\partial^2 v}{\partial X^2} + \ell^2\,\frac{1}{r}\frac{\partial}{\partial r}\left(r\frac{\partial v}{\partial r}\right) + \ell^2\,\frac{1}{r^2}\frac{\partial^2 v}{\partial \theta^2} - \ell^2\,\frac{1}{r^2}\left(v + 2\frac{\partial w}{\partial \theta}\right)\right), \tag{5-3}$$

$$\frac{1}{U_o}\frac{\partial w}{\partial t} + u\frac{\partial w}{\partial X} + v\,\ell\,\frac{\partial w}{\partial r} + w\,\ell\,\frac{1}{r}\frac{\partial w}{\partial \theta} + \ell\,\frac{vw}{r} = -\ell\,\frac{1}{r}\frac{\partial p}{\partial \theta}$$

$$+ \frac{2h}{Re}\frac{1}{\ell}\left(\frac{\partial^2 w}{\partial X^2} + \ell^2\,\frac{1}{r}\frac{\partial}{\partial r}\left(r\frac{\partial w}{\partial r}\right) + \ell^2\,\frac{1}{r^2}\frac{\partial^2 w}{\partial \theta^2} - \ell^2\,\frac{1}{r^2}\left(w - 2\frac{\partial v}{\partial \theta}\right)\right).$$

In the above equations, Re denotes the Reynolds number

$$Re = \rho_f\, U_o^*\, D_H / \mu, \tag{5-4}$$

based on the hydraulic diameter of the annulus,

$$D_H = 2\,H^* = 2\,ha. \tag{5-5}$$

The velocity vector associated with potential flow was denoted by $V_p = U_o^*((1+u_p)\vec{i}_X + v_p\vec{i}_r + w_p\vec{i}_\theta)$, and the related perturbation pressure by p_p.

In this connection, the nondimensional components of the flow velocity in cylindrical coordinates may be written as

$$\begin{aligned} u(X,r,\theta,t) &= u_v(X,r;\theta,t) + u_p(X,r,\theta,t),\\ v(X,r,\theta,t) &= v_v(X,r;\theta,t) + v_p(X,r,\theta,t),\\ w(X,r,\theta,t) &= w_v(X,r;\theta,t) + w_p(X,r,\theta,t),\\ p(X,r,\theta,t) &= p_v(X,r;\theta,t) + p_p(X,r,\theta,t). \end{aligned} \tag{5-6}$$

where u_v, v_v, w_v and p_v are associated with the viscous

effects of the real flow and depend slightly on θ and t; hence, the above notation is used.

In the case of potential flow (μ=0 or Re$\to\infty$), equations (5-3) may be reduced to Euler's equations of motion Now, subtracting the partial differential equations of the potential flow from the full equations (5-2) and (5-3), the governing equations of the remaining viscous flow may be expressed in form of the following nonlinear equations

$$\frac{\partial u_v}{\partial X} + \ell \frac{1}{r}\frac{\partial}{\partial r}(r v_v) + \ell \frac{1}{r}\frac{\partial w_v}{\partial \theta} = 0 \tag{5-7}$$

$$\begin{aligned}
&\frac{1}{U_o}\frac{\partial u_v}{\partial t} + u\frac{\partial u_v}{\partial X} + v\,\ell\frac{\partial u_v}{\partial r} + w\,\ell\frac{1}{r}\frac{\partial u_v}{\partial \theta} + (u_v - 1)\frac{\partial u_p}{\partial X} + v_v\,\ell\frac{\partial u_p}{\partial r} \\
&\quad + w_v\,\ell\frac{1}{r}\frac{\partial u_p}{\partial \theta} = -\frac{\partial p_v}{\partial X} + \frac{2h}{Re}\frac{1}{\ell}\Big(\frac{\partial^2 u}{\partial X^2} + \ell^2\frac{1}{r}\frac{\partial}{\partial r}(r\frac{\partial u}{\partial r}) \\
&\quad + \ell^2\frac{1}{r^2}\frac{\partial u}{\partial \theta^2}\Big),
\end{aligned}$$

$$\begin{aligned}
&\frac{1}{U_o}\frac{\partial v_v}{\partial t} + u\frac{\partial v_v}{\partial X} + v\,\ell\frac{\partial v_v}{\partial r} + w\,\ell\frac{1}{r}(\frac{\partial v_v}{\partial \theta} - w_v) + (u_v - 1)\frac{\partial v_p}{\partial X} \\
&\quad + v_v\ell\frac{\partial v_p}{\partial r} + w_v\ell\frac{1}{r}(\frac{\partial v_p}{\partial \theta} - w_p) = -\ell\frac{\partial p_v}{\partial r} + \frac{2h}{Re}\frac{1}{\ell}\Big(\frac{\partial^2 v}{\partial X^2} \\
&\quad + \ell^2\frac{1}{r}\frac{\partial}{\partial r}(r\frac{\partial v}{\partial r}) + \ell^2\frac{1}{r^2}\frac{\partial^2 v}{\partial \theta^2} - \ell^2\frac{1}{r^2}(v + 2\frac{\partial w}{\partial \theta})\Big),
\end{aligned} \tag{5-8}$$

$$\begin{aligned}
&\frac{1}{U_o}\frac{\partial w_v}{\partial t} + u\frac{\partial w_v}{\partial X} + v\,\ell\frac{\partial w_v}{\partial r} + w\,\ell\frac{1}{r}(\frac{\partial w_v}{\partial \theta} + v_v) + (u_v - 1)\frac{\partial w_p}{\partial X} \\
&\quad + v_v\ell\frac{\partial w_p}{\partial r} + w_v\ell\frac{1}{r}(\frac{\partial w_p}{\partial \theta} + v_p) = -\ell\frac{1}{r}\frac{\partial p_v}{\partial \theta} + \frac{2h}{Re}\frac{1}{\ell}\Big(\frac{\partial^2 w}{\partial X^2} \\
&\quad + \ell^2\frac{1}{r}\frac{\partial}{\partial r}(r\frac{\partial w}{\partial r}) + \ell^2\frac{1}{r^2}\frac{\partial^2 w}{\partial \theta^2} - \ell^2\frac{1}{r^2}(w - 2\frac{\partial v}{\partial \theta})\Big).
\end{aligned}$$

On the basis of a set of assumptions to be introduced later, equations (5-7) and (5-8) will be linearized and solved

analytically by an approximate method, as shown in the next section

5.3 SOLUTION OF VISCOUS FLOW IN NARROW ANNULAR PASSAGE

The unsteady potential flow, which is of course irrotational, is expressed in terms of the potential $\Phi(X,r,\theta,t)$, as shown in chapter III. This analytical solution of the potential flow is used to get the approximate solution of the viscous flow with Navier-Stokes equation, based on assumptions similar to those made in boundary layer theory.

The major assumptions made in inviscid flow may be available for the viscous flow; i.e., i) the amplitude of oscillation of the flexible centre-body is small, ii) the annulus is narrow ($h<<1$), and hence $z = r-1 << 1$

Taking into consideration the order of magnitude of the various terms in the nondimensional momentum and continuity equations by assuming that the frequency of oscillation is not very high and that the Reynolds number is relatively low, the time-derivative terms may be considered to be small in comparison to the radial component of viscous terms in Navier-Stokes equation. Further, equations (5-7) and (5-8) may be linearized and simplified drastically by introducing following assumptions similarly to the boundary-layer theory because of the narrowness of the annular passage:

a) the radial component of viscous motion, v_v, is considered to be negligible;

b) the circumferential and axial variations in u and w are considered to be negligible, when compared with radial variations of the same velocity components.

Accordingly, equations (5-8) become

$$\frac{\partial^2 u}{\partial z^2} = \frac{Re}{2h}\frac{1}{\ell}\frac{\partial p_v}{\partial X} \qquad \frac{\partial^2 w}{\partial z^2} = \frac{Re}{2h}\frac{1}{r}\frac{\partial p_v}{\partial \theta}$$

$$0 = \frac{\partial p_v}{\partial z} \qquad (5\text{-}9)$$

which are considered as a first attempt towards evaluating the effect of the unsteady viscous terms To specify this problem completely, the necessary boundary conditions are required. Considering a solid surface, it is clear that the velocity components normal and tangential to the surface must be equal to those of the surface itself based on the no slip condition.

With the aid of Figure 7, the total mean velocity may be approximated for the purpose of this viscous flow analysis as

$$U_o^* \bar{V}(X,\theta,t) = U_o^* (\bar{u} \cos \beta + \bar{w} \sin \beta), \qquad (5\text{-}10)$$

where u and w are the average values of the dimensionless axial and circumferential flow velocities across the annular gap, respectively, and the angle β is expressed as

$$\sin \beta = \frac{U_o^* \bar{w}}{U_o^* \bar{V}} \simeq \bar{w}(X,\theta,t), \qquad (5\text{-}11)$$

since the nondimensional total mean velocity is approximately equal to 1, which means that the total mean flow velocity remains approximately constant in magnitude; however, the direction of the total mean flow velocity oscillates through an angle β, associated with the motion of the flexible centre-body.

According to potential flow theory, the dimensionless circumferential flow velocity is expressed in terms of the potential $\phi(X,r,\theta,t)$, as follows:

$$w = \frac{1}{r} \frac{\partial \phi}{\partial \theta} . \qquad (5\text{-}12)$$

Substituting equation (3-17) into the above equation and then integrating over the annular gap, the average value of the dimensionless circumferential flow velocity across the annular gap may be expressed as

$$\bar{w} = \sum_{\kappa} \frac{a_\kappa}{\ell U_o h} (f_{T\kappa} W_{T\kappa} + f_{H\kappa} W_{H\kappa}) \sin\theta \, e^{i\omega t}, \qquad (5\text{-}13)$$

where $f_{T\kappa}$, $f_{H\kappa}$, and $W_{T\kappa}$, $W_{H\kappa}$ are expressed as

$$f_{T\kappa} = G_{T\kappa} \left[i\omega E_{T\kappa}(X) + U(X) E'_{T\kappa}(X) \right],$$

$$f_{H\kappa} = G_{H\kappa} \left[i\omega E_{H\kappa}(X) + U(X) E'_{H\kappa}(X) \right],$$

(5-14)

$$W_{T\kappa} = \int_0^h \frac{-1}{1+z} \left(\cosh(q_\kappa z) + R_1 \sinh(q_\kappa z) \right) e^{-\frac{1}{2}z} \, dz,$$

$$W_{H\kappa} = \int_0^h \frac{-1}{1+z} \left(\cos(c_\kappa z) + R_2 \sin(c_\kappa z) \right) e^{-\frac{1}{2}z} \, dz.$$

where $G_{T\kappa}$, $G_{H\kappa}$, q_κ, c_κ, R_1 and R_2 are given in section 3.3.

Using the chain rule of differentiation, the first two of equations (5-9) may be combined, in terms of the new set of coordinates (ξ,ζ) defined in Figure 7, after multiplication by $\cos\beta$ and $\sin\beta$, respectively, as

$$\frac{\partial^2 V}{\partial z^2} = \frac{Re}{2h} \frac{\partial p_v}{\partial \xi}, \qquad (5\text{-}15)$$

where $V = V(z)$.

Applying the above equation to the usual no-slip boundary condition ($V(0)=0$, $V(h)=0$) yields

$$V(z) = -\frac{Re}{2h} \frac{dp_v}{d\xi} \left(\frac{1}{2} z (h-z) \right). \qquad (5\text{-}16)$$

The relation between the pressure gradient and the total mean flow velocity is important in engineering applications. By integration of the above equation over the entire annular passage, the total mean nondimensional flow velocity, which is of course equal to 1 (approximately), is expressed in terms of the viscous perturbation pressure gradient. Hence,

$$\int_0^h \int_0^{2\pi} (1+z) \, V(z) \cos\beta \, dz d\theta = \pi \left((1+h)^2 - 1 \right), \qquad (5\text{-}17)$$

and then under consideration of the narrowness of the annular clearance ($h<<1$), substituting equation (5-16) into the above equation, evaluating the integral and simplifying yield

$$\frac{dp_v}{d\xi} = -\frac{24}{h}\frac{1}{Re} \tag{5-18}$$

From the relationship between the shear forces and the velocity profile for the case of laminar flow as an Newtonian fluid, the tangential viscous stress on the flexible centre-body surface is expressed as

$$\tau = \mu \frac{U_o^*}{a}\frac{\partial V}{\partial z}\Big|_{z=0} = -\frac{12}{Re}\rho_f U_o^{*2}. \tag{5-19}$$

This shear stress is not dependent on time and is, in magnitude, a little larger than that for a steady and fully developed annular flow having the same geometry and the same total mean flow velocity [27]. This means that the velocity variation in the radial direction is larger than that of the steady annular flow. This difference may be due to the motion of the flexible centre-body. The shear stress acting on the flexible centre-body surface may be separated into two parts, the circumferential and axial components (τ_θ and τ_x), as follows:

$$\begin{aligned} \tau_x &= \tau \cos\beta \approx \tau, \\ \tau_\theta &= \tau \sin\beta, \end{aligned} \tag{5-20}$$

where β is a function of axial position along the flexible centre-body, as given by equation (5-17).

The viscous fluid-dynamic forces acting on the flexible centre-body depend on the circumferential and axial components of the shear stress and the viscosity-related pressure component. The longitudinal and normal frictional forces acting on the flexible centre-body per unit length are given by integrating equation (5-20), as follows:

$$\begin{aligned} F_{vL} &= \int_0^{2\pi} \tau_x \, a \, d\theta, \\ F_{vN} &= -\int_0^{2\pi} [\tau_\theta \sin\theta + \rho_f U_o^{*2} p_v \cos\theta] \, a \, d\theta. \end{aligned} \tag{5-21}$$

Thus, the longitudinal friction force is easily obtained by substituting equation (5-20) as

$$F_{vL} = \frac{24}{Re} \pi \rho_f a U_o^{*2}. \qquad (5\text{-}22)$$

However, some manipulation is required to bring p_v, which is an implicit function of θ, into a convenient form. In this respect, $p_v \cos\theta$ is modified as

$$p_v \cos\theta = \frac{d}{d\theta}(p_v \sin\theta) - \frac{dp_v}{d\theta} \sin\theta \ . \qquad (5\text{-}23)$$

The integral of the first term of the right-hand side in the above equation over the domain is equal to zero; hence, the equation of normal frictional force is modified as follows:

$$F_{vN} = -2\rho_f U_o^{*2} a \int_0^{2\pi} \left(\frac{12}{Re} \sin\theta \sin\beta - \frac{dp_v}{d\xi} \frac{d\xi}{d\theta} \sin\theta \right) d\theta. \qquad (5\text{-}24)$$

Then, with aid of Figure 7, the derivative of ξ, with respect to θ, may be written as

$$\frac{d\xi}{d\theta} = -\ell X \sin\beta \frac{\partial\beta}{\partial\theta} + r \sin\beta + r\beta \cos\beta \frac{\partial\beta}{\partial\theta} \ , \qquad (5\text{-}25)$$

in the vicinity of a point on the surface. Applying equation (5-11) and (5-13) to the above equation, under the consideration of small β and $r \to 1$, yields

$$\frac{d\xi}{d\theta} = \sum_{\kappa} \frac{a_\kappa}{\ell U_o h} \left(f_{T\kappa} W_{T\kappa} + f_{H\kappa} W_{H\kappa} \right) r \sin\theta \ e^{i\omega t}. \qquad (5\text{-}26)$$

Finally, substituting the above equation into equation (5-24) and then integrating over the domain, the normal frictional force acting on the flexible centre-body is expressed as

$$F_{vN} = -\rho_f U_{ref}^2 a\pi \ P_{vN}(X) \ e^{i\omega t}, \qquad (5\text{-}27)$$

where

$$P_{vN} = U_o \left(\frac{1}{\ell}\right) \frac{12}{Re} \frac{2+h}{h^2} \sum_{\kappa} a_\kappa \left(f_{T\kappa} W_{T\kappa} + f_{H\kappa} W_{H\kappa} \right).$$

Taking account of equations (3-25), (3-26) and (3-28), it is possibe to define P_{vN} as

$$P_{vN} = i\omega P_{1\kappa vN}(X) + P_{0\kappa vN}(X) , \qquad (5\text{-}28)$$

where $P_{1\kappa vN}$ and $P_{0\kappa vN}$ are determined in the next chapter. Hence, the normal frictional force, derived from the normal shear stress and the viscous perturbation pressure, comprises the unsteady viscous effect, as discussed before.

The unsteady and steady effects, arising from the longitudinal and axial frictional forces, respectively, will be considered in the analysis of the stability of the system at hand in the next chapter.

CHAPTER VI

VISCOUS EFFECTS ON THE DYNAMICS AND STABILITY OF THE FLEXIBLE CENTRE-BODY

6.1 FORMULATION OF EIGENVALUE PROBLEM OF THE SYSTEM CONSIDERING UNSTEADY VISCOUS EFFECTS

The normal frictional force, derived from the normal shear stress and viscous perturbation pressure, will generate unsteady viscous effects on the system, according to equations (5-27) and (5-28). From these equations, which were derived for the system under consideration and with the aid of a reasonable set of assumptions (i.e., small amplitude motion of the flexible centre-body in a narrow annular passage), we shall now proceed with the determination of the fluid-dynamic damping and stiffness matrices of the system by means of Galerkin's method.

In the present analysis, considering the equation of motion of the flexible centre-body, expressed by equation (2-1), and then subtracting the terms associated with the flexural restoring and the inertia force from the result, the fluid-dynamic damping and stiffness terms arising from the unsteady viscous force are obtained.

For that purpose, the equation of motion of the flexible centre-body, subjected to the unsteady potential and viscous forces, may be expressed as follows;

$$EI \frac{\partial^4 e_o^*}{\partial x^{*4}} + \rho_s A_s \frac{\partial^2 e_o^*}{\partial t^{*2}} = F_p(x^*, t^*) + F_{vN}(x^*, t^*). \qquad (6\text{-}1)$$

Substituting equation (2-3) into the above equation, the equation of motion could be re-written in dimensionless form as

$$\frac{\partial^4 e_o}{\partial X^4} + \frac{\partial^2 e_o}{\partial t^2} = \frac{\ell^{*4}}{aEI} [F_p(X,t) + F_{vN}(X,t)]. \qquad (6\text{-}2)$$

Now, taking account of equations (4-2) and (5-27) and then using the same method as in chapter II, based on Galerkin's method (see equation (2-15)), the following equation may be obtained:

$$\sum_{\kappa} a_{\kappa}\int_0^1 \{ -\omega^2[E_{\kappa}(X) + \sigma P_{2\kappa p}(X)] + i\omega\,\sigma[P_{1\kappa p}(X) + P_{1\kappa vN}(X)] + [\beta_{\kappa}^4 E_{\kappa}(X) + \sigma(P_{0\kappa p}(X) + P_{0\kappa vN}(X))]\} E_j(X)\,dX = 0, \quad (6\text{-}3)$$

where $P_{1\kappa vN}$ and $P_{0\kappa vN}$ are the amplitudes of the nondimensional fluid-dynamic damping and stiffness terms, respectively, which are defined in equation (5-28); it is also recalled that $\sigma=(\rho_f/\rho_s)\cdot(\pi\ell^{*2}/A_s)$. Hence, the terms associated with the unsteady force may be expressed as

$$\sum_{\kappa} a_{\kappa} \int_0^1 \sigma \left(i\omega P_{1\kappa vN}(X) + P_{0\kappa vN}(X) \right) \left(E_{Tj} + E_{Hj} \right) dX, \quad (6\text{-}4)$$

where

$$i\omega P_{1\kappa vN}(X) + P_{0\kappa vN}(X) = U_o \frac{1}{\ell} \frac{12}{Re} \frac{2+h}{h^2} \sum_{\kappa} a_{\kappa}(f_{T\kappa}W_{T\kappa} + f_{H\kappa}W_{H\kappa}), \quad (6\text{-}5)$$

which can be derived from equations (5-27) and (5-28).

The next step is to determine $P_{1\kappa vN}$ and $P_{0\kappa vN}$ from the above equations. Before doing that, considering equations (3-25 to 3-28), it is necessary to divide $f_{T\kappa}$ and $f_{H\kappa}$ into two terms for future use as follows:

$$\begin{aligned} f_{T\kappa} &= G_{T\kappa} [\, i\omega\, E_{T\kappa}(X) + \bar{U}(X)U_o E_{T\kappa}'(X) \,], \\ f_{H\kappa} &= G_{H\kappa} [\, i\omega\, E_{H\kappa}(X) + \bar{U}(X)U_o E_{H\kappa}'(X) \,], \end{aligned} \quad (6\text{-}6)$$

where $\bar{U}(X)\simeq 1$ in the present analysis. Thus, substituting into equation (6-5) yields

$$\begin{aligned} P_{1\kappa vN} &= U_o \frac{1}{\ell} \frac{12}{Re} \frac{2+h}{h^2} \sum_{\kappa} a_{\kappa} [G_{T\kappa}W_{T\kappa}E_{T\kappa}(X) + G_{H\kappa}W_{H\kappa}E_{H\kappa}(X)], \\ P_{0\kappa vN} &= U_o^2 \frac{1}{\ell} \frac{12}{Re} \frac{2+h}{h^2} \sum_{\kappa} a_{\kappa} [G_{T\kappa}W_{T\kappa}E_{T\kappa}'(X) + G_{H\kappa}W_{H\kappa}E_{H\kappa}'(X)], \end{aligned} \quad (6\text{-}7)$$

where $W_{T\kappa}$ and $W_{H\kappa}$, given in equation (5-14), are not functions of X.

Finally, substituting equation (6-7) into equation (6-4) and then considering the relationship between equation (2-15) and equation (2-16), the elements of fluid-dynamic damping and stiffness matrices due to the unsteady viscous force are given by

$$c_{j\kappa uv} = U_o \frac{1}{\ell} \frac{12}{Re} \frac{2+h}{h^2} \sigma \left[G_{T\kappa} W_{T\kappa} I_T + G_{H\kappa} W_{H\kappa} I_H \right],$$

$$k_{j\kappa uv} = U_o^2 \frac{1}{\ell} \frac{12}{Re} \frac{2+h}{h^2} \sigma \left[G_{T\kappa} W_{T\kappa} I_T' + G_{H\kappa} W_{H\kappa} I_H' \right], \qquad (6\text{-}8)$$

where I_T, I_H, I_T' and I_H', defined in equations (4-7d), are numerically determined and the results are given in Appendix C; the suffix "uv" stands for the "unsteady viscous" components of the corresponding matrix. Here, the first and second terms of the numerator, 2+h, may be associated with the viscous perturbation pressure and the shear stress, respectively. Furthermore, the two terms within the brackets, which are functions of β, may be related to $\partial e_r^*/\partial t$ for the damping terms and to $U^*(x^*)(\partial e_r^*/\partial x^*)'$ for the stiffness terms, according to the boundary conditions shown in equation (3-16a)

As expected, the unsteady viscous coupling terms are expressed in terms of Re and h. In the above equation, it is expected that the system is influenced by unsteady viscous terms more and more as the annulus becomes narrower; however, the coefficients within the brackets change with h and ℓ (this change, however, may be small as compared with that of $1/h^2$).

6.2 FORMULATION OF THE EIGENVALUE PROBLEM OF THE SYSTEM CONSIDERING STEADY VISCOUS EFFECTS

6.2.1 The Equation of Motion of the Flexible Centre-Body, Influenced by Viscous Forces

As discussed before, small lateral motion of the centre-body is assumed, such that the displacement e_o^* and its derivatives with respect to x^* are small. Thus, the steady effect is represented by the axial viscous stress, taking $\cos\beta \simeq 1$ and $\tau_x = (12/Re)\rho_f U_o^{*2}$. Integrating over the circumference, the longitudinal force, called the steady viscous force, F_{vL}, was obtained in the previous chapter; i.e. $F_{vL} = (24/Re)\pi a U_o^{*2}$. The effects on the fluid-dynamic coupling terms, generated by inviscid and viscous forces (i.e., F_p and F_{vN}), will be also considered in the present section.

The forces acting on a small element, δx^*, of the flexible centre-body, which has undergone a small lateral motion, are shown in Figure 8(a), considering all inviscid, steady and unsteady viscous terms. Force balances, in x^*- and y^*-directions, yield

$$\frac{\partial T}{\partial x^*} + F_{vL} + F_{px} - (F_p + F_{vN}) \frac{\partial e_o^*}{\partial x^*} = 0,$$

$$\frac{\partial Q}{\partial x^*} + F_{py} + F_p + F_{vN} + F_{vL} \frac{\partial e_o^*}{\partial x^*} + \frac{\partial}{\partial x^*}\left(T \frac{\partial e_o^*}{\partial x^*}\right) - m \frac{\partial^2 e_o^*}{\partial t^{*2}} = 0, \qquad (6\text{-}9)$$

where the terms F_{px} and F_{py} were introduced by Paidoussis [12], using the artifice of a "frozen" deformed element immersed totally (i.e., on the all sides) in a fluid of static pressure p and static-pressure gradient $\partial p/\partial x^*$, and Q is the transverse shear force. The forces $F_{px}\delta x^*$ and $F_{py}\delta x^*$, which are like buoyancy forces, are the resultants of the hydrostatic pressure p (and of the pressure drop due to viscosity) acting on the outer surface of the element.

Accordingly, assuming $p \simeq p(x^*)$ is a linear function of x^* (which is reasonable, as the hydrostatic pressure distribution is modified by the frictional pressure drop - see equation (5-

18)), the balance of forces, with aid of Figure 8(b), is given by

$$\left[- \frac{\partial (pA_s)}{\partial x^*} + F_{px} \right] \delta x^* \vec{I} + \left[F_{py} - \frac{\partial}{\partial x^*} \left((pA_s) \frac{\partial e_o^*}{\partial x^*} \right) \right] \delta x^* \vec{J}$$

$$= - \iint_A p \vec{n} \, dA \doteq - \iiint_{vol} \nabla p \, d(vol) = - \frac{\partial p}{\partial x^*} A_s \, \delta x^* \vec{I} , \qquad (6\text{-}10)$$

where $\vec{n}$ is the normal unit vector acting on the surface and "A" and "vol" represent the area and the volume, as domains of integration. Hence,

$$- F_{px} = \frac{\partial p}{\partial x^*} A_s - \frac{\partial (pA_s)}{\partial x^*},$$

$$F_{py} = \frac{\partial}{\partial x^*} \left(pA_s \frac{\partial e_o^*}{\partial x^*} \right) . \qquad (6\text{-}11)$$

In the above equation, it is noted that the term, F_{px} is equivalent, by analogy, to the tension terms acting on the cross-section of the flexible centre-body, and that if $\partial A_s/\partial x^*=0$, then $F_{px}=0$; in this case it is so.

Under consideration of small amplitude motion of the flexible centre-body, if $e_o^* \approx 0(\epsilon)$, then F_p and F_{vN} are of the same order, so that $(F_p+F_{vN})\partial e_o^*/\partial x^* \approx 0(\epsilon^2)$. Now, substituing equation (6-11) into equation (6-9), and retaining terms of $0(\epsilon)$, only yields

$$\frac{\partial T}{\partial x^*} + F_{vL} = 0, \qquad (6\text{-}12a)$$

$$-EI \frac{\partial^4 e_o^*}{\partial x^{*4}} + F_p + F_{vN} + \frac{\partial}{\partial x^*} \left[(T + pA_s) \frac{\partial e_o^*}{\partial x^*} \right] + F_{vL} \frac{\partial e_o^*}{\partial x^*} - m \frac{\partial^2 e_o^*}{\partial t^{*2}} = 0, \qquad (6\text{-}12b)$$

where the fact that $Q = - \frac{\partial}{\partial x^*} \left(EI \frac{\partial^2 e_o^*}{\partial x^{*2}} \right)$ has been utilized, and EI, in this case, is constant with x^*. For convenience, equation (6-12a) may be re-written as

$$\frac{\partial}{\partial x^*} (T + pA_s) + F_{vL} - \frac{\partial p}{\partial x^*} A_s = 0. \qquad (6\text{-}13)$$

For future purposes, integrating the above equation from 0 to x^* and from x^* to ℓ^*, the following equations are obtained, respectively,

$$(T + pA_s) - (T + pA_s)_0 + \int_0^{x^*} F_{vL}\, dx^* - \frac{\partial p}{\partial x^*} A_s x^* = 0, \qquad (6\text{-}14a)$$

$$(T + pA_s)_{\ell^*} - (T + pA_s) + \int_{x^*}^{\ell^*} F_{vL}\, dx^* - \frac{\partial p}{\partial x^*} A_s(\ell^* - x^*) = 0, \qquad (6\text{-}14b)$$

since, $\partial p/\partial x^*$ is constant with x^*; in these equations, the subscripts "0" and "ℓ^*" represent the quantities in brackets "at $x^*=0$" and "at $x^*=\ell^*$", respectively, Here, taking into account equations (5-1) and (5-18), the static pressure drop may be taken as

$$\frac{\partial p}{\partial x^*} \approx \frac{\partial p_v}{\partial \xi} \frac{\rho_f U_o^{*2}}{a} = -\frac{24}{ah} \frac{1}{Re} \rho_f U_o^{*2}, \qquad (6\text{-}15)$$

which is obviously constant for a system with given geometry and system parameters (i.e., a, h, μ, U_o^{*2}). Thus, substituting equations (6-14a,b), respectively, into equation (6-12b), the equation of motion of the flexible centre-body is expressed by either of the following two equations:

$$EI \frac{\partial^4 e_o^*}{\partial x^{*4}} - \left[(T + pA_s)_0 + \frac{\partial p}{\partial x^*} A_s x^* - \int_0^{x^*} F_{vL}\, dx^* \right] \frac{\partial^2 e_o^*}{\partial x^{*2}} - \frac{\partial p}{\partial x^*} A_s \frac{\partial e_o^*}{\partial x^*} + m \frac{\partial^2 e_o^*}{\partial t^{*2}} = F_p + F_{vN}, \qquad (6\text{-}16a)$$

$$EI \frac{\partial^4 e_o^*}{\partial x^{*4}} - \left[(T + pA_s)_{\ell^*} - \frac{\partial p}{\partial x^*} A_s(\ell^* - x^*) + \int_{x^*}^{\ell^*} F_{vL}\, dx^* \right] \frac{\partial^2 e_o^*}{\partial x^{*2}} - \frac{\partial p}{\partial x^*} A_s \frac{\partial e_o^*}{\partial x^*} + m \frac{\partial^2 e_o^*}{\partial t^{*2}} = F_p + F_{vN}. \qquad (6\text{-}16b)$$

The next step is to consider three cases of axial (physical and fluid-static) boundary conditions, shown in Figure 9; i.e.,

a) case I : totally clamped upstream, but axially sliding at downstream end;

b) case II : axially sliding at upstream end, and totally clamped downstream;

c) case III: both ends absolutely clamped.

Of course, the flexible centre-body is subject to boundary conditions appropriate to an Euler-Bernoulli beam, as shown in equation (2-2).

Considering a slice of the beam at the downstream end of the beam (for case I) or at the upstream end (for case II), it is evident that the combined pressure-tension force at that end is zero; i.e , $(T+pA_s)=0$ at $x^*=\ell^*$ for case I or $(T+pA_s)=0$ at $x^*=0$ for case II, neglecting any "form" (or base) drag (if "guarded" by a rigid body at that end).

On the other hand, the situation is different for case III, which is case where the total length of the flexible centre-body remains constant between fixed supports. There is also a compressive load due to radial contraction, arising via the Poisson-ratio effect; for a thin tubular beam, this is equal to $-2\nu(pA_s)$. This will be found to be negligible later for $pA_s\ell^{*2}<<EI$, but this will come out naturally. Since the total extension of the beam in case III due to the tension is zero at $x^*=\ell^*$, T_{ℓ^*} is obtained easily, as follows:

$$\int_0^{\ell^*} T\, dx^* = \int_0^{\ell^*} \left(T_L + F_{vL}\,(\ell^* - x^*) \right) dx^*$$

$$= T_L\ell^* + F_{vL}\ell^{*2} - \tfrac{1}{2} F_{vL}\ell^{*2} = 0, \qquad (6\text{-}17)$$

where F_{vL} is introduced in equation (5-22), which is obviously constant with x^*. Hence,

$$T_0 = \tfrac{1}{2} F_{vL}\ell^*,$$

$$T_{\ell^*} = -\tfrac{1}{2} F_{vL}\ell^*. \qquad \text{for case III} \quad (6\text{-}18)$$

Thus, taking account of the relationships mentioned

above, it is convenient to modify equations (6-16a,b) for each case, as follows:

(a) for case I

$$EI \frac{\partial^4 e_o^*}{\partial x^{*4}} - \left[- \frac{\partial p}{\partial x^*} A_s (\ell^* - x^*) + \int_{x^*}^{\ell^*} F_{vL}\, dx^* \right] \frac{\partial^2 e_o^*}{\partial x^{*2}}$$

$$- \frac{\partial p}{\partial x^*} A_s \frac{\partial e_o^*}{\partial x^*} + m \frac{\partial^2 e_o^*}{\partial t^{*2}} = F_p + F_{vN}; \qquad (6\text{-}19a)$$

(b) for case II

$$EI \frac{\partial^4 e_o^*}{\partial x^{*4}} - \left[\frac{\partial p}{\partial x^*} A_s x^* - \int_0^{x^*} F_{vL}\, dx^* \right] \frac{\partial^2 e_o^*}{\partial x^{*2}}$$

$$- \frac{\partial p}{\partial x^*} A_s \frac{\partial e_o^*}{\partial x^*} + m \frac{\partial^2 e_o^*}{\partial t^{*2}} = F_p + F_{vN}; \qquad (6\text{-}19b)$$

(c) for case III

$$EI \frac{\partial^4 e_o^*}{\partial x^{*4}} - \left[\frac{1}{2} F_{vL} \ell^* + \frac{\partial p}{\partial x^*} A_s x^* - \int_0^{x^*} F_{vL}\, dx^* \right] \frac{\partial^2 e_o^*}{\partial x^{*2}}$$

$$-(1 - 2\nu)\bar{p} A_s \frac{\partial^2 e_o^*}{\partial x^{*2}} - \frac{\partial p}{\partial x^*} A_s \frac{\partial e_o^*}{\partial x^*} + m \frac{\partial^2 e_o^*}{\partial t^{*2}} = F_p + F_{vN}. \qquad (6\text{-}19c)$$

Clearly all three equations (6-19a,b,c) may be written as one; thus, substituting equations (6-15) and (5-22) into the above equations yields

$$EI \frac{\partial^4 e_o^*}{\partial x^{*4}} + \frac{24}{Re} \pi \left(1 + \frac{1}{h}\right) \rho_{fa} U_o^{*2} \left[x^* - \left(1 - \frac{1}{2}\delta\right) \ell^* \right] \frac{\partial^2 e_o^*}{\partial x^{*2}}$$

$$-(1 - 2\nu)\delta(2 - \delta)\bar{p} A_s \frac{\partial^2 e_o^*}{\partial x^{*2}} + \frac{24}{Re} \pi \frac{1}{h} \rho_f U_o^{*2} \frac{\partial e_o^*}{\partial x^*} + m \frac{\partial^2 e_o^*}{\partial t^{*2}}$$

$$= F_p + F_{vN} \qquad (6\text{-}20)$$

where

		upstream end	downstream end
$\delta = 0$	for case I	(totally clamped,	clamped-sliding)
$\delta = 2$	for case II	(clamped-sliding,	totally clamped)
$\delta = 1$	for case III	(totally clamped,	totally clamped)

It is important to notice that the second term in the above equation is positive; this is as it should be, as the beam is under compression, increasing linearly with x^* for case II; however, for case I(δ=0) it becomes negative, the beam being under tension, decreasing linearly with x^*. It is also noted that the existence of the third term depends on whether the length, ℓ^*, is fixed, as in case III, or not

6.2.2 Nondimensionalization and Formulation of the Eigenvalue Problem, using Galerkin's Method

Before proceeding with the analysis, the equation of motion will be rendered dimensionless by introducing the nondimensional parameters, defined in equations (2-3) Recalling those nondimensional parameters and σ defined in equation (2-11), equation (6-20) is re-written in nondimensional form as

$$\frac{\partial^4 e_o}{\partial X^4} + \frac{24}{Re}\left(1 + \frac{1}{h}\right)\sigma U_o^2 \frac{1}{\ell}\left[X - \left(1 - \frac{1}{2}\delta\right)\right]\frac{\partial^2 e_o}{\partial X^2}$$

$$-(1-2\nu)\delta(2-\delta)\,\Pi\,\frac{\partial^2 e_o}{\partial X^2} + \frac{24}{Re}\frac{1}{h}\sigma U_o^2 \frac{1}{\ell}\frac{\partial e_o}{\partial X} + \frac{\partial^2 e_o}{\partial t^2}$$

$$= -\frac{\ell^{*4}}{aEI}\left(F_p + F_{vN}\right), \qquad (6\text{-}21)$$

where

$$\Pi = \frac{\bar{p}A_s \ell^{*2}}{EI};$$

it is recalled that (1+1/h) is the same as (1+D/D_H), D_H being the hydraulic diameter.

Now, considering the terms associated with steady viscous forces by means of Galerkin's method, introduced in chapter II and IV, the elements of the fluid-dynamic stiffness generated by steady viscous forces are given by

$$k_{j\kappa sv} = -\frac{24}{Re}\sigma U_o^2 \frac{1}{\ell}\left[\frac{D}{D_H}\left(I_T' + I_H'\right) + \left(1 + \frac{D}{D_H}\right)\beta_\kappa^2\left(\left(1 - \frac{1}{2}\delta\right)\left(I_T - I_H\right)\right.\right.$$

$$\left.\left. + \left(I_{XH} - I_{XT}\right)\right)\right] + (1-2\nu)\delta(2-\delta)\Pi\,\beta_\kappa^2\left(I_T - I_H\right), \qquad (6\text{-}22)$$

where

$$I_{XT} = \int_0^1 (E_{T\kappa}E_{Tj} + E_{T\kappa}E_{Hj})X \, dX,$$

$$I_{XH} = \int_0^1 (E_{H\kappa}E_{Tj} + E_{H\kappa}E_{Hj})X \, dX,$$

and I_T, I_H, I_T', I_H' and I_p, represented by equation (4-7d), are less than unity. In the above equation, the subscript "sv" represents the "steady viscous" components of the matrix.

In order to evaluate the fluid-dynamic effects acting on the flexible centre-body in real flow, it is obviously necessary to add the steady and unsteady viscous coupling terms, represented by equations (6-8) and (6-22), to the equivalent inviscid terms, represented by equations (4-6b,c), respectively. Hence, the elements of [M], [C] and [K] are given by

$$\begin{aligned} m_{j\kappa} &= m_{pj\kappa}, \\ c_{j\kappa} &= c_{pj\kappa} + c_{j\kappa uv}, \\ k_{j\kappa} &= k_{pj\kappa} + k_{j\kappa uv} + k_{j\kappa sv}, \end{aligned} \tag{6-23}$$

where the inviscid terms, expressed by subscript "p", are given in equation (4-7a,b,c). From the above equations, it is obvious that the virtual mass is not affected by viscous forces (which should be the case) and that the damping coeffient is not influenced by steady viscous force.

Considering equations (4-6), (6-8) and (6-22), it is noted that the potential and the viscous coupling terms are, explicitly, functions of $1/\ell^2$ and $1/\ell$; respectively (except for case III); thus, it is obvious that, when the length ratio increases, the steady and unsteady viscous effects on the system become larger, as compared to the potential terms; also the mean static pressure effects, for case III, become larger.

6.3 DYNAMICS AND STABILITY OF THE FLEXIBLE CENTRE-BODY IN VISCOUS FLOW

The purpose of this section is to illustrate the general dynamical behaviour of the system, as influenced by the viscous forces determined in chapter V. For that purpose, fluids having high viscosity are chosen in some of the caculations, to accentuate the effect.

In all of the calculations to be presented, the inviscid fluid-dynamic coefficients are obtained by rigorous solution (chapter III), but the viscous ones are only given approximately, shown in chapter V for convenience and simplicity; however, it should be emphasized by the author at this point that, as will be seen later, the approximate solution is good enough for evaluating the viscous effects acting on the system.

In the present analysis, rather than attempting an exhaustive parametric study, the calculations have been conducted according to the annular gap width; so called 3/40, 1/10 and 3/20 gap oil-rubber systems (h=0.075, 0.1 and 0.15). As the wording implies, the flexible centre-body is considered to be made of rubber (U_{ref}=1.198 m/s) and the fluid is taken to be oil (μ=0.007 Pa•s). In order to investigate the unsteady viscous effect, calculations are done with unsteady viscous term included and excluded (potential flow) and the results compared. Then, calculations are done with all viscous forces and the results are compared with those in the previous calculations. In order to evaluate, specfically, the effect of viscosity of fluid, another 1/10 gap oil-rubber system considering the inviscid and unsteady viscous effects is investigated with a viscosity, μ=0.014 Pa•s, higher than the one (μ=0.007 Pa•s) mentioned above, and then the result is compared with the corresponding one (μ=0.007 Pa•s, 1/10 annular gap).

In general, it is impossible to assess the stability of a continuous system directly by considering the dimensionless

damping and stiffness coefficients. Neverthless, considering the orders of magnitude of the equations (6-8) and (6-22), it is possible to expect that the system should be influenced by the unsteady viscous forces more and more when the annulus becomes narrower, as discussed in section 6.1.

Effect of increasing flow velocity

The dynamical behaviour of the system with increasing flow velocity will be discussed by means of an illustrating example, as mentioned before. The dimensionless complex eigenfrequencies, ω, which are expressed in terms of $Im(\omega)$ and $Re(\omega)$, of the lowest three modes (n=5) of the oil-rubber system are plotted versus nondimensional flow velocity U_{01}. Here, if the imaginary part of ω, $Im(\omega)$, is positive, motions will be damped, while if $Im(\omega)<0$, motions will be amplified; i.e., the system will be unstable.

The effects of unsteady viscous forces on the 0.075 gap system, which is compared with the results obtained by inviscid theory, are shown in Figure 10. Of course, the results taking unsteady effects into account include the inviscid effects.

At lower flow velocity, the system is influenced by the unsteady viscous damping coefficient, which is constant with flow velocity. Of course, this behaviour did not appeare in the results by potential flow theory -- the "damping" coefficient of the inviscid force is really a Coriolis effect and it has no effect on system behaviour before divergence. As shown in the Figure, the effects of unsteady viscous forces are primarily to diminish $Re(\omega)$ and to produce $Im(\omega)>0$. These effects are represented by P-V in Figures 10(a) and (b).

As flow velocity increases, the first mode eigenfrequency vanishes at point a, and the locus of $Im(\omega)$ bifurcates. But the two branches of the locus coalesce at point b, without ever reaching a negative value. From this result, it is recognized that first mode buckling, which was shown to occur

in case of inviscid flow, does not appear in the case of this viscous flow. However, the cylinder becomes unstable in its second mode at much higher velocity, fluttering at point C' (in the case of inviscid flow, the onset of coupled-mode flutter occurs at point C). And then, the system regains stability in its second mode at point D'. However, the system may lose stability again by buckling in its second mode, when flow velocity increases further; i.e., at point E'.

Further rise of the flow velocity causes the system to flutter in the third mode at a flow velocity higher than that required for the corresponding flutter in inviscid flow. Here, the third-mode flutter is of no particular interest for the following reasons: (i) the value of $Im(\omega)$ of the second mode still remains negative, since the system already lost stability at lower flow velocity; (ii) the validity of the result is questionable at such high flow velocities, since the flow is turbulent there.

Interestingly, coupled-mode flutter (i.e., between the first and second modes or the third and fourth modes in the case of inviscid flow) does not appear in the case of this viscous flow, as can be seen in Figure 10.

The overall dynamical behaviour of the 0.075 gap oil-rubber systems, considering the steady viscous effects as well, is shown in Figure 11, according to end conditions corresponding to cases I, II and III (see Figure 9). Here, in order to evaluate the mean static pressure effect, two different systems (with Π=5 and Π=50) are considered. As expected, the steady viscous effect on the system is smaller than the inviscid and unsteady viscous effects; but, it should be considered in real problems. Except for case II, the steady viscous effect stabilizes the system; moreover, the system in case I becomes unstable by second mode buckling, so that the critical flow velocity is much higher than those for the other cases. These results also suggest that the system is stabilized by increasing the mean static pressure calculated

from Π; but, this effect, even for Π=50, is very small for the system presented here (ℓ=20).

Table 3 Comparison of the nondimensional critical flow velocities obtained by the potential flow and viscous flow theories of Sections III and V [ℓ^*/a=20, H^*/a=0.075, σ=323.74 and U_{refl}=1)3316m/s]

Unsteady Potential Flow Theory				
	1st mode buckling		coupled-mode flutter (1st and 2nd mode)	
	onset A	restabiliza- B (tion	onset C	restabiliza- D (tion
	1.837	2.762	3.030	4.101

Unsteady Viscous Flow Theory (μ=0.007 Pa•s)					
	1st mode buckling		2nd mode flutter		2nd mode buckling
	onset A′	restabiliza- B′ (tion	onset C′	restabiliza- D′ (tion	onset E′
unsteady viscous effects included:	no buckling		3.342	3.735	4.232
steady and unsteady viscous effects included:					
case I	no buckling		no flutter		4.537
case II	no buckling		2.967	3.532	3.960
case III (Π=5)	no buckling		3.346	3.739	4.244
case III (Π=50)	no buckling		3.409	3.766	4.279

In order to evaluate the viscous effect more easily, the nondimensional flow velocity of the critical points, shown in Figure 10, are tabulated in Table 3. Considering this Table and the corresponding Figure, it is expected that the system for case III with a low mean static pressure is not nearly influenced by the steady viscous effect and the system, for case I, is more stable.

Table 4 Comparison of the nondimensional critical flow velocities obtained by the potential flow and viscous flow theories of Sections III and V [ℓ^*/a=20, H^*/a=0.1, σ=323.74 and U_{ref1}=1.3316m/s]

Unsteady Potential Flow Theory				
	1st mode buckling		coupled-mode flutter (1st and 2nd mode)	
	onset A	restabiliza- B (tion	onset C	restabiliza- D (tion
	2.133	3.208	3.505	4.757

Unsteady Viscous Flow Theory (μ=0.007 Pa•s)				
	1st mode buckling		2nd mode flutter	
	onset A'	restabiliza- B' (tion	onset C'	restabiliza- D' (tion
unsteady viscous effects included:	2.291	2.997	3.558	4.690
steady and unsteady viscous effects included:				
case I	2.492	3.170	3.798	4.915
case II	2.096	2.844	3.328	4.476
case III (Π=10)	2.302	3.014	3.570	4.700
case III (Π=50)	2.371	3.057	3.623	4.737

The same analysis has been performed for the cases of the 0.1 gap and 0.15 gap oil-rubber systems (see Figures 12-15). The general dynamic behaviour of these two systems is qualitatively the same; however, it is different in the former case (h=0.075). As expected through inspection of equations (6-8), the unsteady damping effect, which can be represented by P-V in the Figures, is decreased with increasing h and each of these two systems buckles at point A' in its first mode; accordingly, the critical flow velocities are decreased dramatically as compared with former case (h=0.075).

The nondimensional flow velocities of the points shown in Figures 12-15, where the points A and A' represent the non-

dimensional critical flow velocities for both inviscid and viscous flow theory, are given in Table 4, for the 0.1 gap system, and in Table 5, for the 0.15 gap system. By inspection of the Tables and corresponding Figures, the range of the first mode buckling region represented by A'-B' and of the second fluttering region represented by C'-D', with respect to the corresponding region of inviscid flow, are decreased with increasing annular gap. It is also predicted that the stability behaviour is governed by the inviscid fluid-dynamic forces more and more, when the annulus becomes larger; however, viscous effects are taken into account.

Table 5 Comparison of the nondimensional critical flow velocities obtained by the potential flow and viscous flow theories of Sections III and V [ℓ^*/a=20, H^*/a=0.15, σ=323.74 and U_{refl}=1.3316m/s]

Unsteady Potential Flow Theory				
	1st mode buckling		coupled-mode flutter (1st and 2nd mode)	
	onset A	restabiliza- B (tion	onset C	restabiliza- D (tion
	2.639	3.968	4.307	5.875

Unsteady Viscous Flow Theory (μ=0.007 Pa·s)				
	1st mode buckling		2nd mode flutter	
	onset A'	restabiliza- B' (tion	onset C'	restabiliza- D' (tion
unsteady viscous effects included:	2.661	3.939	4.302	5.866
steady and unsteady viscous effects included:				
case I	2.785	4.075	4.471	6.028
case II	2.538	3.810	4.149	5.709
case III (Π=5)	2.668	3.947	4.315	5.872
case III (Π=50)	2.757	4.013	4.388	5.924

Effect of the relative annular gap

Considering the difference in behaviour noted above and recalling the results of the former case (h=0.075), it is noted that the stabilizing influence of the viscous effects increases with diminishing h at a higher rate, to overcome the destabilizing influence of the inviscid effects, at least for this range of h; furthermore, it is suggested that for a system of a much lower annular gap than those analyzed here, the eigenfrequency, $Re(\omega)$, of the first mode may become zero and the locus of the first mode may be bifurcated at lower flow velocity. Accordingly, it is expected that the system does not lose stablity by second mode flutter; but the cylinder buckles in the second mode at higher flow velocity, which is equivalent to point E' of Figure 10(b).

The typical variation with the relative gap of the lowest critical flow velocity at which the system loses stability is shown in Table 6.

Table 6 Influence of the relative gap H^*/a on the lowest critical flow velocity at instability threshold (unsteady viscous flow theory)
[ℓ^*/a=20, σ=323.74, μ=0.007 Pa·s and U_{refl}=1.3316m/s]

(a) unsteady viscous effects included

H^*/a	Type of instability	Critical flow velocity U_{olcr}
0.075	2nd mode flutter	3.343
0.1	1st mode buckling	2.291
0.15	1st mode buckling	2.661

(b) unsteady and steady viscous effects included

H^*/a	Case	Type of instability	Critical flow velocity U_{olcr}
0.075	I	2nd mode buckling	4.537
	II	2nd mode flutter	2.967
	III(Π-5)	2nd mode flutter	3.346
	III(Π-50)	2nd mode flutter	3.409
0.1	I	2nd mode flutter	2.492
	II		2.096
	III(Π-5)		2.302
	III(Π-50)		2.371

Effect of the fluid viscosity

The dynamical behaviour of the 0.1 gap oil-rubber system considering the inviscid and unsteady viscous effects with μ=0.014 Pa•s is presented in Figure 16. The general dynamical behaviour of this system is then compared to that for μ=0.007 Pa•s and the same relative gap, shown in Figure 12. The influence of the fluid viscosity, μ on the lowest critical flow velocity at instability threshold is shown in Table 7.

Table 7 Influence of the fluid viscosity μ on the lowest critical flow velocity at instability threshold (unsteady viscous effects included)
[ℓ^*/a=20, H^*/a=0.1, σ=323.74, U_{ref1}=1.3316m/s]

μ pa•s	Type of instability	Critical flow velocity U_{olcr}
0*	1st mode buckling	2.291
0.007	1st mode buckling	2.661
0.014	2nd mode flutter	3.819

* potential flow theory

Finally, considering all the above, it is also of interest to remark that viscous effects on the dynamics of the system increase with decreasing the annular gap; the results obtained with decreasing the annular gap are, qualitatively, similar to those obtained with increasing the viscosity of the fluid. Moreover, it is not surprising that the viscous terms of the equation of motion for a narrow annular flow have a profound effect on the dynamical behaviour of the clamped-clamped beam, while having a minor effect for unconfined flow.

The overall dynamic behaviour of the system, illustrated above, is influenced much more by the unsteady viscous terms than by the steady viscous terms, particularly by the unsteady viscous damping term.

CHAPTER VII
CONCLUSIONS

7.1 GENERAL CONCLUSIONS AND DISCUSSION

This thesis has dealt with the dynamics of the flexible centre-body in very narrow annular flow. Its main aim was to evaluate the inviscid and viscous effects on the dynamical behaviour of the system and, especially, on its stability. In this paper, a rigorous method based on potential flow theory and an approximate method for viscous flow have been developed.

The inviscid fluid-dynamic force was derived under the assumptions of small amplitude motion of the flexible centre-body and a very narrow annulus, based on potential flow theory. The analytical model for viscous flow has been developed using a simplfied form of the Navier-Stokes and continuity equations and necessary boundary conditions.

System eigenfrequencies have been calculated while varying (i) the density of fluid and (ii) the annular gap ratio for inviscid flow; for viscous flow calculations were conducted while varying (i) the annular gap ratio, (ii) the viscosity of fluid and (iii) the axial (physical and fluid-static) boundary conditions (see Figure 9). In all cases, the flexible centre-body was taken to be clamped at both extremities, so that, apart from the unsteady viscous forces, the system is in the category of gyroscopic conservative dynamical systems.

In general, the stability characteristics of the system, being determined by the fluid dynamic forces acting on the flexible centre-body, are intimately related to the hydro-dynamic or "virtual" mass of the fluid, which in turn controls the natural frequencies of the system at zero flow velocity: the higher the virtual mass, the lower are the natural frequencies at zero flow velocity. Moreover, it has been known that the virtual mass becomes large with decreasing the

annular gap for confined flow. Thus, the instabilities of the system for confined flow occur at lower flow velocities, but the fundamental nature of stability behaviour is not altered vis-à-vis that of unconfined flow.

In general, it is known that for sufficiently high flow velocity, divergence and flutter are possible in various models. e.g, although the system for confined flow loses stability by divergence, in principle, it could also subject to coupled-mode flutter - by coalescence of two modes in complex frequency. Now, the question arises as to the pertinence of all this complex dynamical behaviour of the real system (see, for example, Figures 2, 3, 10) beyond the critical flow velocity. Strictly speaking, linear theory is only capable of yielding the critical flow velocity where the system first loses stability, and is generally unable to predict postcritical behaviour. Neverthless, it has been shown that, in some cases, it is also capable of predicting the post-critical dynamical behaviour of the system (see, for example, refs. 8 and 12). A similar capability will be presumed to exist here also.

Both qualitative and quantitative aspects of the results obtained in Figures 2 to 6 and in Tables 1 and 2 having been discussed in fair detail already (chapter IV), only some general conclusions, for inviscid flow first, will be presenred here, as follows:

(a) the flexible centre-body becomes unstable by first-mode buckling;

(b) the system is generally subject to both divergence and coupled-mode flutter;

(c) the restabilization of the system in its first mode, prior to the onset of coupled-mode flutter, depends on the $(M/m)^{\frac{1}{2}}$ which is associated with the Coriolis force;

(d) the destabilizing fluid dynamic force becomes larger as the annular passage becomes narrower;

(e) the critical flow velocity is lower if the fluid has larger density.

All of these conclusions are applicalbe to systems with parameters in the range of those covered by the numerical calculations undertaken in this Thesis.

Based on inviscid flow theory analyzed here, it is noted that the dynamical behaviour of the system is similar to that of systems with unconfined flow or with internal flow, as discussed in chapter IV. Moreover, it turns out that the approximate method for the critical flow velocity based on the virtual mass (see Appendix E) is suitable for very slender bodies immersed in a narrow annular flow.

As stated in chapter VI, the dynamical behaviour of the system is modified by the viscous terms. In general, these viscous terms affect only slightly the dynamics of the system for confined flow. The stability characteristics of the system can be approximately determined by potential flow theory; this is so, because, as it is known, the frictional forces, although rendering the system nonconservative, do not greatly alter its fundamental behaviour as determined by the inviscid forces. However, the viscous effects become important as the annulus becomes narrower [22].

The results based on the approximate viscous theory developed in chapter V are compared with those obtained by the potential flow theory in chapter VI in detail. Generally, it turns out that viscous effects, as considered in this analysis at least, have a stabilizing influence on the system. Some interesting conclusions for the dynamic behaviour of the system subject to viscous flow are as follows:

(a) the system is subject to both divergence and single-mode flutter, as opposed to coupled-mode flutter;

(b) although the viscous effect is taken into account, the stability behaviour of a system having relatively large annular gap or lower viscosity of fluid is strongly affected by the inviscid fluid-dynamic force; thus, the system loses stability in the first mode by divergence at a little higher flow velocity as compared with the results obtained by potential flow theory;

(c) *if the viscosity of the fluid is increased or the annular gap ratio decreased, the system loses the stability by second-mode flutter or buckling at a much higher flow velocity than predicted obtained by potential flow theory;*

(d) *the steady viscous effect on the dynamics of the system, i.e , due to the tension terms generated by the longitudinal viscous force, has been shown to be rather weak and stabilizes the system except for end conditions corresponding to case II, moreover, pressurization stabilizes the system, but its effect is relatively small.*

Thus, it is interesting to note that the difference in the instability threshold as given by the two theories (i.e. the potential flow theory and the viscous flow theory) is quite large for very narrow annular flow

Although, the treatment of the viscous effects is based on a considerable number of simplifying approximations, these conclusions may be considered to be reasonable as an attempt to assess the influence of viscous effects on the dynamics of the system

It should be remarked that, in the present analysis, the flow in the narrow annular passage is assumed to be a fully developed laminar flow. At higher flow velocity, approximately beyond the second mode buckling point, the validity of the results is questionable, since, the flow is turbulent. In general, the static pressure drop along the axis is different in turbulent flow; further, the shear stresses acting on the wall are much larger than those in laminar flow. However, it is questionable that the viscous effects on the dynamics of the system in the turbulent flow region are more profound.

In summary, inviscid flow theory predicts that the system would be monotonically destabilized as the annular gap ratio becomes smaller, which means that the critical flow velocity would tend to become smaller; however, the stabilizing influence of the viscous effects increases with diminishing annular gap ratio at a higher rate eventually overcoming the destabilizing influence of the relative gap decrease in

inviscid case (in fact, the steady viscous effects for end conditions corresponding to case II of Figures 11, 13 and 15 destabilize the system). This is one of the principal findings of this work.

In view of the lack of reliable experimental data in the area of very narrow viscous flow about a flexible slender centre-body, it is impossible to compare these results with experiment.

7.2 SUGGESTIONS FOR FUTURE WORK

A theoretical analysis has been developed in this thesis for both potential and viscous flow past the flexible centre-body oscillating in a cylindrical duct having a constant annular passage, in order to determine flow-induced instabilities of the system. As mentioned before, the viscous model developed here is obtained under several assumptions. Therefore, there are several possible directions in which this work can be extened; e.g., it is suggested that for the turbulent flow regime, viscous coupling terms should be modified, as mentioned before.

An attempt should be made to extend the theory to more complex geometries. Better analytical models for studying the unsteady flow in narrow passages would consitute a major step forward, in order to obtain results with wider applicability to real engineering problems. In this respect the non-cylindrical geometries involving axially variable annular flow passages will be considered. This represents an important step in solving the problem of the dynamics and stability of noncylindrical configurations.

In the present analysis, both ends of the flexible centre-body are supposed to be clamped. Thus, it is needed to investigate the dynamics and stability of other systems, having different boundary conditions; e.g., clamped-free or pinned-pinned beams.

Finally, to be able to test the theory, it is obviously necessary to get some experimental results of high quality.

REFERENCE

1. Fritz, R. Z., "The effect of Liquid on the Dynamic Motion of Immersaed Solids", J. Engineering for Industry, Vol. , 1972, pp 167-173

2. Chen, S. S., "Free Vibration of a Coupled Fluid/Structural System", J. of Sound & Vibration, Vol. 21, 1972, pp 387-398

3. Au-Yang, M. K., "Free Vibration of Fluid-Coupled Coaxial Cylindrical Shells of Different Lengths", J. of Applied Mechanics, Vol. 43, 1976, pp 480-484

4. Stokes, G. G., "On Some Cases of Fluid Motion", Proceedings Cambridge Philosophical Society, Vol. 8, 1843, pp 105-137

5. Lamb, H., Hydrodynamics, 6th Edition, Dover, 1943, Ch. 6

6. Chen, S. S. etc, "Added Mass and Damping of a Vibrating Rod in Confined Viscous Fluid", J. of Applied Mechanics, Vol.43, 1976, pp 325-329

7. Yeh, T. T. and Chen, S. S., "Dynamics of a Cylindrical Shell System Coupled By Viscous Fluid", J. Acoustical Society of America, Vol. 62, 1977, pp 262-270

8. Paidoussis, M. P., "Dynamics of Flexible Slender Cylinders in Axial Flow; Part 1: Theory", J. of Fluid Mechanics, Vol. 26, 1966, pp 717-736

9. Paidoussis, M. P., "Dynamics of Flexible Slender Cylinders in Axial Flow; Part 2: Experiment", J. of Fluid Mechanics, Vol. 26, 1966, pp 737-751

10. Paidoussis, M. P., "Stability of Towed, Totally Submerged Flexible Cylinder", J. of Fluid Mechanics, Vol. 34, 1968, pp 273-297

11. Taylor, G. I., "Analysis of the Swimming of Long and Narrow Animals", Proceeding of Royal Society (London), A214, 1952, pp 158-183

12. Paidoussis, M. P., "Dynamics of Cylindrical Structure

Subjected to Axial Flow", J. of Sound & Vibration, Vol. 29, 1973, pp 365-385

13. Paidoussis, M. P. and Issid, N. T., "Dynamics Stability of Pipes Conveying Fluid", J. of Sound & Vibration, Vol. 33, 1974, pp 267-294

14. Paidoussis, M. P. and Pettigrew, M. J., "Dynamics of Flexible Cylinders in Axisymmetrically Confined Axial Flow", J. of Applied Mechanics' Vol. 46, 1979, pp 37-44

15. Paidoussis, M. P. and Ostoja-Starzewski, M., "Dynamics of a Flexible Cylinder in Subsonic Axial Flow", AIAA Journal, Vol. 19, 1981, pp 1467-1475

16. Dowell, E. H. and Widnall, S. E., "Generalized Aerodynamic Forces on an Oscillating Cylindrical Shell; Subsonic and Supersonic Flow", AIAA Journal, Vol. 4, 1966, pp 607-610

17. Chen, S. S., "Vibration of Nuclear Fuel Boundles", Nuclear Engineering Design, Vol. 35, 1975, pp 399-422

18. Paidoussis, M. P. and Suss, S., "Stability of a Cluster of Flexible Cylinders in Bounded Axial Flow", J. of Applied Mechanics, Vol. 44, 1977, pp 401-408

19. Paidoussis, M. P., "Flow Induced Vibrations in Nuclear Ractors and Heat Exchangers: Practical Experience and State of Knowledge", Practical Experience with Flow-Induced Vibration (Eds. E. Naudascher and D. Rockwell), Spriager-Verlag Berlin

20. Hobson D. E., "Fluid-Elastic Instabilities caused by Flow in an annulus", Proceeding 3rd International Conference on Vibration of Nuclear Plant, Keswick, U. K., 1982, pp 440-463

21. Mateescu, D. and Paidoussis, M. P., "The Unsteady Potential Flow in an Axially Variable Annulas and Its Effect on the Dynamics of Oscillating Rigid Centre-Body", J. of Fluids Engineering, Vol. 107, 1985, pp 421-427

22. Mateescu, D. and Paidoussis, M. P., "Unsteady Viscous Effects on the Annular-Flow-Induced Instabilities

of Rigid Cylindrical Body in Narrow Duct", J. of Fluids & Structures, Vol. 1, 1987, pp 197-215

23. Mateescu, D., Paidousis, M. P. and Sim, W. G., "Flow-Induce Instability of a Flexible Cylinder in a Narrow Pipe Conveying Fluid", C. C. A. M., Edmonton, 1987

24. Lighthill, M. J., "Note on the Swimming of Slender Fish", J. of Fluid Mechanics, Vol. 90, 1960, pp 305-317

25. Paidoussis, M. P., Chan, S. P., and Misra, A. K., "Dynamics and Stability of Coaxial Cylindrical Shell Containing Flowing Fluid", J. of Sound & Vibration, Vol. 97, 1985, pp 201-235

26. Meirovich, L., Methods of Analytical Dynamics, McGraw-Hill, Ch. 4

27. Yuan, W. S., Fundation of Fluid Mechanics, Prentice Hall, Ch. 8

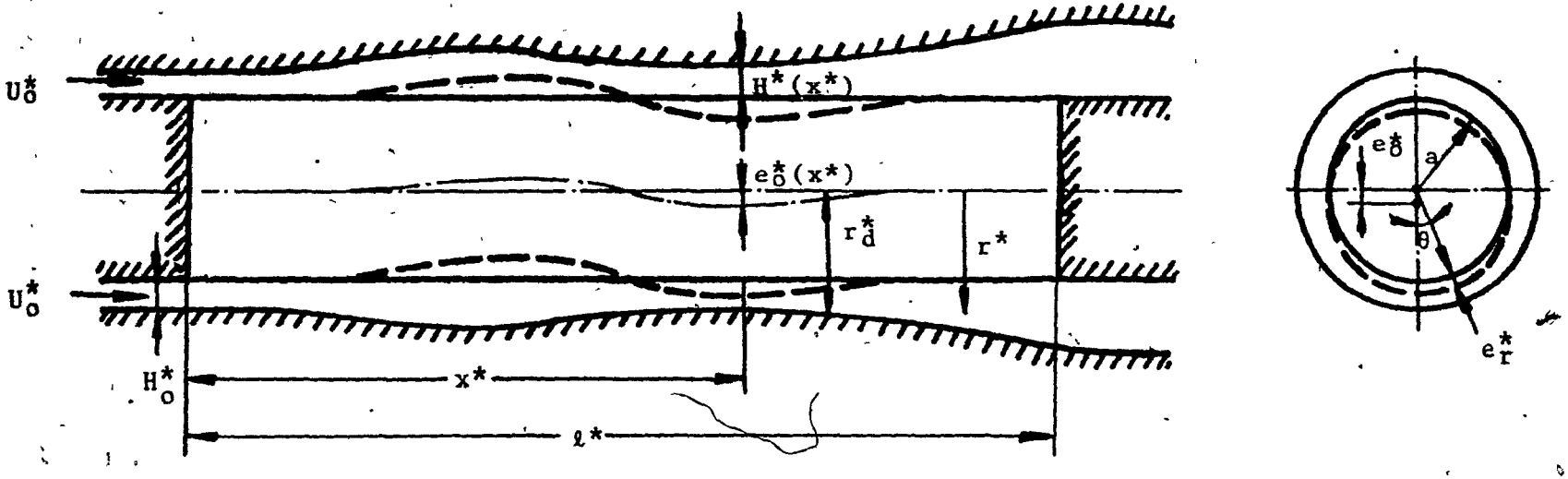

Figure 1 Geometry of the oscillating centre-body inside a duct of variable cross section

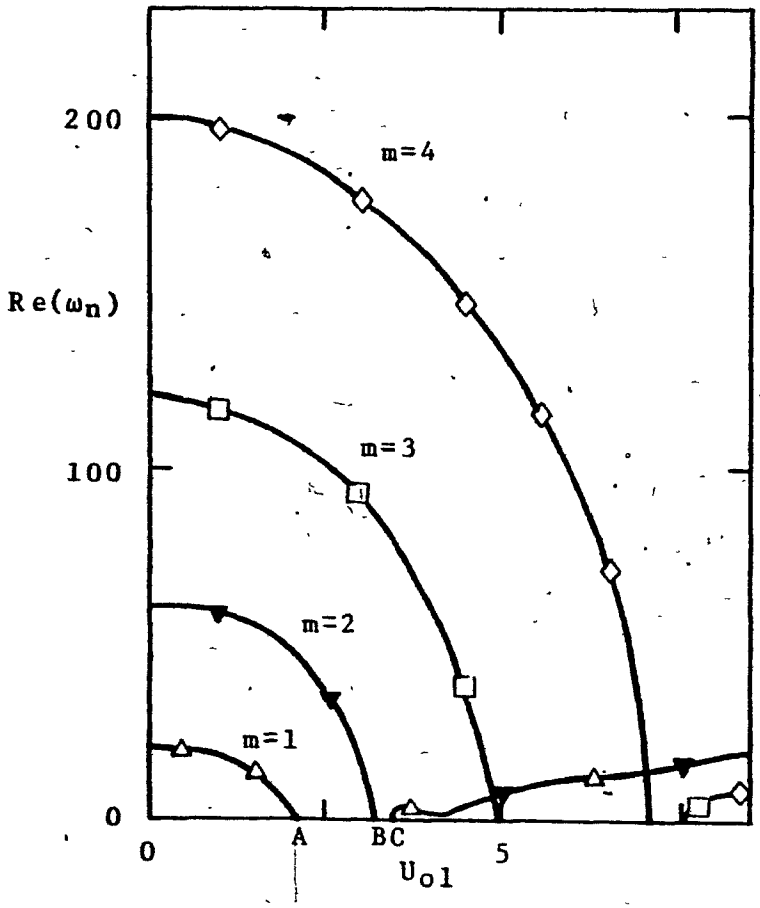

(a) the real components of the nondimensional eigenfrequencies

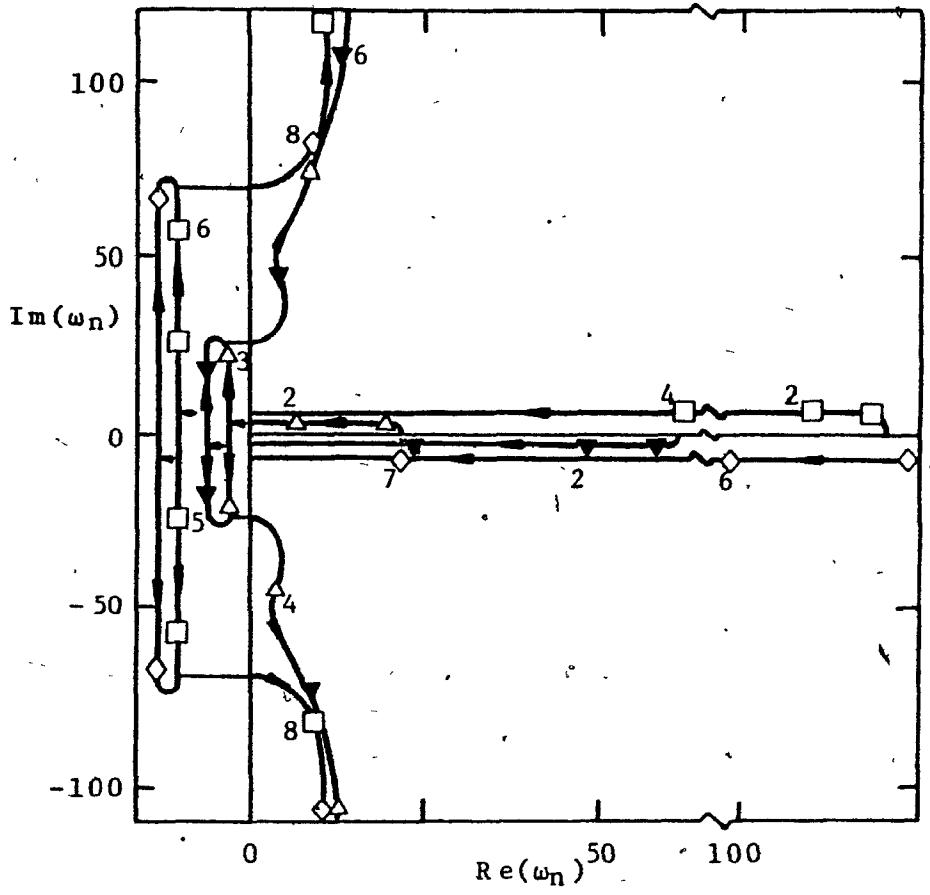

(b) Argand diagram of the real and imaginary parts of the nondimensional eigenfrequencies

Figure 2 The nondimensional eigenfrequencies of the lowest four modes as functions of the nondimensional fluid velocity, U_{o1}, for potential flow (ℓ^*/a=20, H^*/a=0.1, σ=0.4246 and U_{ref1}=36.77m/s):

△ first mode ▼ second mode

□ third mode ◇ fourth mode

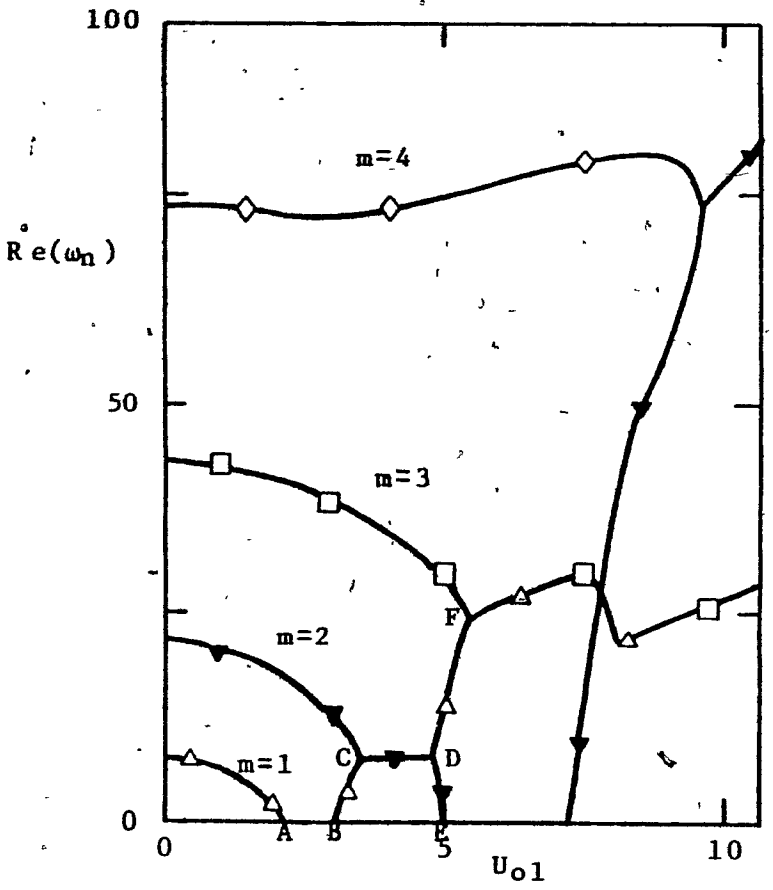

(a) the real components of the nondimensional eigenfrequencies

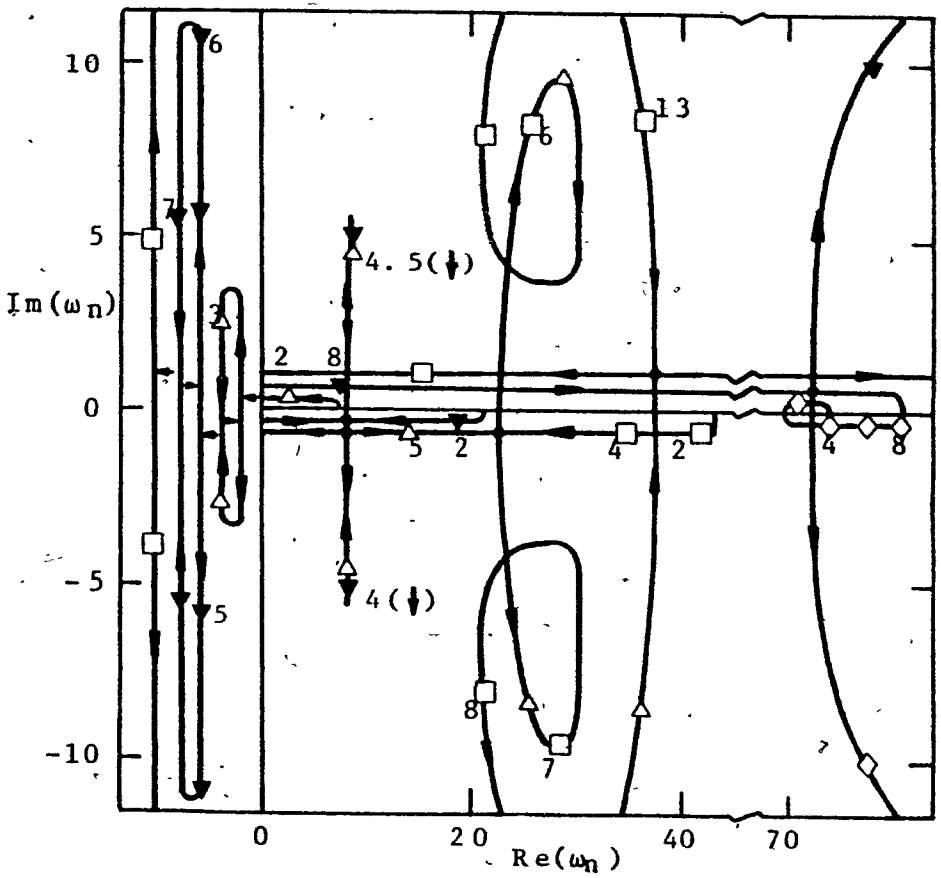

(b) Argand diagram of the real and imaginary parts of the nondimensional eigenfrequencies

Figure 3 The nondimensional eigenfrequencies of the lowest four modes as functions of the nondimensional fluid velocity, U_{o1}, for potential flow (ℓ^*/a=20, H^*/a=0.1, σ=346.62 and U_{ref1}=1.287m/s):

△ first mode ▼ second mode

□ third mode ◇ fourth mode

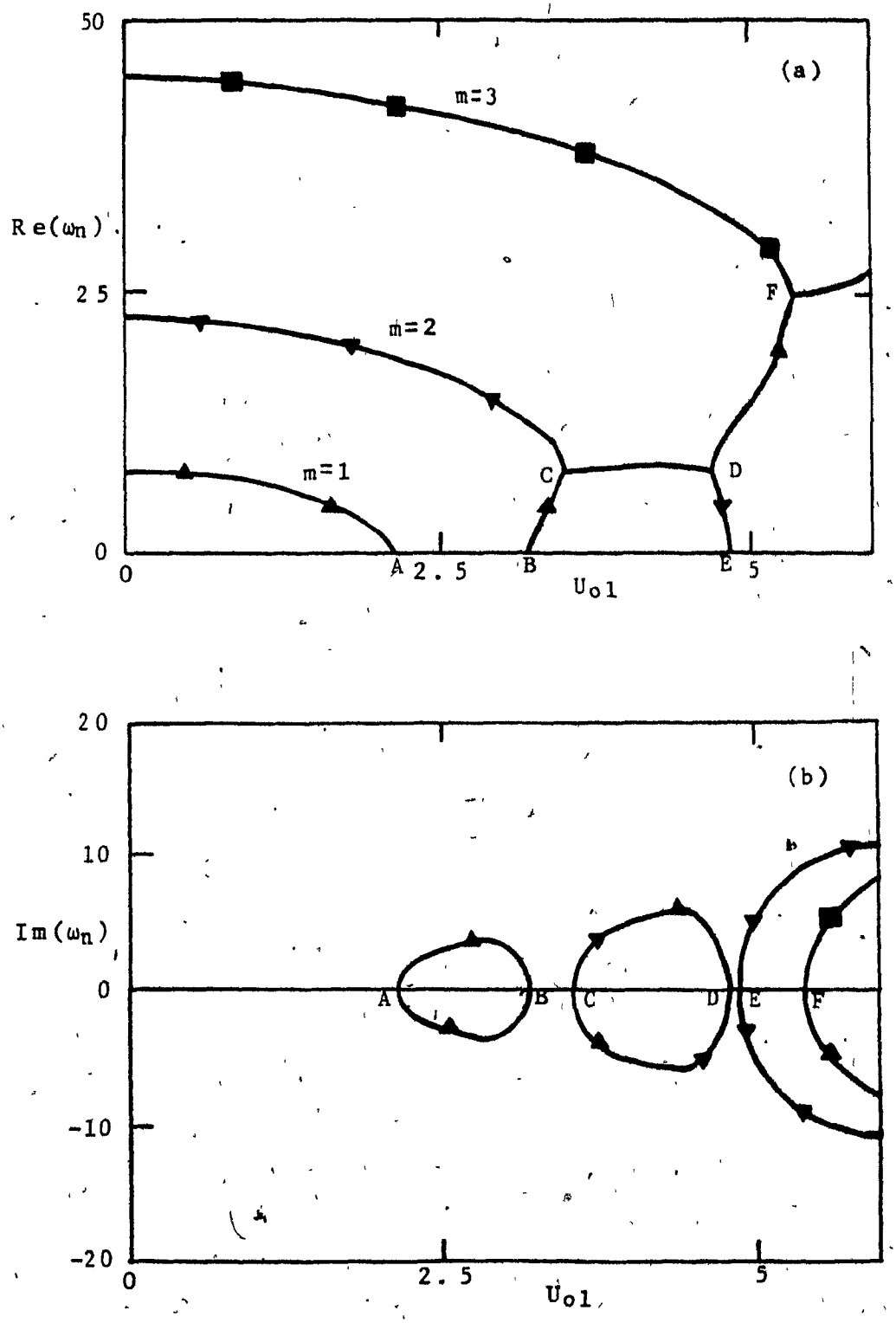

Figure 4 The (a) real and (b) imaginary components of the nondimensional eigenfrequencies of the lowest three modes as functions of the nondimensional fluid velocity, U_{o1}, for potential flow (ℓ^*/a=20, H^*/a=0.1, σ=323.74 and U_{ref1}=1.332m/s):
▲ first mode ▼ second mode
■ third mode

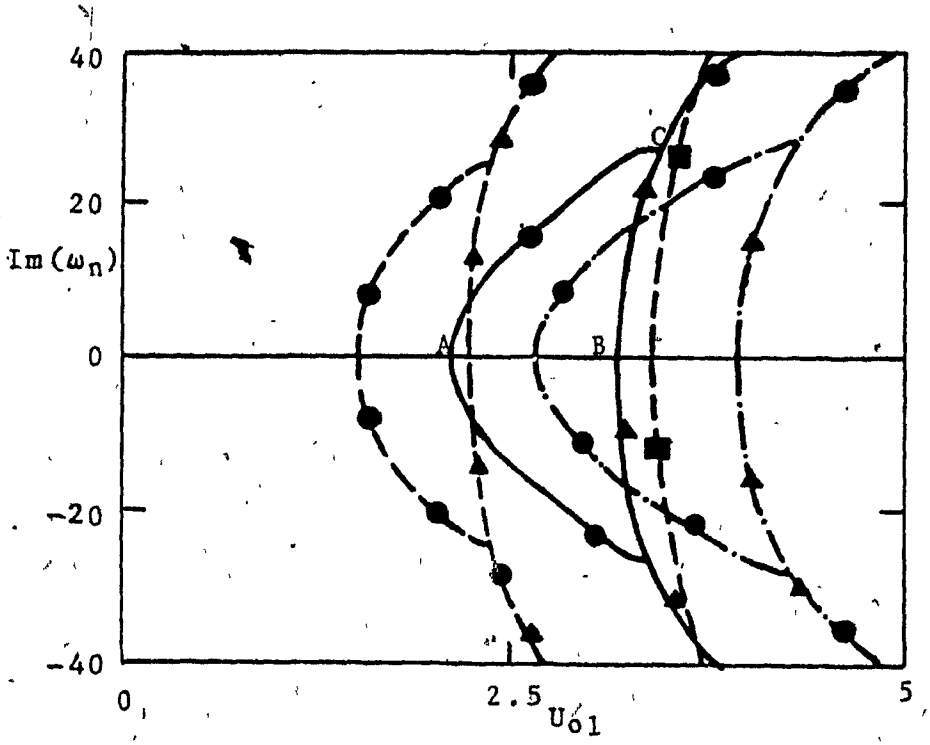

Figure 5 The imaginary components of the nondimensional eigenfrequencies of the lowest two or three modes as functions of the nondimensional fluid velocity, U_{01}, for potential flow, showing the effect of varying H^*/a (ℓ^*/a=20, σ=0.4246 and U_{ref1}=36.77m/s):

——— H^*/a=0.05 ● first mode
——— -0.1 ▲ second mode
—·— -0.15 ■ third mode

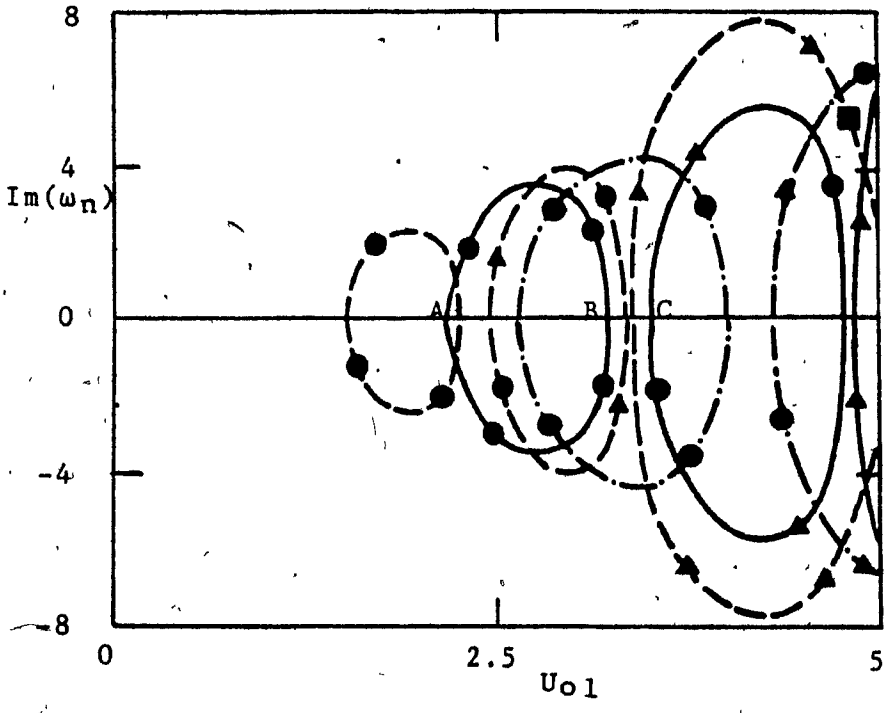

Figure 6 The imaginary components of the nondimensional eigenfrequencies of the lowest two modes as functions of the nondimensional fluid velocity, U_{o1}, for potential flow, showing the effect of varying H^*/a (ℓ^*/a=20, σ=346.62 and U_{ref1}=1.287 m/s):

——— H^*/a=0.05 ● first mode
——— -0.1 ▲ second mode
—·— -0.15

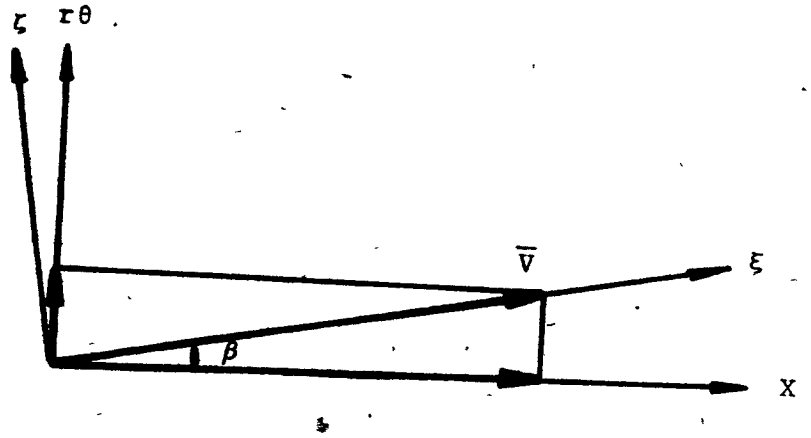

Figure 7 Diagram showing transformation of coordinates and definition of the angle β

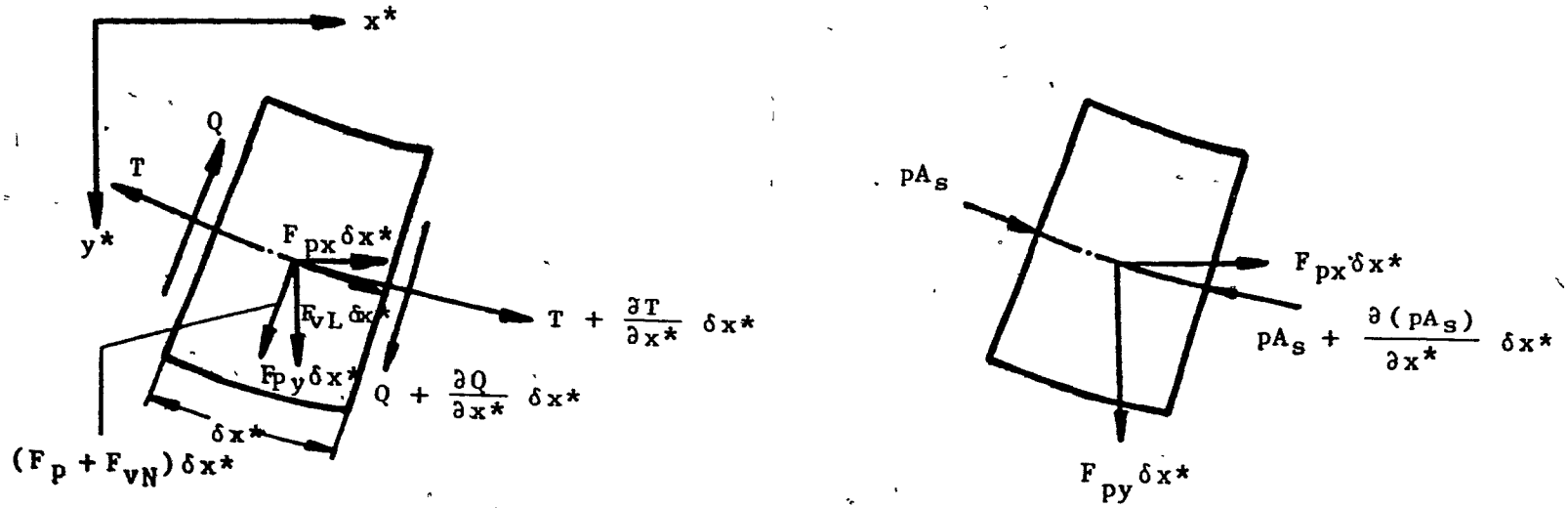

Figure 8 (a) Forces acting on elements of the cylinder and (b) of the equivalent rigid body surrounded by fluid

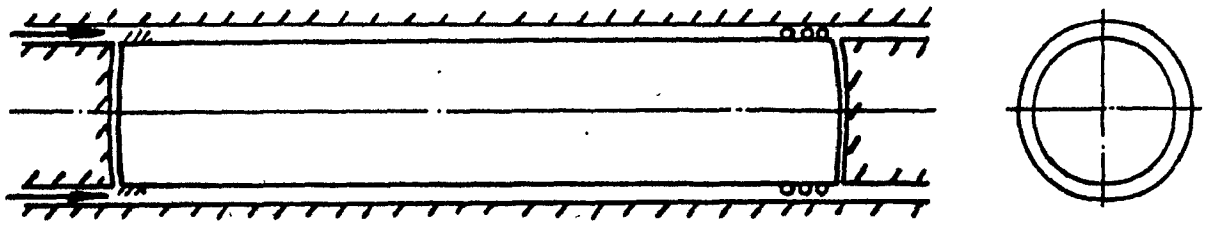

(a) totally clamped at upstream end; clamped but axially sliding at downstream end (case I)

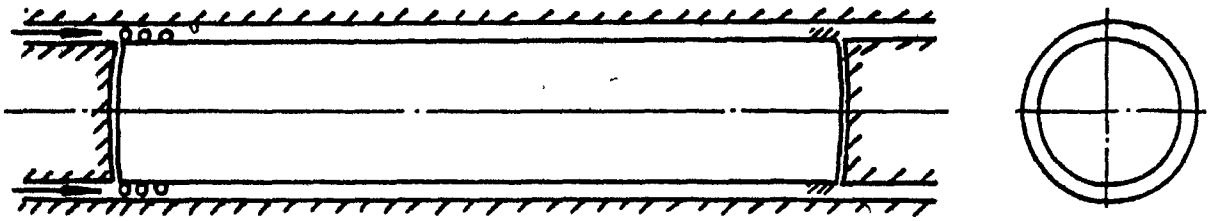

(b) axially sliding at upstream end and totally clamped at downstream end (case II)

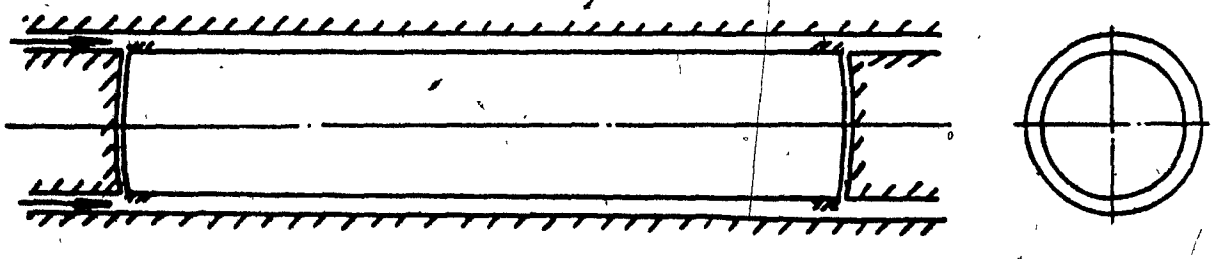

(c) both ends absolutely clamped (case III)

Figure 9 Diagram showing the axial boundary conditions

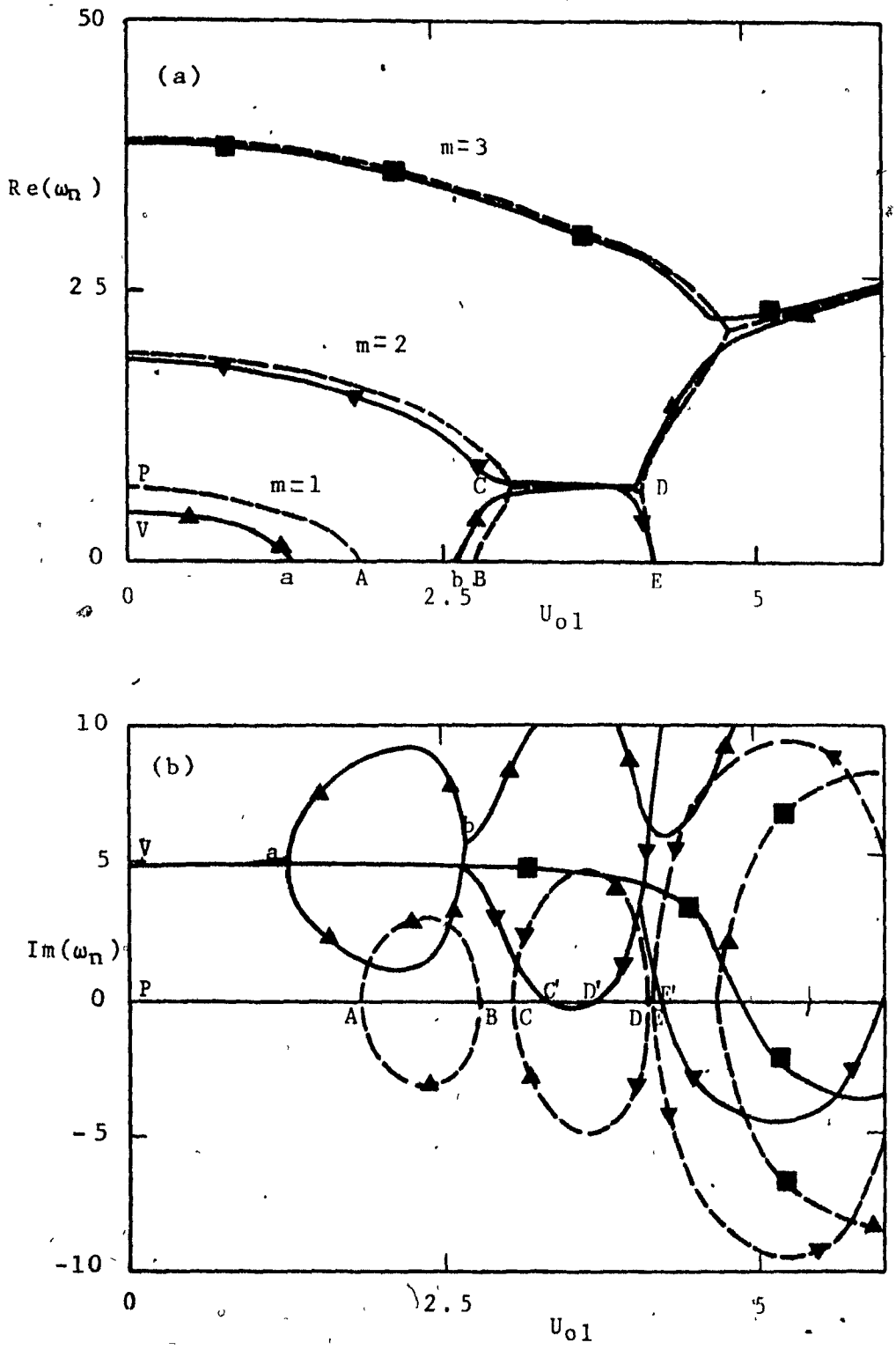

Figure 10 The (a) real and (b) imaginary components of the nondimensional eigenfrequencies of the lowest three modes as functions of the nondimensional fluid velocity, U_{o1}, for potential flow(---) and viscous flow(——) considering potential and unsteady viscous effects (ℓ^*/a=20, H^*/a=0.075, σ=323.74 U_{ref1}=1.3316m/s and μ=0 and 0.007 Pa·s, respectively):

▲ first mode ▼ second mode

■ third mode

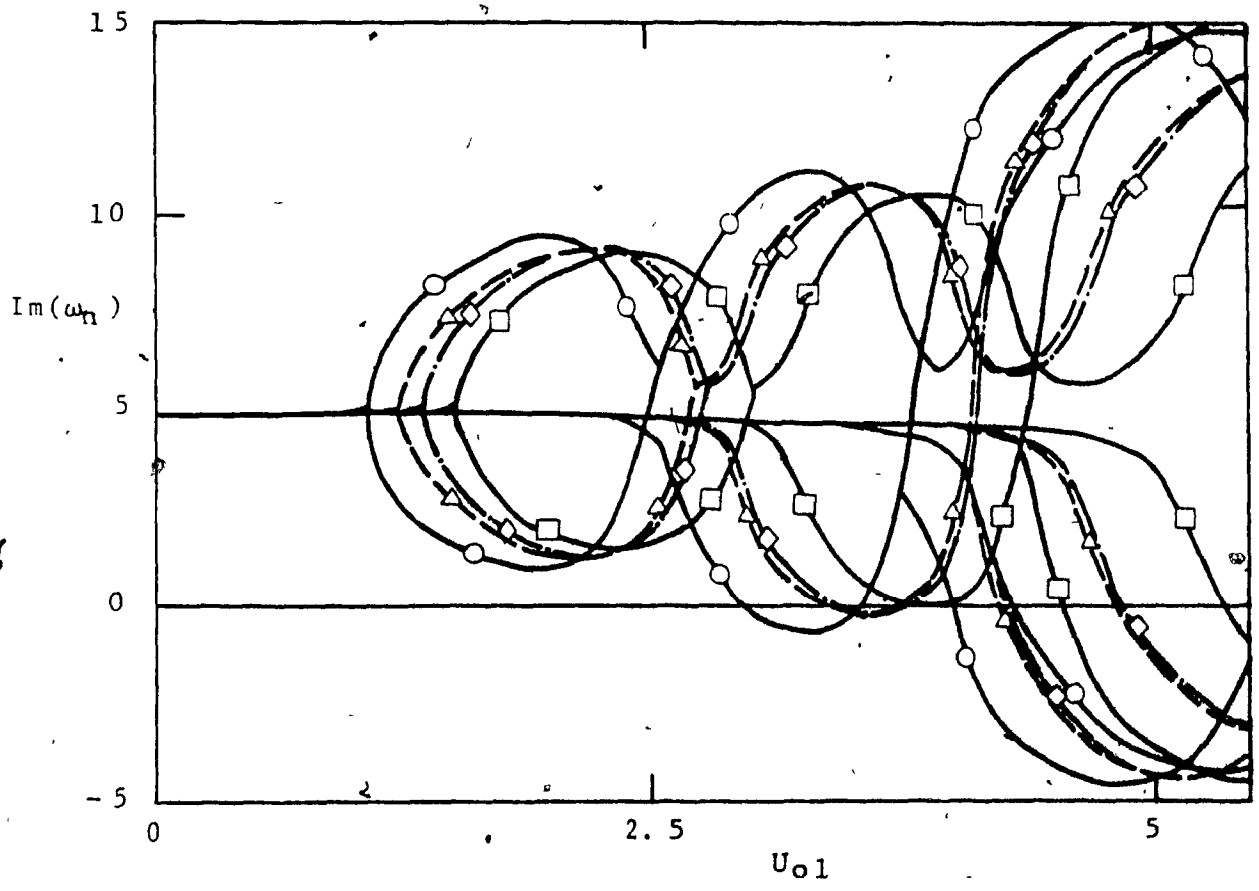

Figure 11 The imaginary components of the nondimensional eigenfrequencies of the lowest three modes as functions of the nondimensional fluid velocity, U_{o1}, for viscous flow considering potential and steady & unsteady viscous effects ($\ell^*/a=20$, $H^*/a=0.075$, $\sigma=323.74$, $U_{ref1}=1.3316$m/s and $\mu=0.007$Pa·s);
—□— case I —△— case III ($\Pi=5$)
—○— case II —◇— case III ($\Pi=50$)
where cases I, II and III correspond to boundary conditions as in (a), (b) and (c) of Fig. 9

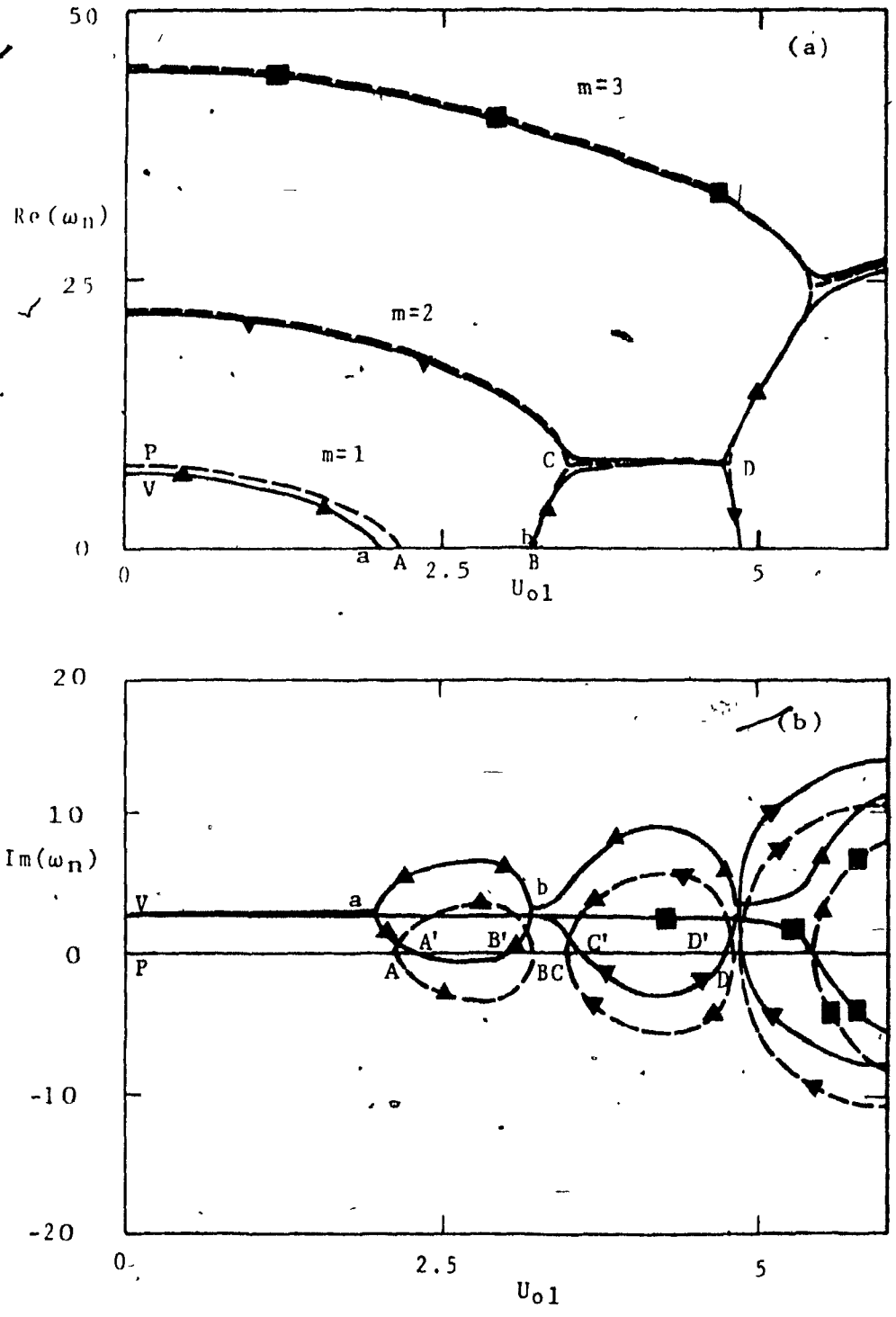

Figure 12. The (a) real and (b) imaginary components of the nondimensional eigenfrequencies of the lowest three modes as functions of the nondimensional fluid velocity, U_{o1}, for potential flow(---) and viscous flow(——) considering potential and unsteady viscous effects (ℓ^*/a=20, H^*/a=0.1, σ=323.74 U_{ref1}=1.3316m/s and μ=0 and 0.007Pa·s, respectively):

▲ first mode ▼ second mode
■ third mode

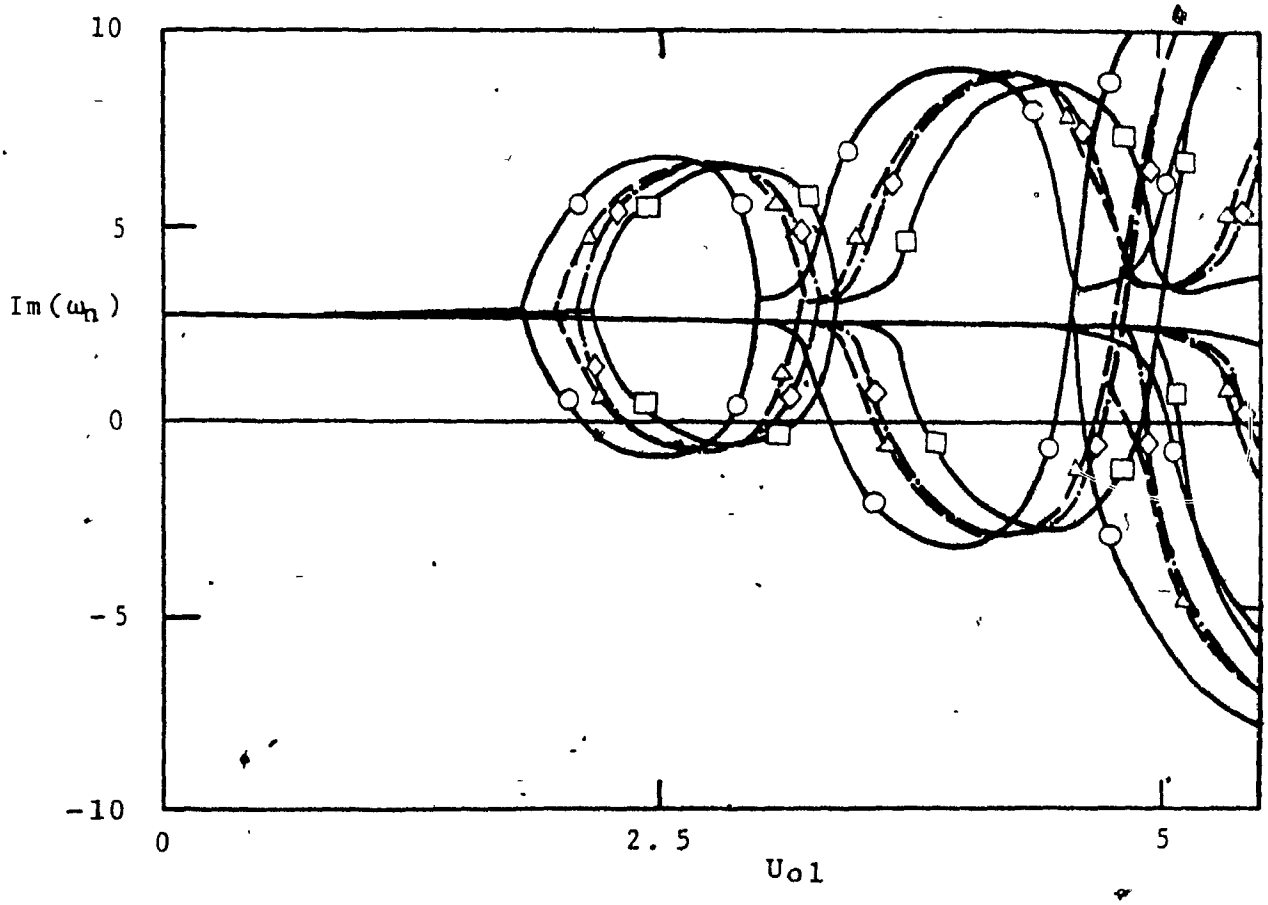

Figure 13 The imaginary components of the nondimensional eigenfrequencies of the lowest three modes as functions of the nondimensional fluid velocity, U_{o1}, for viscous flow considering potential and steady & unsteady viscous effects (ℓ^*/a=20, H^*/a=0.1, σ=323.74, U_{ref1}=1.3316m/s and μ=0.007Pa·s);
case I
case II
case III (Π=10)
case III (Π=50)
where cases I, II and III correspond to boundary conditions as in (a), (b) and (c) of Fig. 9

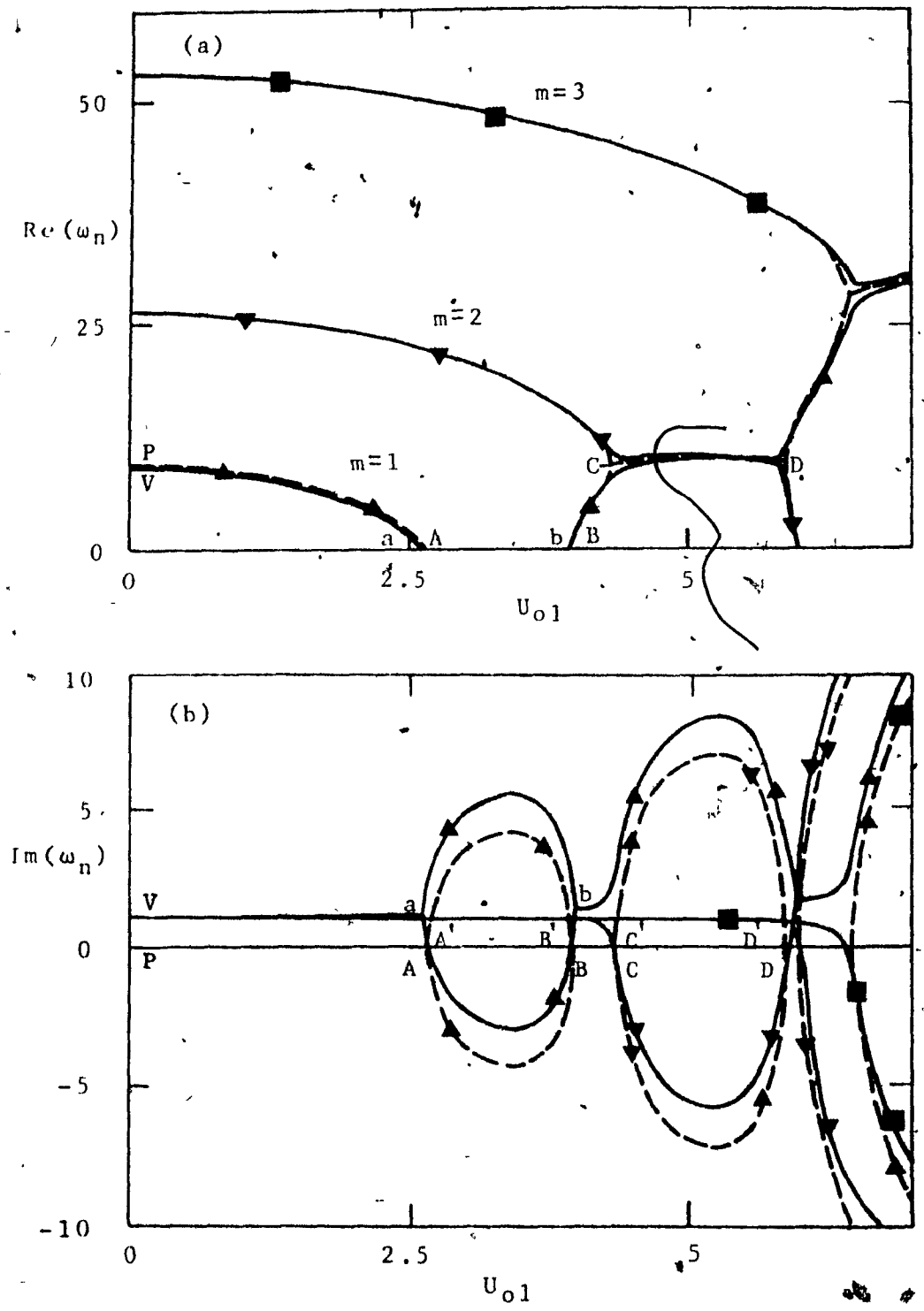

Figure 14 The (a) real and (b) imaginary components of the nondimensional eigenfrequencies of the lowest three modes as functions of the nondimensional fluid velocity, U_{o1}, for potential flow(---) and viscous flow(——) considering potential and unsteady viscous effects (ℓ^*/a=20, H^*/a=0.15, σ=323.74 U_{ref1}=1.3316m/s and μ=0 and 0.007Pa·s, respectively):

▲ first mode ▼ second mode
■ third mode

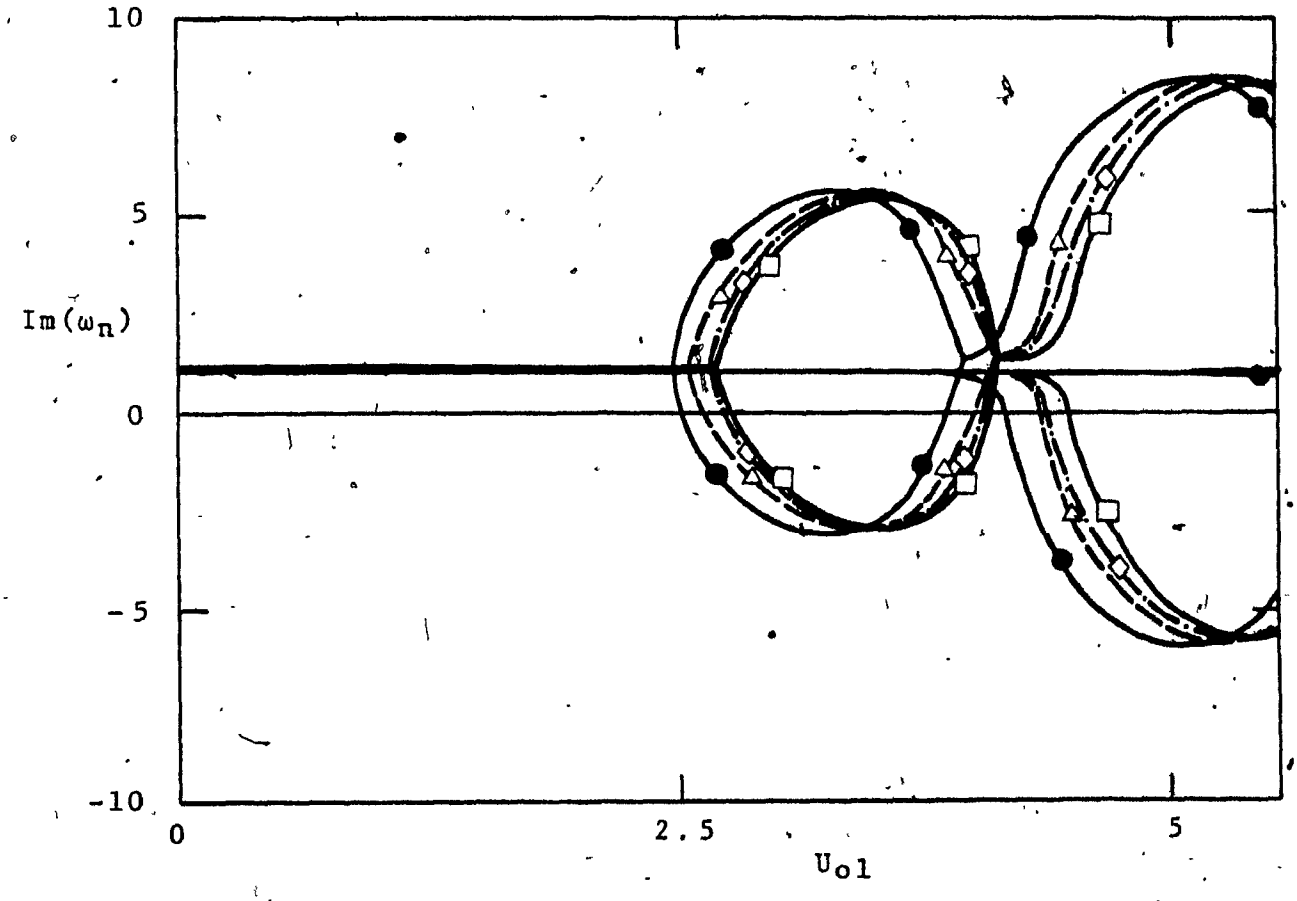

Figure 15 The imaginary components of the nondimensional eigenfrequencies of the lowest three modes as functions of the nondimensional fluid velocity, U_{o1}, for viscous flow considering potential and steady & unsteady viscous effects (ℓ^*/a=20, H^*/a=0.15, σ=323.74, U_{ref1}=1.3316m/s and μ=0.007Pa·s);
—□— case I —△— case III (Π=5)
—●— case II —◇— case III (Π=50)
where cases I, II and III correspond to boundary conditions as in (a), (b) and (c) of Fig. 9

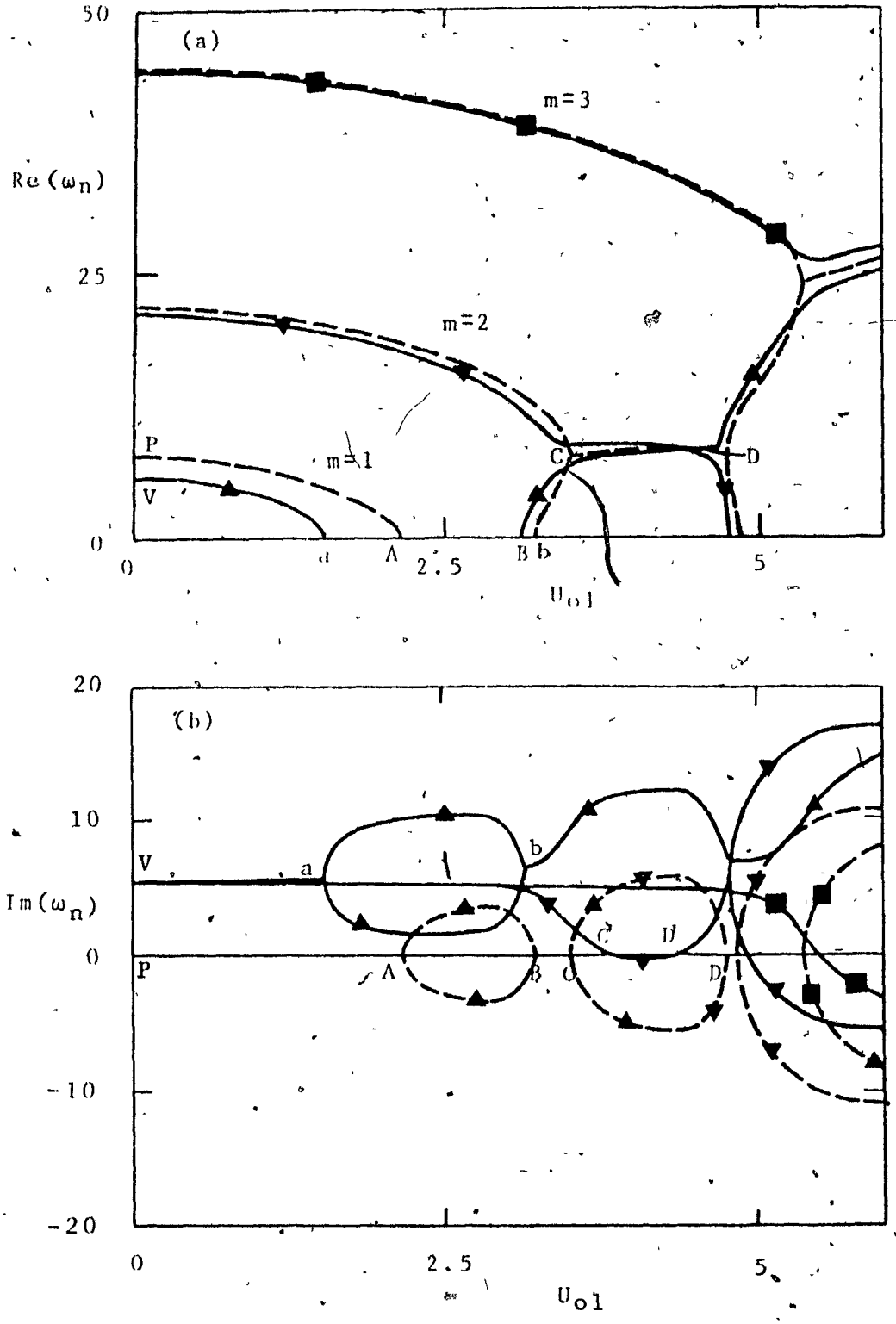

Figure 16 The (a) real and (b) imaginary components of the nondimensional eigenfrequencies of the lowest three modes as functions of the nondimensional fluid velocity, U_{o1}, for potential flow(---) and viscous flow(——) considering potential and unsteady viscous effects (ℓ^*/a=20, H^*/a=0.1, σ=323.74 U_{ref1}=1.3316m/s and μ=0.014Pa•s):
▲ first mode ▼ second mode
■ third mode

APPENDIX A

THE EIGENVALUE PROBLEM FOR THE EULER-BERNOULLI BEAM

A.1 Simple Derivation of Equation of Motion Based on the Hamilton Principle

Under the assumption of slender body theory, which represents that the motions of the flexible centre-body are small enough for rotatory inertia and transverse shear to be negligible, the flexible centre-body is assumed to be an Euler-Bernoulli beam. If they are not, one has to make use of the so-called Timoshenko-beam theory; but this more complex theory will not be discussed here.

To formulate the boundary-value problem, the extended Hamilton principle should be used. The power of this approach becomes evident in that the correct number of boundary conditions and their correct expression are furnished automatically.

The bending moment on a element will be

$$M(x^*,t^*) = EI \frac{\partial \psi(x^*,t^*)}{\partial x^*}, \qquad (A-1)$$

where $\psi(x^*,t^*)$ is the angle

$$\psi(x^*,t^*) \doteq \frac{\partial e_o^*(x^*,t^*)}{\partial x^*}, \qquad (A-2)$$

and where the beam cross section is assumed to be uniform. Now, the potential energy, associated with deformation of the beam (strain energy), and the kinetic energy due to translation are given by

$$V = \frac{1}{2}\int_0^{\ell^*} M(x^*,t^*) \frac{\partial \psi(x^*,t^*)}{\partial x^*} dx^* = \frac{1}{2}\int_0^{\ell^*} EI \left[\frac{\partial^2 e_o^*(x^*,t^*)}{\partial x^{*2}} \right]^2 dx^*, \qquad (A-3)$$

$$T = \frac{1}{2}\int_0^{\ell^*} m_s \left[\frac{\partial e_o^*}{\partial x^*} \right]^2 dx^*.$$

Hence, recalling the Hamilton principle for a conservative system yields

$$\int_{t_1}^{t_2}\int_0^{\ell^*}\left(m_s \frac{\partial e_o^*}{\partial t^*}\frac{\partial}{\partial t^*}(\delta e^*) - EI \frac{\partial^2 e_o^*}{\partial x^{*2}}\frac{\partial^{*2}}{\partial x^{*2}}(\partial e_o^*)\right) \delta x^* dt^* = 0, \quad \text{(A-4)}$$

since the order of integrations with respect to x^* and t is interchangeable and the variational and differentiation operators are commutative.

Integrating by parts the first part of the integral, one gets

$$\delta I_1 = \int_0^{\ell^*} m_s \frac{\partial e_o^*}{\partial t^*}\delta e_o^*\Big|_{t_1}^{t_2} dx^* - \int_{t_1}^{t_2}\int_0^{\ell^*} m_s \frac{\partial^2 e_o^*}{\partial t^{*2}}\delta e_o^*\, dx^*\, dt^*$$

and since the variation δe_o^* must vanish at t_1 and t_2, thus,

$$\delta I_1 = -\int_{t_1}^{t_2}\int_0^{\ell^*} m_s \frac{\partial^2 e_o^*}{\partial t^{*2}}\delta e_o^*\, dx^*\, dt^*. \quad \text{(A-5)}$$

Similarly, for the second part of the integral, one obtains

$$\delta I_2 = \int_{t_1}^{t_2} EI \frac{\partial^2 e_o^*}{\partial x^{*2}}\delta\frac{\partial e_o^*}{\partial x^*}\Big|_0^{\ell^*} dt^* - \int_{t_1}^{t_2}\frac{\partial}{\partial x^*}\left(EI\frac{\partial^2 e_o^*}{\partial x^{*2}}\right)\delta e_o^*\Big|_0^{\ell^*} dt^*$$

$$+ \int_{t_1}^{t_2}\int_0^{\ell^*}\frac{\partial^2}{\partial x^{*2}}\left(EI\frac{\partial^2 e_o^*}{\partial x^{*2}}\right)\delta e_o^*\, dx^* dt^*. \quad \text{(A-6)}$$

Now, the virtual displacements δe_o^* and $\delta(\partial e_o^*/\partial x^*)$ are arbitrary and independent, so they can be taken to be equal to zero at $x^*=0$ and $x^*=\ell^*$. The line integrals and surface integrals may vanish indenpendently. Thus, combining (A-5) and (A-6), the surface integral yields

$$EI \frac{\partial^4 e_o^*}{\partial x^{*4}} + m_s \frac{\partial^2 e_o^*}{\partial t^{*2}} = 0. \quad \text{(A-7)}$$

The boundary conditions are obtained from the vanishing of the line integrals, yielding

$$EI\,\frac{\partial^2 e_o^*}{\partial x^{*2}}\,\delta\left(\frac{\partial e_o^*}{\partial x^*}\right)\Big|_0^{\ell^*} = 0, \qquad \frac{\partial}{\partial x^*}\left(EI\frac{\partial^2 e_o^*}{\partial x^{*2}}\right)\,\delta e_o^*\Big|_0^{\ell^*} = 0. \tag{A-8}$$

Thus, for a uniform beam the following boundary conditions are possible at each extremity:
(i) either $EI(\partial^2 e_o^*/\partial x^{*2})=0$ or $\partial e_o^*/\partial x^*=0$, and
(ii) either $EI(\partial^3 e_o^*/\partial x^{*3})=0$ or $e_o^*=0$.
For a clamped-clamped beam, clearly $e_o^*=0$ and $\partial e_o^*/\partial x^*=0$ must be satisfied. Of course, the differential equation of motion (A-7) must be satisfied for $0\le x^*\le \ell^*$.

A.2 The Eigenvalue Problem

Assuming that the solution of (A-7) is separable in time and space and of the form

$$e_o^*(x^*,t^*) = Y(x^*)\cdot T(t^*). \tag{A-9}$$

Substituting into (A-7) gives

$$-\frac{m_s}{EI}\,\frac{1}{T}\,\frac{d^2T}{dt^{*2}} = \frac{1}{Y}\,\frac{d^4Y}{dx^{*4}} = \lambda^4, \tag{A-10}$$

where the left side of the above depends on t, and the middle side depends on x^* only. Both x^* and t are independent variables, so (A-7) has a solution only if both sides are constant. Hence, the solution takes the form

$$e_o^* = Y(x^*)\,e^{i\Omega t^*}, \tag{A-11}$$

where

$$\Omega^2 = \frac{EI}{m_s^*}\,(\lambda\ell^*)^4, \tag{A-12}$$

and

$$Y(x^*) = A\cos\lambda x^* + B\sin\lambda x^* + C\cosh\lambda x^* + D\sinh\lambda x^*. \tag{A-13}$$

The $Y(x^*)$, called characteristic functions or eigenfunctions, will be determined by application of four boundary conditions, two at each end. The four boundary conditions determine uniquely the shape of the solution, leaving the amplitude arbitrary, and also yield a characteristic equation or frequency equation, which, when solved, gives the character-

istic values of the problem. Here, $\lambda\ell^*$ are the eigenvalues of the problem and are infinite in number; for each one of them, there is a corresponding eigenfrequency Ω, given by (A-12).

Supposing that the beam has clamped ends, the deflection and the slope of the deflection curve must be zero at the clamped ends; thus,

$$Y(0) = Y(\ell^*) = 0, \qquad \left(\frac{dY}{dx^*}\right)\Big|_{x^*=0,\,\ell^*} = 0. \tag{A-14}$$

Substituting equation (A-13) in the above gives

$$A + C = 0, \tag{A-15a}$$
$$A\cos\lambda\ell^* + B\sin\lambda\ell^* + C\cosh\lambda\ell^* + D\sinh\lambda\ell^* = 0, \tag{A-15b}$$
$$\lambda(B + D) = 0, \tag{A-15c}$$
$$\lambda(-A\sin\lambda\ell^* + B\cos\lambda\ell^* + C\sinh\lambda\ell^* + D\cosh\lambda\ell^*) = 0. \tag{A-15d}$$

Equation (A-15a) yields A=-C and (A-15c) B=-D. Substituting into -15b and -15d gives

$$\begin{aligned} A(\cos\lambda\ell^* - \cosh\lambda\ell^*) &= -B(\sin\lambda\ell^* - \sinh\lambda\ell^*), \\ \lambda A(-\sin\lambda\ell^* - \sinh\lambda\ell^*) &= -\lambda B(\cos\lambda\ell^* - \cosh\lambda\ell^*). \end{aligned} \tag{A-16}$$

Elimination A and B and then simplifying yields

$$\cosh\beta_\kappa \cos\beta_\kappa = 1, \tag{A-17}$$

where $\beta_\kappa = \lambda\ell^*$.

Equation (A-17) is the characteristic equation for a clamped-clamped beam. It is a transcendental equation, the solution of which will give the infinite set of admissible solutions, i.e., the infinite set of eigenvalues β_κ. Solving equation (A-17) numerically, e.g., by the secant method, the first five of the infinite set of eigenvalues β_κ are given below

$$\begin{aligned} \beta_1 &= 4.7300407, & \beta_2 &= 7.8532046, \\ \beta_3 &= 10.9956078, & \beta_4 &= 14.1371655, \\ \beta_5 &= 17.2787597 \end{aligned} \tag{A-18}$$

Introducing the above in equation (A-12), it is possible to obtain the infinite set of eigenfrequencies, Ω_κ, as follows:

$$\Omega_\kappa = \beta_\kappa^2 \left(\frac{EI}{m_s \ell^4}\right)^{\frac{1}{2}} . \qquad (A-19)$$

Now, introducing the nondimensional parameter $X = x^*/\ell^*$ and comparison functions $E_\kappa(X)$, shown in Chapter II, and then substituting back to equation (A-13) for the κth mode, $Y_\kappa(X)$ are expressed as

$$Y_\kappa(X) = a_\kappa E_\kappa(X) = a_\kappa \left(E_{T\kappa} + E_{H\kappa}\right), \qquad (A-20)$$

where

$$E_{T\kappa}(X) = -\cos(\beta_\kappa X) + \sigma_\kappa \sin(\beta_\kappa X),$$

$$E_{H\kappa}(X) = \cosh(\beta_\kappa X) - \sigma_\kappa \sinh(\beta_\kappa X),$$

are the trigonometric and hyperbolic compoments of $E_\kappa(X)$, and

$$\sigma_\kappa = \frac{\cosh(\beta_\kappa) - \cos(\beta_\kappa)}{\sinh(\beta_\kappa) - \sin(\beta_\kappa)} . \qquad (A-21)$$

APPENDIX B

THE GENERAL SOLUTION OF A DAMPED SYSTEM

B.1 General Discussion

In many ways the assumption that systems possess no damping is a mathematical convenience rather than a reflection of physical evidence. However, there are cases in which the damping effect cannot be ignored. Also, in a limited number of these cases, the analysis of the corresponding undamped systems can be used to obtain the response of the damped systems.

There are many mathematical models representing damping: i.e., linear viscous, Coulomb and structural damping. The most important type of damping in vibration study is linear viscous damping. According to this model the damping takes the form of a force proportional in magnitude to the velocity and acting in the direction opposite to the direction of the velocity. In contrast with viscous damping, Coulomb damping, which is also refered to as dry friction, has a constant magnitude. Structural damping is associated with internal energy dissipation due to the hysteresis effect in cyclic stress, for which reason it is also called hysteretic damping.

In some special cases, the classical modal matrix, obtained from the eigenvalue problem associated with the undamped system, can be used successfully to uncouple the equations of motion of a viscously damped linear system. Unfortunately, this is not always possible. The general case of viscous damping can be treated by transforming a set of n ordinary differential equations of second order into a set of 2n ordinary differential equations of first order. The eigenvalues and eigenvectors associated with the latter set of equations are complex quantities.

Damped continuous systems can sometimes be treated by

assuming a solution, in the form of a superposition of classical normal modes, which leads to a set of ordinary differential equations. The problem of solving the partial differential equations associated with the continuous systems is reduced to the problem of solving a set of ordinary differential equations resembling, in structure, the equations describing a discrete system; this is done by many of the approximate methods of solution for continuous systems (e.g., Galerkin's method).

In the next section, a technique for obtaining a set of uncoupled co-ordinates of the damped system, equivalent to that of the undamped system, will be shown.

B.2 The General Solution of a Damped System

Using Galerkin's method based on the expansion theorem, the problem of solving the partial differential equation associated with a continuous system has now been rendered discrete and, upon truncating the summation at r=n, the equation of motion may be written in matrix form as follows:

$$M\ddot{q} + C\dot{q} + Kq = Q. \qquad (B\text{-}1)$$

Here, in order to allow the determination of the response within the desired accuracy, it is assumed that the order of this matrix equation is sufficiently high.

According to the viscous flow theory for the problem at hand, it is noted that M is diagonal, but C and K are not, and, moreover, they are not symmetric; however, the inviscid flow theory, based on the slender body theory, predicts that K should be symmetric. In the present thesis, the asymmetry in C and K is entirely due to the presence of fluid forces; e.g, for the inviscid flow, the asymmetry of C is due to the Coriolis forces. Thus, equation (B-1) represents a coupled set of equations and cannot be decoupled easily. Here, a quite

general method will be presented.

Let the following square and column partitioned matrices of order 2n be defined as

$$B = \begin{bmatrix} 0 & M \\ M & C \end{bmatrix}, \quad E = \begin{bmatrix} -M & 0 \\ 0 & K \end{bmatrix}, \quad z = \begin{Bmatrix} \dot{q} \\ q \end{Bmatrix}, \quad F = \begin{Bmatrix} 0 \\ Q \end{Bmatrix}. \tag{B-2}$$

Hence, the equation of motion may be written in form

$$B\dot{z} + Ez = F, \tag{B-3}$$

where B is generally not symmetric. This equation is the so-called reduced equation For the homogeneous form of this equation and with solution of the form

$$z = e^{\mu t^*} u, \tag{B-4}$$

the eigenvalue problem

$$(\mu I + Y)u = 0 \tag{B-5}$$

is obtained, where Y represents $B^{-1} \cdot E$, and u are the corresponding eigenvectors.

For nontrivial solution, the determinant of the left-hand side of the above equation is zero, which relationship gives 2n eigen-values of the matrix Y, μ_i. For a stable system, the μ_i are either real and negative or complex conjugate with a negative real part.

Let consider now that 2n values of μ have been found and that they are dictinct. Proceeding in the same way as for conservative systems, it may be shown that weighted orthogonality holds for this system also, namely

$$u_s^T B u_r = 0 \quad \text{and} \quad u_s^T E u_r = 0, \quad \text{for } r \neq s. \tag{B-6}$$

Defining the modal matrix

$$A = [\, u_1, u_2, \cdots\cdots u_{2n} \,], \tag{B-7}$$

one must have $A^T BA = P = \text{diag.}$ and $A^T EA = S = \text{diag.}$, an easily proven result by virtue of the orthogonality of the set of μ_i.

Reverting now to the non-homogeneous equation (B-3) and introducing

$$z = Ay \,, \tag{B-8}$$

one obtains

$$P\dot{y} + Sy = N \,, \tag{B-9}$$

or

$$\dot{y} + [\mu]y = P^{-1}N \,, \tag{B-10}$$

where $N = A^T F$, and $[\mu] = P^{-1}S$ in view of the orthogonality property discussed above. Hence, the system has been decoupled and equation (B-10) may be rewritten in the form

$$\dot{y}_i + \mu_i y_i = (1/P_{ii})N_i, \quad i = 1, 2, \cdots, 2n. \tag{B-11}$$

The solution is of the form

$$y_i = (y)_o \, e^{\mu_i t^*} + \frac{1}{P_{ii}} \int_0^{t^*} e^{\mu_i (t^* - t)} N_i(t) \, dt. \tag{B-12}$$

The solution in terms of the original co-ordinates can now be obtained by the transformation $z = Ay$, so that

$$z_i = \sum_{j=1}^{2n} a_{ij} y_i, \tag{B-13}$$

which yields both q_i and $\dot{q}_i$.

APPENDIX C

THE INTEGRALS OF THE EIGENFUNCTION PRODUCT NEEDED FOR THE GALERKIN'S METHOD

As shown in chapters IV and VI, the continuous system must be rendered discrete, which may be accomplished by application of Galerkin's method. Here, it is assumed that an approximate solution of the equation of motion of the flexible centre-body has the form of an infinite series,

$$e_o(X,t) = e^{i\omega t} \sum_{\kappa} a_\kappa E_\kappa(X), \qquad (C-1)$$

where the $E_\kappa(X)$ is a set of suitable comparison functions satisfying all the boundary conditions of a clamped-clamped Euler-Bernoulli beam.

In this respect, the added mass, stiffness and damping matrices due to the fluid flow were expressed in terms of the integrals of the eigenfunction products,

$$I_T = \int_0^1 (E_{T\kappa}(X)E_{Tj}(X) + E_{T\kappa}(X)E_{Hj}(X))\, dX,$$

$$I_H = \int_0^1 (E_{H\kappa}(X)E_{Tj}(X) + E_{H\kappa}(X)E_{Hj}(X))\, dX,$$

$$I_T' = \int_0^1 (E_{T\kappa}'(X)E_{Tj}(X) + E_{T\kappa}'(X)E_{Hj}(X))\, dX,$$

$$I_H' = \int_0^1 (E_{H\kappa}'(X)E_{Tj}(X) + E_{H\kappa}'(X)E_{Hj}(X))\, dX, \qquad (C-2)$$

$$I_p = I_T + I_H, \qquad I_p' = I_T' + I_H',$$

$$I_{XT} = \int_0^1 (E_{T\kappa}(X)E_{Tj}(X) + E_{T\kappa}(X)E_{Hj}(X))X\, dX,$$

$$I_{XH} = \int_0^1 (E_{H\kappa}(X)E_{Tj}(X) + E_{H\kappa}(X)E_{Hj}(X))X\, dX,$$

$$I_p'' = \beta_\kappa^2 (I_{XT} - I_{XH}) - \int_0^1 E_\kappa''(X)E_j(X)\, dX,$$

where the subscripts "T" and "H" represent the trigonometric and hyperbolic components of E_κ, respectively. Thus, it is possible to separate each of the integrals into two parts; e.g., $I_T = I_{TT} + I_{TH}$ - one associated with purely trigonometric terms and the other with trigonometric(κ) and hyperbolic(j) ones.

In this Thesis, five-mode Galerkin descriptions of the continuous system are employed in the solution of the equation of motion, so that each of the integrals could be represented by a 5x5 matrix. It is possible to compute the elements of the integrals in the above equation, using an analytical method or a numerical method.

Because of economical benefit in computer programming, the analytical method is adopted for evaluating the elements of the integrals (i.e., I_{TT}, $I_{T'H}$ ····· etc.) in this Thesis; but, the results are compared with those obtained numerically. The numerical results are obtained by using Simpson's rule, which was found to be most suitable for this case. The analytical results and the numerical ones are shown in Tables C-1 and -2, respectively. The numerical results agree with the analytical ones.

On the other hand, the constants I_p, I_p' and I_p'', in view of the orthonormal property of the comparison functions utilized, were given in reference [13], as follows:

$$I_p = \int_0^1 E_\kappa(X) E_j(X)\, dX = \begin{cases} 0, & \text{for } j \neq \kappa \\ 1, & \text{for } j = \kappa \end{cases}$$

$$I_p' = \int_0^1 E_\kappa'(X) E_j(X)\, dX = \begin{cases} \dfrac{4\beta_\kappa^2\beta_j^2}{\beta_\kappa^4 - \beta_j^4}\left((-1)^{\kappa+j} - 1\right), & \text{for } j \neq \kappa \\ 0, & \text{for } j = \kappa \end{cases}$$

(C-3)

$$I_p'' = \int_0^1 E_\kappa''(X) E_j(X) X\, dX = \beta_\kappa^2 (I_{XH} - I_{XT})$$

$$- \frac{4\beta_\kappa^2\beta_j^2(\beta_\kappa\sigma_\kappa - \beta_j\sigma_j)}{\beta_\kappa^4 - \beta_j^4}(-1)^{\kappa+j} - \frac{3\beta_\kappa^4 + \beta_j^4}{\beta_\kappa^4 - \beta_j^4} I_p', \quad \text{for } j \neq \kappa$$

$$- \frac{1}{2}\beta_\kappa\sigma_\kappa(2 - \beta_\kappa\sigma_\kappa), \quad \text{for } j = \kappa$$

where σ_κ and β_κ (or σ_j and β_j) are defined in Appendix A. They are useful to check the results obtained by the analytical and numerical methods.

In fact, it is tedious working to obtain the integrals I_{XT} and I_{XH} analytically. Here, in order to compute the elements of integral I_p", the above equation is used directly in view of the economical benefit in computer programming.

Table C-1 Analytical Results of the Integrals

ITT(J,K)=INTEGRALS OF ETK*ETJ

774939920011436	.000000000000000	-.128853274792887	.000000000000000	-.091472084645410
000000000000000	.873342081666445	000000000000000	-.090860847978029	.000000000000000
-.128853274792887	.000000000000000	.909024097627064	.000000000000000	-.070739587057529
000000000000000	-.090860847978029	000000000000000	.928265809821772	.000000000000001
-.091472084645410	000000000000000	-.070739587057529	.000000000000001	.942125416419723

ITH(J,K)=INTEGRALS OF ETK*EHJ

.000000000000000	.000000000000000	088611259767178	.000000000000000	.078718284251028
.000000000000005	000000000000000	-.000000000000002	.048008430862115	-.000000000000004
-.088611259767203	000000000000010	.000000000000000	-.000000000000005	.029960118777843
-.000000000003437	-.048008430860180	-.000000000000788	.000000000000000	.000000000000507
-.078718284270662	000000000013045	-.029960118785307	.000000000003144	.000000000000000

IHT(J,K)=INTEGRALS OF EHK*ETJ

.000000000000000	.000000000000005	-.088611259767203	-.000000000003437	-.078718284270662
000000000000000	.000000000000000	.090000000000010	-.048008430860180	.000000000013045
.088611259767178	-.000000000000002	.000000000000000	-.000000000000788	-.029960118785307
.000000000000000	.048008430862115	-.000000000000005	.000000000000000	.000000000003144
078718284251028	-.000000000000004	029960118777843	.000000000000507	.000000000000000

IHH(J,K)=INTEGRALS OF EHK*EHJ

.225060079988564	-.000000000000011	128853274792923	.000000000004304	.091472084668227
-.000000000000011	.126657918333572	-.000000000000037	.090860847974379	-.000000000019842
.128853274792923	-.000000000000037	090975902372987	.000000000003181	.070739587075193
000000000004304	090860847974379	.000000000003181	.070734190172534	-.000000000013317
.091472084668227	-.000000000019842	.070739587075193	-.000000000013317	.057874583609149

IT'T(J,K)=INTEGRALS OF ET'K*ETJ

.000000000000000	-4.997371653432706	000000000000000	-2.992445634069410	- 000000000000003
2.997371653432706	.000000000000001	-7.000384301615965	-.000000000000001	-3.667254852428516
.000000000000000	5.000384301615965	.000000000000000	-8.999972951174813	-.000000000000001
.992445634069410	.000000000000000	6.999972951174811	.000000000000000	-11.000001610670720
- 000000000000001	1.667254852428517	.000000000000000	9.000001610670717	-.000000000000002

IT'H(J,K)=INTEGRALS OF ET'K*EHJ

.000000000000002	2 336745843801025	.000000000000002	2.389916571120489	.000000000000003
1.401555905627957	-.000000000000134	2.271033745208532	-.000000000000159	2.411551608648733
-.000000000000287	1.622202581844236	-.000000000000560	2.215351292734058	-.000000000000652
.792616661001032	.000000000053176	1.723049525813948	.000000000080490	2.178219262877507
- 000000000159587	1 096370796194176	-.000000000369737	1 782179455406007	-.000000000498861

IH'T(J,K)=INTEGRALS OF EH'K*ETJ

.000000000000000	.598444094372176	-.000000000000273	1.207383338918478	-.000000000339264
-.336745843801027	-.000000000000001	377797418156325	.000000000027314	.903629204304686
-.000000000000001	-.271033745208398	.000000000000000	.276950474105562	-.000000000129124
-.389916571120491	.000000000000025	-.215351292733498	.000000000000000	.217820545092854
000000000000000	-.411551608648602	.000000000000094	-.178219262957999	.000000000000002

IH'H(J,K)=INTEGRALS OF EH'K*EHJ

-.000000000000002	-1.279834330855183	.000000000000395	-1.511780388007983	.000000000403105
-.720165669144948	.000000000000134	-1.164547695882026	-.000000000051613	-1.374152048995303
.000000000000154	-.835452304118667	.000000000000560	-1.125124843153130	.000000000305199
-.488219611911797	-.000000000028741	-.874875156766943	-.000000000080490	-1.099993165947896
.000000000103108	-.625847951503468	.000000000194212	-.900006814470475	.000000000498861

Table C-2 Numerical Results of the Integrals

ITT(J,K)=INTEGRALS OF ETK*ETJ

.774939919850388	.000000000000000	-.128853276467218	.000000000000000	-.091472089241162
.000000000000000	.873342079983130	.000000000000000	-.090860852596908	.000000000000000
-.128853276467218	.000000000000000	.909024093009563	.000000000000000	-.070739596873819
.000000000000000	-.090860852596908	.000000000000000	.929265800005343	.000000000000000
-.091472089241162	.000000000000000	-.070739596873819	.000000000000000	.942125398491749

ITH(J,K)=INTEGRALS OF ETK*EHJ

-.000000000000006	.000000000000000	.088611260710356	.000000000000000	.078718287748852
.000000000000005	-.000000000000077	-.000000000000003	.048008432787970	-.000000000000004
- 088611260710329	.000000000000022	-.000000000000424	.000000000000004	.029960121993302
-.000000000003305	- 048008432786313	-.000000000000771	-.000000000001350	.000000000000253
- 078718287772238	.000000000019182	-.029960122009308	.000000000010884	-.000000000012255

IHT(J,K)=INTEGRALS OF EHK*ETJ

-.000000000000006	.000000000000005	-.088611260710329	-.000000000003305	-.078718287772238
.000000000000000	-.000000000000077	.000000000000022	-.048008432786313	.000000000019182
.088611260710356	- 000000000000003	-.000000000000424	-.000000000000771	-.029960122009308
.000000000000000	.048008432787970	.000000000000004	-.000000000001350	.000000000010884
.078718287748852	-.000000000000004	.029960121993302	.000000000000253	-.000000000012255

IHH(J,K)=INTEGRALS OF EHK*EHJ

.225060060348563	-.000000000000010	.128853276466659	.000000000004200	.091472089265303
-.000000000000010	.126657920016269	-.000000000000055	.090860852590008	-.000000000024772
.128853276466659	-.000000000000055	.090975906987201	.000000000003121	.070739596884920
.000000000004200	.090860852590008	.000000000003121	.070734199977328	-.000000000018488
.091472089265303	-.000000000024772	.070739596884920	-.000000000018488	.057874601515698

IT'T(J,K)=INTEGRALS OF ET'K*ETJ

.000000000000002	2.336745841076659	.000000000000002	2.389916566172267	.000000000000002
1.401555903962348	-.000000000000128	2.271033730551539	-.000000000000147	2.411551574185962
- 000000000000415	1 622202571382817	-.000000000000805	2.215351246306660	-.000000000000891
.792618659183219	000000000051009	1.723049489717693	.000000000074784	2.178219150086121
-.000000000174688	1.096370780586723	-.000000000410590	1.782179363212716	-.000000000589675

IT'H(J,K)=INTEGRALS OF ET'K*EHJ

.000000000000000	-4.997371653582502	.000000000000001	-2.992445639493663	.000000000000000
2.997371653460497	.000000000000001	-7.000384301752223	.000000000000001	-3.667254858664959
.000000000000001	5.000384301730262	.000000000000001	-8.999972951366624	-.000000000000002
.992445635642961	.000000000000001	6 999972951321562	.000000000000000	-11.000001610903090
.000000000000000	1 667254855305057	.000000000000000	9.000001610861107	-.000000000000001

IH'T(J,K)=INTEGRALS OF EH'K*ETJ

.000000000000000	.598444096804806	-.000000000000079	1.207383366887110	-.000000000249922
-.336745845294017	-.000000000000005	.377797426084113	.000000000028713	903629268062638
.000000000000000	-.271033750860648	.000000000000100	.276950492282876	-.000000000007866
-.389916580511707	.000000000000020	-.215351306857863	-.000000000001545	.217820579760917
.000000000000000	-.411551637666602	.000000000000250	-.178219291365601	.000000000143044

IH'H(J,K)=INTEGRALS OF EH'K*EHJ

-.000000000000002	-1 279834337589577	.000000000000172	-1.511780428889665	.000000000314117
-.720165673200070	.000000000000134	-1.164547727843871	-.000000000052645	-1.374152167942588
.000000000000256	-.835452326946606	000000000000560	-1.125124940514880	000000000217448
-.488219625561150	-.000000000028173	- 874875232493575	-.000000000080491	-1.099993418218183
.000000000126343	-.625848005644773	.000000000250022	-.900007004656320	000000000498810

APPENDIX D

THE COMPUTER PROGRAM

The program is used for calculating the eigenfrequencies of the system; moreover, from the results, it is possible to determine the region of the stability of the flexible centre-body subjected to an annular flow. The dynamical behaviour of the system can be studied at different annular mean flow velocities. The same program is applied to the system for evaluating the inviscid effects and/or the unsteady and steady effects by changing the coefficient "Delta".

The whole program is written in FORTRAN IV Language. It can be run on a personal digital computer. All calculations, except subroutine SORT, are carried out in real and complex arithmetic with double precision. The program has the following structure:

(1) MAIN PROGRAM (after calculating all the necessary eigenvalues, the elements of mass, damping and stiffness matrix are computed);

(2) SUBROUTINE ANA (it is used for obtaining the elements of the integrals shown in Appendix B);

(3) SUBROUTINE ZANLYT (as an IMSL subroutine, it is useful for calculating the roots of functions; therefore, it could be used for obtaining the eigenfrequencies of the system with the aid of the subroutine DET and the necessary subroutines - i.e., SUBROUTINE UERTST, USPKD and UGETIO);

(4) SUBROUTINE DET (it is called by subroutine ZANLYT to compute the determinent - see equation 4-9);

(5) SUBROUTINE SORT (it is called by MAIN PROGRAM to sort the eigenfrequencies according to ascending order of magnitude).

Eventually, the annular mean flow velocity is incremented in the MAIN PROGRAM and the iteration procedure is repeated, as mentioned before.

A sample listing of the program and its output results (with ℓ=20, h=0.1, σ=323.74 and μ=0.007) are shown in the pages that follow.

```
      PROGRAM RZVFS
      IMPLICIT REAL*8 (A-H,O-Z)
      DIMENSION EM(5,5),EC(5,5),EK(5,5),D1(5,5),D2(5,5),D3(5,5),D4(5,5)
      DIMENSION D5(5,5),BT(5),SGM(5),AI(5),INFER(10),WT(5),WH(5)
      DIMENSION GT(5),GH(5),DEL(3),A(5,5)
      REAL DATA1(5,3),DATA2(5,3)
      COMPLEX*16 EI(10),DET,CA(5,5)
      COMMON EM,EC,EK
      EXTERNAL DET
      CHARACTER*80 FNAME2
C
  448 FORMAT(A)
      WRITE(*,452)
  452 FORMAT(' OUTPUT FILE NAME-'\)
      READ(*,448) FNAME2
      OPEN(6,FILE=FNAME2,STATUS='NEW')
C
      DATA EPS,NSIG,KN,NGUESS,IN,ITMAX/.1D-3,11,0,0,10,100/
      DATA AI,NITER,N/4.6D0,7.7D0,10.8D0,14.0D0,17.2D0,50,5/
      DATA PIE,DATA1/.3141592D1,15*0.0/
      DETA DEL/0.D0,2.D0,1.D0/
C
C     SECANT METHOD
C
      DO 2 I=1, N
       XX=AI(I)
       X=AI(I)+0.2D0
       F=DCOS(X)*DCOSH(X)-.1D1
       FF=DCOS(XX)*DCOSH(XX)-.1D1
        DO 4 J=1, NITER
        XN=1.D6*(X*FF-XX*F)/((FF-F)*1.D6)
        FN=DCOS(XN)*DCOSH(XN)-.1D1
        F=FF
        FF=FN
        X=XX
        XX=XN
        C=DABS(FF-F)
        CN=.1D-14
        IF(C.LT.CN) GO TO 6
    4   CONTINUE
    6   SGM(I)=(DCOSH(XN)-DCOS(XN))/(DSINH(XN)-DSIN(XN))
        BT(I)=XN
    2   WRITE(6,50)I,BT(I),I,SGM(I)
C
    8 WRITE(*,80)
      READ(*,*) FM,BL,HO,RA,UFI,SS,IK,VOF
      WRITE(*,52) FM,BL,HO,RA,UFI,SS,IK,VOF
      WRITE(*,82)
      READ(*,*) IANS
      IF(IANS.EQ.2) GO TO 8
      H=HO/RA
   10  WRITE(*,84)
       READ(*,*) BM,E,POI,VFOF,IDELTA
       WRITE(*,54) BM,E,POI,VFOF,IDELTA
```

```
      WRITE(*,82)
      READ(*,*) IANS
      IF(IANS.EQ.2) GO TO 10
      WRITE(6,55) BM,FM,BL,RA,HO,VOF,E,POI,VFOF,IDELTA
      CV=.125D1
      DO 12 J=1, N
       BJ=BT(J)
       SGMJ=SGM(J)
        DO 12 K=1, N
         BK=BT(K)
        IF(J.NE.1) GO TO 18
        RK=BK/(BL/RA)
        RKS=RK**2
        QK=DSQRT(RKS+CV)
        Q=QK*H
        GT(K)=(-QK+.5D0*DTANH(Q))/(QK**2-.25D0)/DTANH(Q)
        RT=(QK*DSINH(Q)-.5D0*DCOSH(Q))/(-QK*DCOSH(Q)+.5D0*DSINH(Q))
        IF(RKS.LT.CV) GO TO 14
        CK=DSQRT(RKS-CV)
        C=CK*H
        GH(K)=(CK-.5D0*DTAN(C))/(CK**2+.25D0)/DTAN(C)
        RH=(CK*DSIN(C)+.5D0*DCOS(C))/(CK*DCOS(C)-.5D0*DSIN(C))
        GO TO 16
   14     CK=DSQRT(CV-RKS)
        C=CK*H
        GH(K)=(-CK+.5D0*DTANH(C))/(CK**2-.25D0)/DTANH(C)
        RH=(-CK*DSINH(C)+.5D0*DCOSH(C))/(CK*DCOSH(C)-.5D0*DSINH(C))
C
   16   IF(IDELTA.EQ.1) GO TO 18
        DA=0.0D0
        SIMPT=FT(DA,RT,Q)
        SIMPH=FH(DA,RH,C)
        XH=DA
        DO 20 I=1,NITER
         XH=XH+DH
         TERMT=.2D1*FT(XH,RT,Q)
         TERMH=.2D1*FH(XH,RH,C)
         SIMPT=SIMPT+TERMT
         SIMPH=SIMPH+TERMH
         IF(I.NE.I/2*2) SIMPT=SIMPT+TERMT
   20    IF(I.NE.I/2*2) SIMPH=SIMPH+TERMH
        WT(K)=DH*(SIMPT-TERMT/.2D1)/.3D1
        WH(K)=DH*(SIMPH-TERMH/.2D1)/.3D1
C
   18    SGMK=SGM(K)
         CALL ANA(BK,BJ,SGMK,SGMJ,A1,A2,A3,A4)
         D1(J,K)=A1
         D2(J,K)=A2
         D3(J,K)=A3
         D4(J,K)=A4
         IF(IDELTA.EQ.1) GO TO 12
         B4=BK**4-BJ**4
         X=4.D0*(BK*BJ)**2*(BK*SGMK-BJ*SGMJ)/B4*(-1.D0)**(K+J)
         D5(J,K)=(X-(3.D0*BK**4+BJ**4)/B4*(A3+A4))/BK**2
```

```
  12   CONTINUE
         CI=.25D0*PIE*(RA**4-(VFOF*RA)**4)
         AREA=PIE*RA**2
         SAREA=PIE*(RA**2-(VFOF*RA)**2)
         UREF=DSQRT(E*CI/(BM*SAREA*BL**2))
         UREF1=DSQRT(E*CI/(FM*AREA*BL**2))
         RO=PIE*BL**2/SAREA*(FM/BM)
         RM=FM*AREA/(FM*AREA+BM*AREA)
         WRITE(6,56) RO,RM,UREF,UREF1,H
         WRITE(*,56) RO,RM,UREF,UREF1,H
         IF(IDELTA.NE.1) GO TO 22
CCCCCCCCCCCCCCCCCCCCCCCCCCCCCC
C          INVISCID           C
CCCCCCCCCCCCCCCCCCCCCCCCCCCCCC
         WRITE(6,86)
         WRITE(6,88) (I,I=1,5)
         WRITE(6,90)
         UF=UFI
  22   DO 24 L=1,IK
        UO=UF/UREF
        UO1=UF/UREF1
        WRITE(*,*)UF,UO,UO1
        DO 26 J=1,N
         DO 26 K=1, N
         BK=BT(K)
         EM1=(1.D0-RO*GT(K)*(RA/BL)**2)*D1(J,K)
         EM(J,K)=EM1+(1.D0-RO*GH(K)*(RA/BL)**2)*D2(J,K)
         ECN1=GT(K)*D3(J,K)+GH(K)*D4(J,K)
         EC(J,K)=-RO*UO*(RA/BL)**2*.2D1*ECN1
         EKN1=BK**4*(D1(J,K)+D2(J,K))
         EKN2=GT(K)*D1(J,K)-GH(K)*D2(J,K)
  26     EK(J,k)=EKN1+RO*(UO*BK*RA/BL)**2*EKN2
       CALL ZANLYT(DET,EPS,NSIG,KN,NGUESS,IN,EI,ITMAX,INFER,IER)
       DO 28 K=1,10
  28    WRITE(*,58)K,EI(K)
       CALL SORT(EI,L,DATA1,DATA2)
       WRITE(6,60) UO1,((DATA2(I,J),J=1,3),I=1,5)
       DO 30 I=1,5
        DO 30 K=1,3
  30    DATA1(I,K)=DATA2(I,K)
  24   UF=UF+SS
       IF(IDELTA.EQ.1) GO TO 47
CCCCCCCCCCCCCCCCCCCCCCCCCCCCCCCCCCCCC
C       INVISCID + UNSTEADY        C
CCCCCCCCCCCCCCCCCCCCCCCCCCCCCCCCCCCCC
       WRITE(6,92)
       WRITE(6,88) (I,I=1,5)
       WRITE(6,90)
       UF=UFI
       DO 34 L=1,IK
        UO=UF/UREF
        UO1=UF/UREF1
        RE=.2D1*FM*UF*HO/VOF
        WRITE(*,*)UF,UO,UO1,RE
```

```
      DO 36 J=1,N
       DO 36 K=1, N
       BK=BT(K)
       ECN1=GT(K)*D3(J,K)+GH(K)*D4(J,K)
       ECV1=WT(K)*GT(K)*D1(J,K)+WH(K)*GH(K)*D2(J,K)
       ECN=-RO*UO*(RA/BL)**2*.2D1*ECN1
       ECV=-RO*UO*(RA/BL)*1.2D1*(2.D0+H)*ECV1/(RE*H**2)
       EC(J,K)=ECN+ECV
       EKN1=BK**4*(D1(J,K)+D2(J,K))
       EKN2=GT(K)*D1(J,K)-GH(K)*D2(J,K)
       EKN=EKN1+RO*(UO*BK*RA/BL)**2*EKN2
       EKV1=WT(K)*GT(K)*D3(J,K)+WH(K)*GH(K)*D4(J,K)
       EKV=-RO*UO**2*(RA/BL)*1.2D1*(2.D0+H)*EKV1/(RE*H**2)
 36    EK(J,K)=EKN+EKV
      CALL ZANLYT(DET,EPS,NSIG,KN,NGUESS,IN,EI,ITMAX,INFER,IER)
      DO 38 K=1,10
 38    WRITE(*,58)K,EI(K)
      CALL SORT(EI,L,DATA1,DATA2)
      WRITE(6,60) UO1,((DATA2(I,J),J=1,3),I=1,5)
      DO 40 I=1,5
       DO 40 K=1,3
 40    DATA1(I,K)=DATA2(I,K)
 34   UF=UF+SS
CCCCCCCCCCCCCCCCCCCCCCCCCCCCCCCCCCCCCCCCC
C      INVISCID + UNSTEADY + STEADY       C
CCCCCCCCCCCCCCCCCCCCCCCCCCCCCCCCCCCCCCCCC
      WRITE(6,94)
      DO 51 I1=1,3
      DEL1=1.D0-.5D0*DEL(I1)
      IF(I1.NE.3) GO TO 42
 41   WRITE(*,96)
      READ(*,*) T
 42   UF=UFI
      WRITE(6,98)I1,T
      WRITE(6,88) (I,I=1,5)
      WRITE(6,90)
      DO 44 L=1,IK
       UO=UF/UREF
       UO1=UF/UREF1
       RE=.2D1*FM*UF*HO/VOF
       WRITE(*,*)UF,UO,UO1,RE
       DO 46 J=1,N
        DO 46 K=1, N
        BK=BT(K)
        IF(I1.NE.1) GO TO 43
        X=D3(J,K)+D4(J,K)
        XX=D2(J,K)-D1(J,K)
        A(J,K)=1.D0/H*X-BK**2*(1.D0+1.D0/H)*(XX*DEL1-D5(J,K))
        TM=DEL(I1)*(2.D0-DEL(I1))*(1.D0-2.D0*POI)*T*BK**2
 43     ECN1=GT(K)*D3(J,K)+GH(K)*D4(J,K)
        ECV1=WT(K)*GT(K)*D1(J,K)+WH(K)*GH(K)*D2(J,K)
        ECN=-RO*UO*(RA/BL)**2*.2D1*ECN1
        ECV=-RO*UO*(RA/BL)*1.2D1*(2.D0+H)*ECV1/(RE*H**2)
        EC(J,K)=ECN+ECV
```

```
      EKN1=BK**4*(D1(J,K)+D2(J,K))
      EKN2=GT(K)*D1(J,K)-GH(K)*D2(J,K)
      EKN=EKN1+RO*(UO*BK*RA/BL)**2*EKN2
      EKV1=WT(K)*GT(K)*D3(J,K)+WH(K)*GH(K)*D4(J,K)
      EKV2=2.4D1*RO*UO**2(RA/BL)/RE*A5(J,K)-TM*(D2(J,K)-D1(J,K))
      EKV=-RO*UO**2*(RA/BL)*1 2D1*(2.D0+H)*EKV1/(RE*H**2)
 46   EK(J,K)=EKN+EKV+EKV2
      CALL ZANLYT(DET,EPS,NSIG,KN,NGUESS,IN,EL,ITMAX,INFER,IER)
      DO 48 K=1,10
 48    WRITE(*,58)K,EI(K)
      CALL SORT(EI,L,DATA1,DATA2)
      WRITE(6,60) UO1,((DATA2(I,J),J=1,3),I=1,5)
      DO 50 I=1,5
       DO 50 K=1,3
 40    DATA1(I,K)=DATA2(I,K)
 44   UF=UF+SS
      IF(I1.NE.3) GO TO 51
      WRITE(*,100)
      READ(*,*) IANS
      IF(IANS.EQ.1) GO TO 41
51   CONTINUE
47   CONTINUE
C
 50   FORMAT(5X,'BT(',I1,')=',F17.14,5X,'SGM(',I1,')=',F17.14)
 52   FORMAT(//,5X,'FM=',D9.4,5X,'BL=',D9.4,5X,'HO=',D9.4,5X,'RA=',D9.4,
     1   /,5X'UFI=',D9.4,5X,'SS=',D9.4,5X,'IK=',I5,5X,'VOF=',D9.4)
 54   FORMAT(//,5X,'BM=',D9.4,5X,'E=',D9.4,5X,'POI=',D9.4,5X,/,5X,
     1       'VFOF=',D9.4,5X,'IDELTA',I1)
 55   FORMAT(//,5X,'BD=',D9.4,5X,'FD=',D9.4,5X,'BL=',D9.4,5X,
     1       'RA=',D9.4,5X,'HO=',D9.4,/,5X,'VOF=',D8.3,5X,'E=',D10.5,
     1       5X,'POI=',D8.3,5X,'VFOF=',D7.2,5X,'IDELTA=',I1)
 56   FORMAT(//,5X,'RO=',F9.4,5X,'RM=',F9.4,5X,'URF=',F9.4,5X,
     1       'URF1=',F9.4,5X,'H=',F9.4)
 58   FORMAT(5X,'EIGENVALUE(',I2,')=',2D16.8)
 60   FORMAT(2X,F7.4,5(2X,3F7.2))
C
 80   FORMAT(' ENTER: (1) FM=MASS OF THE FLUID',/,7X,'(2) BL=LENGTH OF
     1BODY',/,7X,'(3) HO=CLEARANCE',/,7X,'(4) RA=RADIUS OF BODY',/,7X,
     1'(5) UFI=IN. FLUID VEL',/,7X,'(6) SS= STEP SIZE OF F.VEL',/,
     17X,'(7) IK= ITERATION NO.',/,7X,'(8) VOF=VISCOSITY OF FLUID')
 82   FORMAT(' *** IS THIS TRUE ? ***  1= YES    2=NO')
 84   FORMAT(' ENTER: (1) BM=MASS OF THE BODY',/,7X,'(2) E=YOUNG'S
     1MODULUS',/,7X,'(3) POI=POISSON'RATIO',/,7X,'(4) VFOF=VOID FACTOR
     1OF FLEX. BODY',/,7X,'(5) IDELTA = 1, ONLY INVISCID EFFECT',/,
     1 18X,'= 2, ONLY VISCOUS EFFECT',/,18X,'= 3, BOTH EFFECTS')
 86   FORMAT(///,5X,'INVISCID FLOW')
 88   FORMAT(/,4X,'UO2',5X,5(7X,1('MODE    ',I1),7X))
 90   FORMAT(/,10X,5('  REAL1  REAL2   IMAG  '),/,3X,125('-'))
 92   FORMAT(///,5X,'INVISCID + UNSTEADY')
 94   FORMAT(///,5X,'INVISCID + UNSTEADY + STEADY')
 96   FORMAT(/,'T=?')
 98   FORMAT(//,5X,'CASE  ',I1,5X,'T=',F9.4)
 100  FORMAT(/,'*** DO YOU WANT ANOTHER T ? *** 1=YES,  2=NO')
C
```

```
      FUNCTION FH(Z,RH,C)
      DOUBLE PRECISION Z,C,FH,RH
      FH-(DCOS(C)+RH*DSIN(C))*DEXP(-.5DO*Z)/(1.DO+Z)
      RETURN
      END
C
      FUNCTION FT(Z,RT,Q)
      DOUBLE PRECISION Z,Q,FT,RT
      FT-(DCOSH(Q)+RT*DSINH(Q))*DEXP(-.5DO*Z)/(1.DO+Z)
      RETURN
      END
C
C
      STOP
      END
C
C
C
C
C
C
C
C
C
C
C
C
C
C
C
C
C
C
C
C
C
C
C
C
C
C
C
C
C
C
C
C
C
C
C
C
C
C
C
```

```
CCCCCCCCCCCCCCCCCCCCCCCCCCCCCCCCCCCCCCCCCCCCCC
C       *** SUBROUTINE ANA ***              C
CCCCCCCCCCCCCCCCCCCCCCCCCCCCCCCCCCCCCCCCCCCCCC
      SUBROUTINE ANA(BK,BJ,SGMK,SGMJ,A1,A2,A3,A4)
      IMPLICIT REAL*8 (A-H,O-Z)
      IF(BK.EQ.BJ) GO TO 10
      BP=BK+BJ
      BM=BK-BJ
      SUMA=DSIN(BM)/.2D1/BM+DSIN(BP)/.2D1/BP
      SUMB=SGMK*(DSIN(BM)/.2D1/BM-DSIN(BP)/.2D1/BP)
      SUMC=-DCOS(BM)/.2D1/BM+DCOS(BP)/.2D1/BP+BJ/(BP*BM)
      SUMD=SGMK*(DCOS(BM)/.2D1/BM+DCOS(BP)/.2D1/BP-BK/(BP*BM))
      TT=SUMA+SGMJ*(SUMB+SUMC)+SUMD
      GO TO 20
   10 SUM1=DSIN(.2D1*BJ)/.4D1/BJ+SGMJ**2*(.5D0-DSIN(.2D1*BJ)/.4D1/BJ)
      TT=SUM1+.5D0-SGMJ*(DSIN(BJ))**2/BJ
C
   20 BS=BJ**2+BK**2
      SUMA=(BJ*DCOS(BK)+BK*DSIN(BK))/BS
      SUMB=SGMK*(BJ*DSIN(BK)-BK*DCOS(BK))/BS
      SUMC=(BJ+SGMK*BK)/BS
      SUMD=SGMK*(BJ*DSIN(BK)+BK*DCOS(BK))/BS
      SUME=(-BJ*DCOS(BK)+BK*DSIN(BK))/BS
      SUMF=(SGMK*BK-BJ)/BS
      SUM1=.5D0*(SGMJ-.1D1)*DEXP(BJ)*(SUMA-SUMB)
      SUM2=-.5D0*(SGMJ-.1D1)*SUMC
      SUM3=-.5D0*(SGMJ+.1D1)*DEXP(-BJ)*(SUMD+SUME)
      SUM4=.5D0*(SGMJ+.1D1)*SUMF
      TH=SUM1+SUM2+SUM3+SUM4
C
       SKP1=SGMK+.1D1
       SKM1=SGMK-.1D1
       SUMA=SKM1*DEXP(BK)*(BK*DCOS(BJ)+BJ*DSIN(BJ))/BS
       SUMB=SKM1*DEXP(BK)*SGMJ*(BK*DSIN(BJ)-BJ*DCOS(BJ))/BS
       SUMC=SKM1*(BK+SGMJ*BJ)/BS
       SUMD=SKP1*DEXP(-BK)*SGMJ*(BK*DSIN(BJ)+BJ*DCOS(BJ))/BS
       SUME=SKP1*DEXP(-BK)*(-BK*DCOS(BJ)+BJ*DSIN(BJ))/BS
       SUMF=SKP1*(SGMJ*BJ-BK)/BS
       SUM1=.5D0*(SUMA-SUMB-SUMC)
       SUM2=-.5D0*(SUMD+SUME-SUMF)
       HT=SUM1+SUM2
C
        IF (BK.EQ.BJ) GO TO 40
        APB=((.1D1+SGMJ)*(.1D1+SGMK))/(.4D1*BP)
        AMB=((.1D1-SGMJ)*(.1D1-SGMK))/(.4D1*BP)
        SMA=AMB*DEXP(BP)-APB*DEXP(-BP)
        SMB=(.1D1-SGMK*SGMJ)*DSINH(BM)+(SGMK-SGMJ)*(.1D1-DCOSH(BM))
         HH=SMB/(.2D1*BM)+(SGMK+SGMJ)/(.2D1*BP)+SMA
        GO TO 50
   40   AMB=((.1D1-SGMJ)**2)/(.8D1*BJ)
        APB=((.1D1+SGMJ)**2)/(.8D1*BJ)
        SM1=AMB*DEXP(.2D1*BJ)-APB*DEXP(-.2D1*BJ)
        HH=(SGMJ/BJ+(.1D1-SGMJ**2))/.2D1+SM1
C
```

```
 50     SKB=SGMK*BK*BJ
        SUMA=(BK*BJ+SGMK*BK**2)*DEXP(BJ)*DSIN(BK)/BS
        SUMB=(SKB-BK**2)*DEXP(BJ)*DCOS(BK)/BS
        SUMC=(BK**2-SKB)/BS
        SUMD=(SGMK*BK**2-BK*BJ)*DEXP(-BJ)*DSIN(BK)/BS
        SUME=-(SKB+BK**2)*DEXP(-BJ)*DCOS(BK)/BS
        SUMF=+(BK**2+SKB)/BS
        SUM1=.5D0*(1.D0-SGMJ)*(SUMA+SUMB+SUMC)
        SUM2=.5D0*(1.D0+SGMJ)*(SUMD+SUME+SUMF)
        TDH=SUM1+SUM2
C
        IF(BK.EQ.BJ) GO TO 60
        SB=SGMK*SGMJ*BK
        SUMA=(BK+SB)*DCOS(BM)/.2D1/BM
        SUMB=(BK-SB)*DCOS(BP)/.2D1/BP
        SUMC=(SGMJ*BK-SGMK*BK)*DSIN(BM)/.2D1/BM
        SUMD=-(SGMJ*BK+SGMK*BK)*DSIN(BP)/.2D1/BP
       SUME=-(BK+SB)/.2D1/BM-(BK-SB)/.2D1/BP
       TDT=SUMA+SUMB+SUMC+SUMD+SUME
       GO TO 70
 60    TDT=-.5D0*((DSIN(BJ))**2+SGMJ*DSIN(.2D1*BJ)-(SGMJ*DSIN(BJ))**2)
C
 70     SKM=BK*.5D0*(1.D0-SGMK)
        SKP=BK*.5D0*(1.D0+SGMK)
        SUMA=-SKM*(DEXP(BK)*(BK*DCOS(BJ)+BJ*DSIN(BJ))-BK)/BS
        SUMB=SKP*(DEXP(-BK)*(-BK*DCOS(BJ)+BJ*DSIN(BJ))+BK)/BS
        SUMC=SKM*(DEXP(BK)*(BK*DSIN(BJ)-BJ*DCOS(BJ))+BJ)/BS
        SUMD=SKP*(DEXP(-BK)*(BK*DSIN(BJ)+BJ*DCOS(BJ))-BJ)/BS
       HDT=SUMA+SUMB+SGMJ*(SUMC+SUMD)
C
       IF(BK.EQ.BJ) GO TO 80
       SBK=SGMK*SGMJ*BK
       APB=(BK*(.1D1+SGMJ)*(.1D1+SGMK))/(.4D1*BP)
       AMB=(BK*(.1D1-SGMJ)*(.1D1-SGMK))/(.4D1*BP)
       SMA=AMB*DEXP(BP)+APB*DEXP(-BP)-(BK+SBK)/(.2D1*BP)
       SMB=(BK-SBK)*DCOSH(BM)-(BK-SBK)-(SGMK-SGMJ)*DSINH(BM)*BK
        HDH=SMB/(.2D1*BM)+SMA
        GO TO 85
 80     APB=((.1D1+SGMJ)**2)/.8D1
        AMB=((.1D1-SGMJ)**2)/.8D1
        SMA=AMB*DEXP(.2D1*BJ)+APB*DEXP(-.2D1*BJ)
         HDH=SMA-(.1D1+SGMJ**2)/.4D1
C
 85     A1=TT+TH
        A2=HT+HH
        A3=TDT+TDH
        A4=HDT+HDH
        RETURN
        END
C
C
C
C
C
```

```
CCCCCCCCCCCCCCCCCCCCCCCCCCCCCCCCCCCCCCCCCCCCCCCCCCC
C          COMPLEX FUNCTION DET                    C
CCCCCCCCCCCCCCCCCCCCCCCCCCCCCCCCCCCCCCCCCCCCCCCCCCC
      COMPLEX*16 FUNCTION DET(EI)
      IMPLICIT REAL*8(A-H,O-Z)
      DIMENSION CA(5,5),L(5),M(5),DA2(5,5),DA1(5,5),DA0(5,5)
      COMPLEX*16 CA,PIVOT,HOLD,EI
      COMMON DA2,DA1,DA0
      N=5
      DO 1 I=1,N
        DO 1 J=1,N
    1     CA(I,J)=EI**2*DA2(I,J)+EI*DA1(I,J)+DA0(I,J)
      N1=N-1
      DET=(1.D0,0.D0)
      DO 10 I=1,N
      L(I)=I
   10 M(I)=I
      DO 100 LMNT=1,N1
      PIVOT=(0.D0,0.D0)
      DO 20 I=LMNT,N
      NROW=L(I)
      DO 20 J=LMNT,N
      NCOL=M(J)
      IF(CDABS(PIVOT).GE.CDABS(CA(NROW,NCOL))) GO TO 20
      NPR=I
      NPC=J
      PIVOT=CA(NROW,NCOL)
   20 CONTINUE
      IF(NPR.EQ.LMNT) GO TO 22
      DET=-DET
      KEEP=L(NPR)
      L(NPR)=L(LMNT)
      L(LMNT)=KEEP
   22 IF(NPC.EQ.LMNT) GO TO 26
      DET=-DET
      KEEP=M(NPC)
      M(NPC)=M(LMNT)
      M(LMNT)=KEEP
   26 DET=DET*PIVOT
      IF(CDABS(PIVOT).LT.0.1D-8) GO TO 333
      JAUG=LMNT+1
      NPR=L(LMNT)
      NPC=M(LMNT)
      DO 100 I=JAUG,N
      NROW=L(I)
      HOLD=CA(NROW,NPC)/PIVOT
      DO 100 J=JAUG,N
      NCOL=M(J)
  100 CA(NROW,NCOL)=CA(NROW,NCOL)-HOLD*CA(NPR,NCOL)
      DET=DET*CA(NROW,NCOL)
  333 RETURN
      END
C
C
```

```
CCCCCCCCCCCCCCCCCCCCCCCCCCCCCCCCCCCCCCCCCCCCCCCC
C        SUBROUTINE  ZANLYT                      C
CCCCCCCCCCCCCCCCCCCCCCCCCCCCCCCCCCCCCCCCCCCCCCCC
      SUBROUTINE ZANLYT(F,EPS,NSIG,KN,NGUESS,N,X,ITMAX,INFER,IER)
      DOUBLE PRECISION RZERO,RTEN,RHUN,RP01,AX,EPS1,QZ,EPS,TPQ
      DIMENSION X(1),INFER(1)
      COMPLEX*16 X,D,DD,DEN,FPRT,FRT,H,RT,T1,T2,T3,TEM,Z0,Z1,Z2,BI,F,
     1           XX,XL,Y0,Y1,Y2,X0,ZERO,P1,ONE,FOUR,P5
      DATA ZERO,P1,ONE/(.0D0,.0D0);(.1D0,.0D0),(1.D0,.0D0)/
      DATA FOUR,P5/(4.D0,.0D0),(.5D0,.0D0)/
      DATA RZERO,RTEN,RHUN,AX,ICKMAX,RP01/.0D0,1.D1,1.D2,.1D0,3,.01D0/
      IER=0
      IF(N.LT.1) GO TO 9005
      EPS1=RTEN**(-NSIG)
      EPS1=DMIN1(EPS1,RP01)
      KNP1=KN+1
      KNPN=KN+N
      KNPNG=KN+NGUESS
      DO 5 I=1,KNPN
      INFER(I)=0
      IF(I.GT.KNPNG) X(I)=ZERO
    5 CONTINUE
      L=KNP1
   10 JK=0
      ICK=0
      XL=X(L)
   15 IC=0
      H=AX
      H=P1*H
      IF(CDABS(XL).GT.AX) H=P1*XL
      RT=XL+H
      NN=20
      GO TO 50
   20 Z0=FPRT
      Y0=FRT
      X0=RT
      RT=XL-H
      NN=25
      GO TO 50
   25 Z1=FPRT
      Y1=FRT
      H=XL-RT
      D=H/(RT-X0)
      RT=XL
      NN=30
      GO TO 50
   30 Z2=FPRT
      Y2=FRT
   35 DD=ONE+D
      T1=Z0*D*D
      T2=Z1*DD*DD
      XX=Z2*DD
      T3=Z2*D
      BI=T1-T2+XX+T3
```

```
      DEN=BI*BI-FOUR*(XX*T1-T3*(T2-XX))
      T1=CDSQRT(DEN)
      QZ=RHUN*DMAX1(CDABS(BI),CDABS(T1))
      T2=BI+T1
      TPQ=CDABS(T2)+QZ
      IF(TPQ.EQ.QZ) T2=ZERO
      T3=BI-T1
      TPQ=CDABS(T3)+QZ
      IF(TPQ.EQ.QZ) T3=ZERO
      DEN=T2
      QZ=CDABS(T3)-CDABS(T2)
      IF(QZ.GT.RZERO) DEN=T3
      NN=30
      IF(CDABS(DEN).LE.RZERO) GO TO 65
      D=-XX/DEN
      D=D+D
      H=D*H
      RT=RT+H
      IF(CDABS(H).LE.EPS1*DMAX1(CDABS(RT),AX)) GO TO 70
      IF(IC.NE.0) GO TO 15
      NN=40
      GO TO 50
   40 QZ=CDABS(FPRT)-CDABS(Z2)*RTEN
      IF(QZ.GE.RZERO) GO TO 45
      Z0=Z1
      Z1=Z2
      Z2=FPRT
      Y0=Y1
      Y1=Y2
      Y2=FRT
      GO TO 35
   45 CONTINUE
      D=D*P5
      H=H*P5
      RT=RT-H
   50 JK=JK+1
      IF(JK.GT.ITMAX) GO TO 75
      FRT=F(RT)
      FPRT=FRT
      IF(L.EQ.1) GO TO 60
      LM1=L-1
      DO 55 I=1,LM1
      TEM=RT-X(I)
      IF(CDABS(TEM).EQ.RZERO) GO TO 65
   55 FPRT=FPRT/TEM
   60 CONTINUE
      IF(CDABS(FPRT).LE.EPS.AND.CDABS(FRT).LE.EPS) GO TO 80
      IF(NN.EQ.20) GO TO 20
      IF(NN.EQ.25) GO TO 25
      IF(NN.EQ.30) GO TO 30
      IF(NN.EQ.40) GO TO 40
   65 CONTINUE
      IF(IC.NE.0) GO TO 15
```

```
      TEM=RTEN*EPS1
      IF(CDABS(RT).GT.AX) TEM=TEM*RT
      RT=RT+TEM
      D=(H+TEM)*D/H
      H=H+TEM
      GO TO 50
   70 CONTINUE
      IF(IC.NE.0) GO TO 80
      IC=1
      Z0=Y1
      Z1=Y2
      Z2=F(RT)
      XL=RT
      ICK=ICK+1
      IF(ICK.LE.ICKMAX) GO TO 35
      JK=ITMAX+JK
   75 IER=33
   80 X(L)=RT
      INFER(L)=JK
      L=L+1
      IF(L.LE.KNPN) GO TO 10
      IF(IER.NE.0) CALL UERTST(IER,'ZANLYT')
 9005 RETURN
      END
C
C
C
C
C
C
C
C
C
C
C
C
C
C
C
C
C
C
C
C
C
C
C
C
C
C
C
C
C
C
```

```
CCCCCCCCCCCCCCCCCCCCCCCCCCCCCCCCCCCCCCCCCCCCCCCCCCCCCCCCCCCCCCCCCCCC
C       SUBROUTINE       UERTST                                      C
CCCCCCCCCCCCCCCCCCCCCCCCCCCCCCCCCCCCCCCCCCCCCCCCCCCCCCCCCCCCCCCCCCCC
      SUBROUTINE UERTST(IER,NAME)
      INTEGER IER,I,IEQ,IEQDF,IOUNIT,LEVEL,LEVOLD,NIN,NMTB
      INTEGER NAME(1),NAMEQ(6),NAMSET(6),NAMUPK(6)
      DATA NAMSET/'U','E','R','S','E','T'/
      DATA NAMEQ/6*' '/
      DATA LEVEL,IEQDF,IEQ/4,0,'-'/
      CALL USPKD(NAME,6,NAMUPK,NMTB)
      CALL UGETIO(1,NIN,IOUNIT)
      IF(IER.GT.999) GO TO 25
      IF(IER.LT.-32) GO TO 55
      IF(IER.LE.128) GO TO 5
      IF(LEVEL.LT.1) GO TO 30
      IF(IEQDF.EQ.1) WRITE(IOUNIT,35) IER,NAMEQ,IEQ,NAMUPK
      IF(IEQDF.EQ.0) WRITE(IOUNIT,35) IER,NAMUPK
      GO TO 30
    5 IF(IER.LE.64) GO TO 10
      IF(LEVEL.LT.2) GO TO 30
      IF(IEQDF.EQ.1) WRITE(IOUNIT,40) IER,NAMEQ,IEQ,NAMUPK
      IF(IEQDF.EQ.0) WRITE(IOUNIT,40) IER,NAMUPK
      GO TO 30
   10 IF(IER.LE.32) GO TO 15
      IF(LEVEL.LT.3) GO TO 30
      IF(IEQDF.EQ.1) WRITE(IOUNIT,45) IER,NAMEQ,IEQ,NAMUPK
      IF(IEQDF.EQ.0) WRITE(IOUNIT,45) IER,NAMUPK
      GO TO 30
   15 CONTINUE
      DO 20 I=1,6
      IF(NAMUPK(I).NE.NAMSET(I)) GO TO 25
   20 CONTINUE
      LEVOLD=LEVEL
      LEVEL=IER
      IER=LEVOLD
      IF(LEVEL.LT.0) LEVEL=4
      IF(LEVEL.GT.4) LEVEL=4
      GO TO 30
   25 CONTINUE
      IF(LEVEL.LT.4) GO TO 30
      IF(IEQDF.EQ.1) WRITE(IOUNIT,50) IER,NAMEQ,IEQ,NAMUPK
      IF(IEQDF.EQ.0) WRITE(IOUNIT,50) IER,NAMUPK
   30 IEQDF=0
      RETURN
   35 FORMAT(19H *** TERMINAL ERROR,10X,7H(IER = ,I3,
     1       20H) FROM IMSL ROUTINE ,6A1,A1,6A1)
   40 FORMAT(27H *** WARNING WITH FIX ERROR,2X,7H(IER = ,I3,
     1       20H) FROM IMSL ROUTINE ,6A1,A1,6A1)
   45 FORMAT(18H *** WARNING ERROR,11X,7H(IER = ,I3,
     1       20H) FROM IMSL ROUTINE ,6A1,A1,6A1)
   50 FORMAT(20H *** UNDEFINED ERROR,9X,7H(IER = ,I5,
     1       20H) FROM IMSL ROUTINE ,6A1,A1,6A1)
   55 IEQDF=1
      DO 60 I=1,6
```

```
   60   NAMEQ(I)=NAMUPK(I)
   65   RETURN
        END
C
C
C
CCCCCCCCCCCCCCCCCCCCCCCCCCCCCCCCCCCCCCCCCC
C       SUBROUTINE   UGETIO              C
CCCCCCCCCCCCCCCCCCCCCCCCCCCCCCCCCCCCCCCCCC
        SUBROUTINE UGETIO(IOPT,NIN,NOUT)
        INTEGER IOPT,NIN,NOUT,NIND,NOUTD
        DATA NIND,NOUTD/5,6/
        IF(IOPT.EQ.3) GO TO 10
        IF(IOPT.EQ.2) GO TO 5
        IF(IOPT.NE.1) GO TO 9005
        NIN=NIND
        NOUT=NOUTD
        GO TO 9005
    5   NIND=NIN
        GO TO 9005
   10   NOUTD=NOUT
 9005   RETURN
        END
C
C
CCCCCCCCCCCCCCCCCCCCCCCCCCCCCCCCCCCCCCCCCC
C       SUBROUTINE      USPKD            C
CCCCCCCCCCCCCCCCCCCCCCCCCCCCCCCCCCCCCCCCCC
        SUBROUTINE USPKD(PACKED,NCHARS,UNPAKD,NCHMTB)
        INTEGER NC,NCHARS,NCHMTB
        LOGICAL*2 UNPAKD(1),PACKED(1),LBYTE,LBLANK
        INTEGER*2 IBYTE,IBLANK
        EQUIVALENCE(LBYTE,IBYTE)
        DATA LBLANK,IBYTE,IBLANK/3*' '/
        NCHMTB=0
        IF(NCHARS.LE.0) RETURN
        NC=MINO(129,NCHARS)
        NWORDS=NC*4
        J=1
        DO 110 I=1,NWORDS,4
        UNPAKD(I)=PACKED(J)
        UNPAKD(I+1)=LBLANK
        UNPAKD(I+2)=LBLANK
        UNPAKD(I+3)=LBLANK
  110   J=J+1
        DO 200 N=1,NWORDS,4
        NN=NWORDS-N-2
        LBYTE=UNPAKD(NN)
        IF(IBYTE.NE.IBLANK) GO TO 210
  200   CONTINUE
        NN=0
  210   NCHMTB=(NN+3)/4
        RETURN
        END
```

```
CCCCCCCCCCCCCCCCCCCCCCCCCCCCCC
C       SORT PROGRAM          C
CCCCCCCCCCCCCCCCCCCCCCCCCCCCCC
      SUBROUTINE SORT(EI,L,DATA1,DATA2)
      IMPLICIT REAL (A-H,O-Z)
      DOUBLE PRECISION AI,R
      DIMENSION DATA1(5,3),DATA2(5,3),DATA3(10,2)
      COMPLEX*16 EI(10)
      S=0.0
      DO 1 I=1,10
       AI=AIMAG(EI(I))
       R=REAL(EI(I))
       IF(DABS(AI).LT.1.D-5) AI=1.D-5
       IF(DABS(R).LT1.D-5) R=1.D-5
       DI=SNGL(AI)
       DR=SNGL(R)
       ID=IFIX(DI)
       IR=IFIX(DR)
       DATA3(I,1)=FLOAT(IR)
       S=S+DATA3(I,1)/1.E1
 1     DATA3(I,2)=FLOAT(ID)
      DO 2 I=1,10,2
       N=I+1
       M=(I+1)/2
       M1=0
       DO 3 J=N,10
        DAI=DATA3(I,2)
        DAJ=-DATA3(J,2)
        IF(DAI.NE.DAJ) GO TO 3
        IF(DATA3(I,1).EQ.DATA3(J,1)) GO TO 50
        IF(DAI.NE.0.) GO TO 3
        SA=(DATA3(I,1)+DATA3(J,1))/2.
        SC=ABS(SA-S)
        IF(SC.EQ.0.) GO TO 50
        M1=M1+1
        IF(M1.EQ.1) GO TO 60
        SB=(DATA3(I,1)+DATA3(I+1,1))/2.
        SD=ABS(SB-S)
        IF(SD.LT.SC) GO TO 70
        GO TO 60
 50     M1=4
 60     DO 4 K=1,2
         DR=DATA3(J,K)
         DATA3(J,K)=DATA3(I+1,K)
 4       DATA3(I+1,K)=DR
 70     IF(M1.EQ.4) GO TO 80
 3     CONTINUE
 80    DATA2(M,3)=ABS(DAI)
       IF(DATA3(I,1).GT.DATA3(I+1,1)) GO TO 90
       DR=DATA3(I,1)
       DATA3(I,1)=DATA3(I+1,1)
       DATA3(I+1,1)=DR
 90    DATA2(M,1)=DATA3(I,1)
       DATA2(M,2)=DATA3(I+1,1)
```

```
  2   CONTINUE
C
      IF(L.EQ.1) GO TO 170
      DO 10  I=1,5
       DO 11 J=I,5
        DI=ABS(DATA2(J,3)-DATA1(I,3))
        IF(I.EQ.J) GO TO 160
       IF(DI-D) 140,150,11
 140   DO 12 K=1,3
        DR=DATA2(J,K)
        DATA2(J,K)=DATA2(I,K)
 12     DATA2(I,K)=DR
       GO TO 160
 150   DR=ABS(DATA1(I,1)-DATA2(I,1))
       DI=ABS(DATA1(I,1)-DATA2(J,1))
       IF(DI.GT.DR) GO TO 10
       DO 13 K=1,3
        DR=DATA2(J,K)
        DATA2(J,K)=DATA2(I,K)
 13     DATA2(I,K)=DR
       GO TO 10
 160   D=DI
 11   CONTINUE
 10  CONTINUE
 170 RETURN
     END
```

BT(1)= 4.73004074486270 SGM(1)= .98250221457624
BT(2)= 7.85320462409584 SGM(2)= 1.00077731190727
BT(3)=10 99560783800167 SGM(3)= 99996645012541
BT(4)=14.13716549125746 SGM(4)= 1.00000144989766
BT(5)=17 27875965739948 SGM(5)= .99999893734438

BD=.1154D+04 FD= 9340D+03 EL=.5000D+00 RA= 2500D-01 HD= 2500D-02
VOF= 700D-02 E=.26500D+07 POI= 470D+00 VFOF= 00D+00 IDELTA= 3
RO= 323 7435 RM= 4473 URF= 1 1980 URF1= 1.3316

INVISCID

UO1	MODE 1			MODE 2			MODE 3			MODE 4			MODE 5		
	IMAG1	IMAG2	REAL	IMAG1	IMAG2	REAL	IMAG1	IMAG2	REAL	IMAG1	IMAG2	REAL	IMAG1	IMAG2	REAL
.0000	.00	00	7.67	.00	.00	21 80	00	.00	44 41	.00	00	76.29	00	00	114.13
1502	.00	.00	7 64	00	00	21 78	00	00	44 40	00	00	76 27	00	00	114.17
.3004	.00	00	7.56	00	00	21 73	00	00	44 37	00	00	76.23	00	00	114 31
.4506	00	.00	7 43	00	00	21 65	00	00	44 31	00	00	76 15	00	00	114.52
6008	00	00	7.24	00	00	21.53	00	00	44 23	00	00	76 05	00	00	114 83
7509	00	.00	6 99	00	00	21 38	00	00	44.13	00	00	75 93	00	.00	115 21
9011	.00	00	6.69	00	.00	21 19	00	00	44 01	00	00	75.79	00	00	115 67
1.0513	.00	.00	6 33	00	.00	20 97	00	00	43 86	00	.00	75 64	00	.00	116 21
1.2015	00	00	5.91	00	.00	20.71	00	00	43 68	00	00	75.48	.00	.00	116.81
1.3517	.00	00	5.42	00	00	20 42	.00	.00	43 48	00	00	75.31	00	00	117 48
1.5019	.00	00	4 86	.00	.00	20 09	00	.00	43 24	.00	.00	75.15	00	00	118.20
1.6521	00	.00	4 21	.00	.00	19 72	00	00	42 98	00	00	75 00	.00	.00	118.98
1 8023	.00	00	3 45	00	00	19 31	.00	.00	42 69	00	00	74 86	.00	.00	119.81
1 9525	.00	.00	2 50	.00	00	18 85	.00	00	42 37	.00	00	74 73	.00	00	120 69
2.1027	.00	.00	1.00	.00	00	18 35	00	00	42 03	00	00	74.62	.00	.00	121 61
2.2528	1 92	-1.92	.00	00	.00	17.80	00	00	41.65	00	00	74 53	00	.00	122 58
2.4030	2 75	-2 75	00	00	00	17 20	00	.00	41 24	00	.00	74.47	00	00	123.55
2.5532	3 22	-3 22	00	00	00	16 54	.00	00	40 81	00	00	74.43	.00	00	124 57
2.7034	3.44	-3.44	00	.00	00	15.80	.00	00	40 36	00	.00	74 42	.00	00	125 61
2.8536	3.39	-3 39	.00	.00	.00	14.99	00	00	39 88	00	00	74 44	.00	00	126 69
3.0038	2.98	-2 98	00	00	00	14.06	00	00	39.38	00	00	74 48	00	00	127.78
3.1540	1.76	-1 76	.00	00	.00	13.00	.00	.00	38.85	00	00	74.55	.00	00	128.89
3.3042	00	00	2 76	.00	.00	11 68	.00	.00	38 31	00	00	74 64	00	.00	130.02
3 4544	00	00	5.50	.00	.00	9 69	.00	00	37 75	.00	00	74 76	00	.00	131.17
3.6046	-2 80	-2 80	7 81	2 80	2.80	7 81	00	00	37.16	00	00	74 90	00	00	132.33
3.7547	-4.21	-4 21	7 97	4 21	4 21	7.97	00	00	36 56	00	.00	75.06	00	00	133.51
3.9049	-5.04	-5 04	8 09	5 04	5 04	8.09	00	00	35.94	00	00	75 24	.00	00	134.69
4.0551	-5.54	-5.54	8.17	5.54	5 54	8 17	.00	.00	35 29	00	00	75.44	00	00	135 89
4.2053	-5 74	-5 74	8 21	5.74	5 74	8 21	.00	00	34 62	00	00	75 86	00	00	137.09
4 3555	-5 64	-5 64	8.20	5.64	5 64	8.20	00	.00	33 91	.00	00	75.90	.00	00	138 30
4.5057	-5 12	-5.12	8.12	5 12	5 12	8 12	00	00	33.17	.00	00	76 14	00	.00	139 52
4 6559	-3.77	-3 77	7.86	3.77	3.77	7.86	00	.00	32.36	00	00	76 40	00	00	140 74
4 8061	.00	00	10.33	00	.00	3.67	00	00	31 48	00	00	76 67	00	00	141.96
4.9563	.00	.00	13.56	5 17	-5.17	00	00	00	30 47	00	00	76 95	00	00	143.19
5.1065	00	00	16.23	7.25	-7.25	00	00	.00	29 25	.00	.00	77 24	00	00	144 42
5 2566	00	.00	19 16	8 52	-8.52	00	00	00	27 55	.00	.00	77 53	00	00	145.66
5.4068	-2.10	-2.10	23.93	9.42	-9 42	.00	2.10	2 10	23.93	00	.00	77.83	.00	00	146.89
5.5570	-4.91	-4.91	24 49	10.07	-10.07	00	4.91	4 91	24.49	.00	.00	78 13	00	.00	148 12
5.7072	-6.45	-6.45	25.04	10 52	-10.52	.00	6.45	6 45	25 04	.00	00	78 43	.00	.00	149.36
5 8574	-7.56	-7.56	25.58	10.80	-10.80	.00	7.56	7.56	25 58	00	00	78 73	00	00	150 59

INVISCID + UNSTEADY

UP1	MODE 1			MODE 2			MODE 3			MODE 4			MODE 5		
	IMAG1	IMAG2	REAL	IMAG1	IMAG2	REAL	IMAG1	IMAG2	REAL	IMAG1	IMAG2	REAL	IMAG1	IMAG2	REAL
.0000	2.70	2.70	7.18	2.68	2.68	21.63	2.65	2.65	44.33	2.61	2.61	76.24	2.61	2.61	114.10
.1502	2.70	2.70	7.15	2.68	2.68	21.62	2.65	2.65	44.32	2.61	2.61	76.23	2.61	2.61	114.14
.3004	2.70	2.70	7.07	2.68	2.68	21.57	2.65	2.65	44.29	2.61	2.61	76.18	2.60	2.60	114.28
.4506	2.71	2.71	6.93	2.68	2.68	21.48	2.65	2.65	44.23	2.61	2.61	76.11	2.60	2.60	114.49
.6008	2.71	2.71	6.74	2.67	2.67	21.36	2.64	2.64	44.15	2.61	2.61	76.01	2.60	2.60	114.80
.7509	2.72	2.72	6.48	2.67	2.67	21.21	2.64	2.64	44.05	2.61	2.61	75.89	2.59	2.59	115.18
.9011	2.73	2.73	6.17	2.67	2.67	21.02	2.64	2.64	43.93	2.61	2.61	75.75	2.59	2.59	115.64
1.0513	2.74	2.74	5.80	2.67	2.67	20.80	2.64	2.64	43.78	2.61	2.61	75.59	2.58	2.58	116.18
1.2015	2.75	2.75	5.36	2.67	2.67	20.53	2.64	2.64	43.60	2.61	2.61	75.43	2.58	2.58	116.78
1.3517	2.76	2.76	4.84	2.66	2.66	20.24	2.63	2.63	43.39	2.61	2.61	75.27	2.57	2.57	117.45
1.5019	2.78	2.78	4.24	2.66	2.66	19.90	2.63	2.63	43.16	2.61	2.61	75.11	2.56	2.56	118.17
1.6521	2.80	2.80	3.53	2.66	2.66	19.53	2.63	2.63	42.90	2.61	2.61	74.95	2.55	2.55	118.95
1.8023	2.81	2.81	2.63	2.65	2.65	19.11	2.62	2.62	42.60	2.60	2.60	74.81	2.55	2.55	119.78
1.9525	2.83	2.83	1.30	2.65	2.65	18.65	2.62	2.62	42.28	2.60	2.60	74.68	2.54	2.54	120.66
2.1027	4.63	1.08	.00	2.64	2.64	18.14	2.62	2.62	41.93	2.60	2.60	74.57	2.53	2.53	121.57
2.2528	5.60	.16	00	2.64	2.64	17.58	2.61	2.61	41.56	2.59	2.59	74.48	2.52	2.52	122.53
2.4030	6.18	-.37	00	2.63	2.63	16.96	2.61	2.61	41.15	2.59	2.59	74.42	2.51	2.51	123.51
2.5532	6.54	- 67	00	2.62	2.62	16.28	2.60	2.60	40.72	2.58	2.58	74.38	2.50	2.50	124.53
2.7034	6.68	- 74	.00	2.61	2.61	15.53	2.60	2.60	40.26	2.57	2.57	74.37	2.49	2.49	125.58
2.8536	6.58	- 55	00	2.60	2.60	14.69	2.59	2.59	39.78	2.56	2.56	74.38	2.48	2.48	126.65
3.0038	6.09	04	00	2.57	2.57	13.74	2.58	2.58	39.27	2.56	2.56	74.42	2.47	2.47	127.75
3.1540	4.57	1.70	00	2.53	2.53	12.61	2.57	2.57	38.74	2.55	2.55	74.49	2.46	2.46	128.86
3.3042	3.28	3.28	3.30	2.42	2.42	11.19	2.56	2.56	38.19	2.54	2.54	74.58	2.45	2.45	129.99
3.4544	4.04	4.04	6.25	1.68	1.68	8.95	2.55	2.55	37.63	2.53	2.53	74.70	2.44	2.44	131.14
3.6046	6.29	6.29	7.38	-.53	-.53	8.26	2.54	2.54	37.04	2.52	2.52	74.84	2.43	2.43	132.30
3.7547	7.49	7.49	7.67	-1.69	-1.69	8.27	2.52	2.52	36.43	2.50	2.50	75.00	2.42	2.42	133.47
3.9049	8.25	8.25	7.86	-2.41	-2.41	8.32	2.51	2.51	35.80	2.49	2.49	75.18	2.40	2.40	134.66
4.0551	8.70	8.70	7.98	-2.82	-2.82	8.35	2.48	2.48	35.15	2.48	2.48	75.38	2.39	2.39	135.85
4.2053	8.88	8.88	8.07	-2.95	-2.95	8.35	2.46	2.46	34.46	2.47	2.47	75.60	2.38	2.38	137.05
4.3555	8.76	8.76	8.10	-2.77	-2.77	8.29	2.43	2.43	33.75	2.45	2.45	75.83	2.37	2.37	138.26
4.5057	8.21	8.21	8.07	-2.16	-2.16	8.13	2.39	2.39	32.99	2.44	2.44	76.07	2.36	2.36	139.48
4.6559	6.78	6.78	7.91	- 65	- 65	7.72	2.34	2.34	32.17	2.42	2.42	76.33	2.35	2.35	140.70
4.8061	3.44	3.44	10.63	2.78	2.78	2.87	2.27	2.27	31.26	2.41	2.41	76.60	2.34	2.34	141.93
4.9563	3.50	3.50	13.80	8.39	-2.67	.00	2.17	2.17	30.23	2.39	2.39	76.88	2.32	2.32	143.15
5.1065	3.69	3.69	16.50	10.36	-4.61	.00	1.99	1.99	28.97	2.38	2.38	77.16	2.31	2.31	144.38
5.2566	4.19	4.19	19.45	11.60	-5.83	00	1.51	1.51	27.26	2.36	2.36	77.45	2.30	2.30	145.62
5.4068	6.15	6.15	22.36	12.48	-6.68	00	-.43	-.43	25.49	2.34	2.34	77.75	2.29	2.29	146.85
5.5570	8.23	8.23	23.54	13.12	-7.30	.00	-2.50	-2.50	25.43	2.32	2.32	78.05	2.28	2.28	148.09
5.7072	9.64	9.64	24.31	13.57	-7.72	00	-3.89	-3.89	25.76	2.30	2.30	78.35	2.26	2.26	149.32
5.8574	10.69	10.69	24.97	13.85	-7.98	.00	-4.92	-4.92	26.19	2.28	2.28	78.65	2.25	2.25	150.55

INVISCID + UNSTEADY + STEADY

CASE 1 T= 0000

UO1	MODE 1			MODE 2			MODE 3			MODE 4			MODE 5		
	IMAG1	IMAG2	REAL	IMAG1	IMAG2	REAL	IMAG1	IMAG2	REAL	IMAG1	IMAG2	REAL	IMAG1	IMAG2	REAL
0000	2 70	2 70	7 18	2 68	2 68	21 63	2 65	2 65	44 33	2 61	2 61	76 24	2 61	2 61	114.10
1502	2 70	2 70	7 20	2 68	2 68	21 68	2 65	2 65	44 39	2 61	2 61	76 30	2 61	2 61	114 22
3004	2 70	2 70	7 16	2 68	2 68	21 68	2 65	2 65	44 42	2 61	2 61	76 33	2 60	2 60	114 43
4506	2 70	2.70	7 07	2 68	2 68	21 66	2 65	2 65	44 43	2 62	2 62	76 33	2 60	2 60	114 73
6008	2.71	2 71	6 92	2 68	2 68	21 60	2 65	2 65	44 42	2 62	2 62	76 30	2 59	2 59	115 11
7509	2 72	2 72	6 72	2 67	2 67	21 50	2 65	2 65	44.39	2 62	2 62	76 25	2 58	2 58	115 57
9011	2 72	2 72	6 46	2 67	2 67	21 37	2 64	2 64	44 33	2 62	2 62	76 18	2 57	2 57	116 11
1 0513	2 73	2 73	6 15	2 67	2 67	21 20	2 64	2 64	44 24	2 63	2 63	76 10	2 56	2 56	116 72
1 2015	2 74	2 74	5 78	2 67	2 67	21 00	2 64	2 64	44 13	2 63	2 63	76 01	2 55	2 55	117 40
1 3517	2 76	2 76	5 35	2 67	2 67	20 76	2 64	2 64	43 99	2 63	2 63	75 92	2 54	2.54	118 15
1 5019	2 77	2 77	4 84	2 67	2 67	20 49	2 64	2 64	43 83	2 64	2 64	75 82	2 53	2 53	118 85
1 6521	2.78	2 78	4 26	2 66	2 66	20 17	2 64	2 64	43.63	2 64	2.64	75 74	2 51	2 51	119 81
1 8023	2 80	2 80	3 58	2 66	2 66	19 82	2 64	2 64	43 41	2 64	2 64	75 66	2 50	2 50	120 72
1 9525	2 81	2 81	2 74	2 66	2 66	19 42	2 64	2 64	43 16	2 64	2 64	75 60	2 48	2.48	121 68
2 1027	2 83	2 83	1 57	2 66	2.66	18 98	2 64	2 64	42 87	2 64	2 64	75 56	2 47	2.47	122 67
2 2528	4 34	1 37	00	2 66	2 66	18.49	2 64	2 64	42 56	2 64	2 64	75 53	2 45	2.45	123 71
2.4030	5.38	.37	00	2 65	2 65	17.96	2 64	2 64	42 23	2 64	2 64	75 54	2 43	2.43	124 78
2 5532	5 99	- 20	00	2.65	2.65	17.37	2 64	2.64	41.86	2.64	2 64	75 56	2 42	2 42	125 88
2 7034	6 37	- 52	.00	2 65	2.65	16 72	2 64	2.64	41.47	2 63	2.63	75 61	2 40	2 40	127.00
2.8536	6 54	- 64	00	2 64	2.64	16 00	2 63	2 63	41 06	2 63	2 63	75.69	2 38	2 38	128 16
3.0038	6.49	- 52	00	2.63	2 63	15 21	2.63	2 63	40.62	2 62	2 62	75 78	2 37	2 37	129 33
3.1540	6 12	- 08	.00	2 62	2 62	14 32	2 63	2 63	40.16	2.62	2 62	75 82	2 35	2.35	130.53
3 3042	5 11	1 05	00	2 60	2 60	13 30	2 62	2 62	39 69	2 61	2 61	76 08	2 33	2.33	131 74
3.4544	3 16	3 16	2 35	2 54	2 54	12 07	2 62	2.62	39.19	2.60	2 60	76 28	2 32	2.32	132.97
3 6046	3 37	3.37	4.85	2.37	2 37	10 39	2 61	2.61	38.68	2 60	2 60	76 47	2 30	2.30	134 22
3.7547	5 18	5 18	7 27	.59	.59	8 40	2 60	2 60	38 15	2 59	2 59	76 69	2 28	2 28	135.48
3 9049	6 80	6.80	7 67	-1.00	-1.00	8 28	2 60	2 60	37 60	2 58	2.58	76 94	2 26	2.26	136 75
4.0551	7.74	7.74	7 85	-1 90	-1 90	8 30	2 58	2.58	37 04	2 57	2 57	77 21	2 25	2 25	138.02
4.2053	8 33	8.33	7 97	-2.44	-2 44	8 31	2 57	2 57	36 46	2 56	2 56	77 49	2 23	2.23	139 31
4.3555	8 64	8 64	8 03	-2 71	-2 71	8 30	2 55	2 55	35 86	2 55	2 55	77 78	2 21	2 21	140.61
4 5057	8 68	8.68	8 04	-2 70	-2 70	8 24	2 53	2 53	35.24	2 54	2 54	78 11	2 19	2 19	141.91
4 6559	8.39	8.39	8.00	-2 36	-2 36	8 10	2 51	2.51	34 59	2 52	2 52	78 44	2 17	2 17	143 22
4.8061	7.56	7 56	7.84	-1 47	-1 47	7 81	2 48	2 48	33 90	2 51	2.51	78 78	2 16	2.16	144 53
4.9563	4.97	4 97	7 58	1 19	1 19	6 97	2 44	2 44	33 16	2 50	2 50	79 13	2 14	2.14	145.85
5.1065	3.37	3.37	11 76	6 59	- 82	.00	2 39	2 39	32 36	2.49	2 49	79 50	2 12	2 12	147 17
5.2566	3.44	3 44	14.28	9.49	-3 67	.00	2 31	2 31	31 45	2 47	2 47	79 87	2 10	2 10	148 49
5 4068	3 58	3.58	16.62	11.01	-5 16	00	2 19	2 19	30 40	2 46	2 46	80 24	2.08	2 08	149.82
5 5570	3 85	3 85	19 11	12.05	-6 17	00	1 93	1 93	29.05	2 45	2 45	80 62	2 06	2.06	151.15
5.7072	4 77	4 77	22 09	12.81	-6.90	.00	1 04	1 04	27.16	2 43	2 43	81 01	2.05	2.05	152 47
5.8574	7.05	7.05	24 03	13.36	-7 42	.00	-1 22	-1 22	26.28	2 42	2 42	81.40	2 03	2 03	153 80

CASE 2 T= 0000

U01	MODE 1			MODE 2			MODE 3			MODE 4			MODE 5		
	IMAG1	IMAG2	REAL	IMAG1	IMAG2	REAL	IMAG1	IMAG2	REAL	IMAG1	IMAG2	REAL	IMAG1	IMAG2	REAL
0000	2 70	2 70	7 18	2 68	2.68	21 63	2 65	2 65	44 33	2 61	2 61	76.24	2 61	2.61	114.10
1502	2 70	2 70	7 11	2.68	2 68	21 56	2 65	2 65	44 25	2.61	2 61	76 15	2 61	2 61	114.07
3004	2 70	2 70	6 98	2 68	2.68	21 45	2 65	2 65	44 15	2 61	2.61	76 03	2 60	2 60	114.12
4506	2 71	2 71	6 79	2 68	2 68	21 30	2 65	2 65	44 03	2.62	2 62	75 89	2 60	2 60	114 26
6008	2 71	2 71	6 55	2 67	2 67	21 12	2 65	2 65	43 89	2.62	2 62	75 71	2 59	2.59	114 49
7509	2 72	2 72	6 24	2 67	2 67	20 91	2 65	2 65	43 72	2 62	2 62	75 52	2 58	2.58	114 79
9011	2 73	2 73	5 86	2 67	2 67	20 66	2 64	2 64	43 52	2 62	2 62	75 30	2 57	2 57	115.17
1 0513	2 74	2 74	5 42	2 67	2 67	20 38	2.64	2 64	43 30	2.63	2.63	75 08	2 56	2 56	115 63
1 2015	2 75	2 75	4 90	2 67	2 67	20.05	2 64	2 64	43.08	2 63	2 63	74 85	2 55	2 55	116 15
1 3517	2 76	2 76	4 28	2 66	2 66	19.69	2 64	2 64	42 78	2 63	2 63	74 61	2 54	2 54	116 74
1 5019	2 78	2 78	3 54	2 66	2 66	19 30	2 64	2 64	42 48	2 64	2 64	74 38	2 53	2 53	117 39
1 6521	2 79	2 79	2 60	2 66	2 66	18 85	2 64	2 64	42 14	2 64	2 64	74 15	2 51	2 51	118 09
1 8023	2 81	2 81	1 12	2 65	2 65	18 37	2 64	2 64	41 78	2 64	2 64	73 94	2 50	2 50	118.84
1 9525	4 80	87	00	2 65	2 65	17 83	2 64	2 64	41 39	2 64	2 64	73 75	2 48	2 48	119 63
2 1027	5 74	- 03	00	2 64	2 64	17 25	2 64	2 64	40 97	2 64	2 64	73 57	2 46	2 46	120 47
2 2528	6 32	- 56	00	2 64	2 64	16 60	2 63	2 63	40 52	2 64	2.64	73 41	2 45	2 45	121 34
2 4030	6 67	- 85	00	2 63	2 63	15 89	2 63	2 63	40 04	2 64	2 64	73 28	2 43	2 43	122 24
2 5532	6 79	- 90	00	2 62	2 62	15 10	2 63	2 63	39 53	2 63	2 63	73 17	2 41	2 41	123 18
2 7034	6 64	- 66	00	2 60	2 60	14 20	2 63	2 63	39 00	2 63	2 63	73 09	2 39	2 39	124 14
2 8586	6 01	08	00	2 57	2 57	13 17	2 62	2 62	38 44	2 63	2 63	73.04	2 38	2 38	125.13
3 0038	3 13	3 13	45	2 51	2 51	11 92	2 61	2 61	37 86	2 62	2 62	73 01	2 36	2 36	126.14
3 1540	3 36	3 36	4 27	2 32	2 32	10 17	2 61	2 61	37 25	2 61	2.61	73 01	2.34	2 34	127.17
3 3042	5 37	5 37	6 99	35	35	8 14	2 60	2 60	36 62	2 60	2 60	73 03	2.32	2 32	128.21
3 4544	7 07	7.07	7 47	-1 32	-1 32	8 12	2 59	2 59	35 97	2.60	2.60	73.08	2 30	2 30	129 28
3 6046	8 07	8 07	7 73	-2 27	-2 27	8 22	2 57	2 57	35 29	2 59	2 59	73 15	2 28	2.28	130.35
3.7547	8 70	8 70	7 82	-2 86	-2 86	8 31	2 56	2 56	34 58	2 58	2 58	73.23	2 27	2.27	131.44
3 9049	9.04	9 04	8 07	-3 15	-3 15	8 38	2.54	2 54	33 83	2 57	2 57	73 34	2.25	2.25	132.53
4.0551	9 10	9 10	8 18	-3 15	-3 15	8.41	2.51	2 51	33 05	2.55	2 55	73 47	2 23	2.23	133.64
4 2053	8 80	8 80	8 24	-2 79	-2 79	8 38	2 47	2 47	32.22	2 54	2.54	73 61	2 21	2.21	134.75
4.3555	7 93	7 93	8 22	-1 83	-1 83	8.22	2 43	2 43	31 31	2 53	2.53	73.76	2.19	2.19	135.87
4 5057	5 25	5 25	8 17	.95	95	7 54	2.36	2.36	30.29	2.52	2 52	73.92	2.17	2.17	137.00
4.6559	3 49	3.49	12 91	6 20	-.48	00	2.25	2.25	29 11	2 50	2.50	74.10	2.15	2 15	138.13
4 8061	3.71	3 71	16 16	9 44	-3.65	00	2 02	2.02	27 61	2 49	2 49	74.28	2 13	2.13	139.26
4.9563	4 57	4 57	19 75	11 03	-5 21	.00	1.18	1.18	25.40	2.47	2 47	74 47	2 11	2 11	140.39
5 1065	7.30	7.30	22 12	12.10	-6 25	.00	-1.53	-1.53	24.28	2 45	2 45	74.66	2.09	2.09	141 53
5 2566	9 19	9.19	23 04	12.87	-6.99	00	-3.39	-3 39	24.54	2 44	2.44	74.86	2.07	2.07	142.67
5 4068	10 50	10 50	23 76	13 41	-7 51	00	-4.68	-4.68	24.98	2 42	2.42	75.05	2.04	2.04	143 80
5 5570	11 49	11 49	24 42	13 77	-7 84	.00	-5.64	-5 64	25.48	2 40	2.40	75.24	2.02	2.02	144.94
5 7072	12 25	12 25	25.05	13.96	-7 99	.00	-6 38	-6.38	25.99	2.38	2.38	75.43	2.00	2.00	146.07
5 8574	12 84	12 84	25.68	13 98	-7 97	.00	-6 94	-6.94	26 52	2.36	2.36	75.62	1.98	1.98	147.21

CASE 3 T= 10 0000

UO1	MODE 1			MODE 2			MODE 3			MODE 4			MODE 5		
	IMAG1	IMAG2	REAL	IMAG1	IMAG2	REAL	IMAG1	IMAG2	REAL	IMAG1	IMAG2	REAL	IMAG1	IMAG2	REAL
0000	2 70	2 70	7 24	2.68	2 68	21 71	2 65	2 65	44 42	2.61	2 61	76 34	2 61	2.61	114.20
1502	2.70	2 70	7 21	2.68	2 68	21 70	2 65	2 65	44 41	2.61	2 61	76 33	2 61	2 61	114.25
3004	2 70	2 70	7 13	2 68	2 68	21 64	2 65	2 65	44 38	2 61	2 61	76 28	2 60	2 60	114 38
4506	2 70	2 70	6 99	2 68	2 68	21 56	2 65	2 65	44 32	2 62	2 62	76 21	2 60	2 60	114 60
.6008	2 71	2 71	6 80	2 68	2 68	21 44	2 65	2 65	44 24	2 62	2 62	76 11	2 59	2 59	114 90
7509	2 72	2.72	6 55	2 67	2.67	21 29	2 65	2 65	44 14	2 62	2 62	75 98	2 58	2 58	115 29
9011	2 72	2 72	6 24	2 67	2.67	21 10	2 64	2.64	44 02	2 62	2 62	75 84	2 57	2 57	115.75
1 0513	2 73	2 73	5 87	2 67	2 67	20 87	2 64	2 64	43 87	2 63	2 63	75 69	2 56	2 56	116 28
1 2015	2 75	2 75	5.43	2 67	2 67	20 61	2 64	2 64	43 69	2 63	2 63	75 53	2 55	2 55	116.88
1 3517	2 76	2 76	4 92	2 67	2 67	20 32	2 64	2 64	43 48	2 63	2 63	75 36	2 54	2 54	117 55
1 5019	2.77	2 77	4 32	2 66	2 66	19 98	2 64	2 64	43 25	2 64	2 64	75 20	2 53	2 53	118.28
1 6521	2 79	2 79	3 62	2.66	2 66	19.60	2 64	2 64	42 99	2 64	2 64	75 05	2 51	2 51	119 06
1 8023	2 80	2 80	2 75	2 66	2 66	19 19	2 64	2 64	42 69	2 64	2 64	74 90	2 50	2 50	119 89
1 9525	2 82	2 82	1 49	2 66	2 66	18 73	2 64	2 64	42 37	2 64	2 64	74 77	2 48	2 48	120 76
2 1027	4 48	1 20	00	2 65	2 65	18 22	2 64	2 64	42 02	2 64	2 64	74 66	2 47	2 47	121 68
2 2528	5 51	22	00	2 65	2 65	17 66	2 64	2 64	41 65	2 64	2 64	74 58	2 45	2 45	122 64
2 4030	6.12	- 35	00	2 65	2 65	17 05	2 64	2 64	41 24	2 64	2 64	74 51	2 43	2 43	123.62
2 5532	6 50	-.67	00	2.64	2 64	16 37	2 63	2 63	40 81	2 64	2 64	74 47	2 42	2 42	124 64
2 7034	6 66	- 76	00	2 63	2.63	15 62	2 63	2 63	40 35	2 63	2 63	74 46	2 40	2 40	125 69
2 8536	6 57	- 60	00	2 62	2.62	14 79	2 63	2 63	39 87	2 63	2 63	74 47	2 38	2 38	126 76
3 0038	6 12	- 06	00	2 60	2 60	13 84	2 62	2 62	39 36	2 62	2 62	74 51	2.36	2 36	127.86
3 1540	4 76	1 43	.00	2 56	2 56	12 73	2 62	2 62	38 83	2 62	2 62	74 58	2 35	2 35	128 97
3 3042	3 21	3 21	3 10	2 48	2 48	11 33	2 61	2 61	38 28	2 61	2.61	74 67	2 33	2.33	130.10
3.4544	3 78	3.78	6 06	1.94	1 94	9.12	2 61	2.61	37 72	2 60	2 60	74 78	2 31	2 31	131 25
3 6046	6.16	6 16	7 41	- 40	- 40	8 21	2 60	2 60	37 13	2.59	2 59	74 92	2 29	2 29	132.41
3.7547	7.42	7 42	7 70	-1.62	-1 62	8 24	2 59	2 59	36 52	2 58	2 58	75 08	2.27	2.27	133 59
3 9049	8 20	8 20	7 88	-2 36	-2.36	8.30	2 57	2 57	35 89	2 57	2 57	75 26	2 26	2 26	134 77
4.0551	8.68	8 68	8 00	-2.79	-2.79	8 33	2 56	2 56	35 24	2 56	2 56	75 46	2 24	2.24	135.97
4 2053	8.88	8 88	8 09	-2.94	-2.94	8 34	2 53	2.53	34 56	2 55	2 55	75 68	2 22	2.22	137.17
4 3555	8.78	8 78	8.12	-2 79	-2.79	8.28	2.51	2.51	33 84	2 54	2 54	75 91	2 20	2.20	138 38
4.5057	8.27	8 27	8.08	-2.22	-2 22	8 15	2.48	2.48	33 09	2 53	2.53	76 16	2.18	2.18	139.60
4 6559	6.94	6.94	7 92	- 81	- 81	7 78	2.43	2 43	32 27	2 51	2.51	76.41	2.16	2.16	140 82
4 8061	3.42	3 42	10.34	2 80	2.80	3.52	2.37	2 37	31 37	2 50	2 50	76 68	2.14	2.14	142.04
4.9563	3 46	3 46	13 62	8.22	-2.44	.00	2.28	2 28	30 35	2 49	2 49	76 96	2.12	2.12	143.27
5.1065	3 63	3 63	16 33	10.29	-4.47	00	2 12	2.12	29 11	2 47	2 47	77 24	2.10	2 10	144.51
5 2566	4.06	4 06	19.25	11 56	-5.71	00	1 72	1.72	27.43	2 46	2 46	77 53	2 09	2 09	145 74
5.4068	5 93	5 93	22.35	12 46	-6 59	00	-.13	-.13	25.48	2 44	2 44	77 83	2.07	2 07	146.97
5.5570	8.13	8.13	23.58	13.12	-7 21	00	-2.31	-2.31	25.37	2 43	2.43	78.13	2.05	2 05	148.21
5 7072	9.59	9.59	24.34	13.58	-7.64	.00	-3 75	-3.75	25.71	2.41	2 41	78 42	2.03	2 03	149 44
5.8574	10.66	10.66	24.99	13.88	-7 91	.00	-4.80	-4 80	26.15	2.39	2 39	78.72	2.01	2.01	150.68

CASE 3 T= 50 0000

UO1	MODE 1			MODE 2			MODE 3			MODE 4			MODE 5		
	IMAG1	IMAG2	REAL	IMAG1	IMAG2	REAL	IMAG1	IMAG2	REAL	IMAG1	IMAG2	REAL	IMAG1	IMAG2	REAL
0000	2 70	2.70	7.47	2 68	2.68	22 03	2 65	2.65	44 78	2 61	2.61	76 74	2.61	2.61	114.62
.1502	2 70	2.70	7.45	2.68	2 68	22.01	2 65	2 65	44.77	2.61	2.61	76.72	2.61	2.61	114.66
3004	2 70	2.70	7.37	2 68	2.68	21 96	2.65	2.65	44.73	2.61	2.61	76.68	2.60	2.60	114.80
4506	2 70	2 70	7 23	2.68	2 68	21 87	2.65	2.65	44.68	2.62	2.62	76.60	2.60	2.60	115 01
.6008	2 71	2 71	7 04	2 68	2.68	21.75	2 65	2.65	44.60	2 62	2 62	76.50	2 59	2.59	115.32
.7509	2.72	2.72	6 80	2 67	2 67	21.60	2.65	2.65	44 50	2 62	2.62	76 38	2.58	2.58	115.70
9011	2 72	2.72	6.50	2 67	2 67	21.41	2 64	2 64	44 38	2 62	2.62	76.24	2 57	2.57	116 16
1 0513	2.73	2 73	6 14	2 67	2 67	21 19	2 64	2 64	44 22	2.63	2.63	76 08	2.56	2 56	116.70
1 2015	2 74	2.74	5 71	2 67	2.67	20 93	2 64	2 64	44 05	2 63	2.63	75 92	2 55	2.55	117.30
1 3517	2.76	2.76	5 22	2.67	2 67	20 63	2 64	2 64	43 84	2.63	2.63	75 75	2 54	2.54	117.97
1.5019	2 77	2.77	4 65	2.67	2 67	20.30	2.64	2.64	43 61	2.64	2 64	75 59	2 53	2.53	118.70
1.6521	2 78	2 78	3 99	2.66	2 66	19.92	2.64	2 64	43.35	2 64	2.64	75 43	2.51	2 51	119.48
1 8023	2.80	2.80	3 19	2 66	2 66	19.51	2 64	2 64	43.06	2 64	2 64	75.29	2.50	2.50	120 31
1.9525	2.82	2 82	2.15	2.66	2.66	19 05	2.64	2 64	42.74	2 64	2.64	75 16	2 48	2 48	121.19
2 1027	3 58	2 09	00	2 66	2 66	18 55	2 64	2 64	42 39	2.64	2.64	75 05	2 47	2.47	122.10
2.2528	5.13	58	00	2.65	2 65	17.99	2 64	2 64	42 01	2 64	2 64	74 96	2.45	2.45	123.06
2.4030	5.89	- 12	00	2 65	2 65	17 39	2.64	2.64	41.60	2.64	2.64	74 89	2.43	2.43	124.05
2 5532	6 35	- 53	00	2 64	2 64	16 72	2 64	2.64	41.17	2.64	2.64	74 85	2.42	2.42	125.07
2 7034	6 59	- 72	.00	2.64	2 64	15 99	2.63	2.63	40.71	2 63	2.63	74 83	2.40	2.40	126 12
2.8536	6.60	-.65	00	2 63	2.63	15 17	2.63	2.63	40.23	2.63	2.63	74.85	2.38	2.38	127.19
3.0038	6.29	-.26	.00	2.61	2.61	14.25	2.63	2.63	39.73	2.62	2.62	74.88	2.36	2.36	128.28
3.1540	5 37	.77	.00	2.58	2.58	13.20	2 62	2.62	39 20	2.62	2 62	74.95	2.35	2.35	129.40
3.3042	3.16	3.16	2 19	2 53	2.53	11 91	2.62	2 62	38.65	2.61	2.61	75.04	2.33	2.33	130.53
3.4544	3 41	3.41	4.85	2.31	2.31	10.10	2 61	2.61	38.09	2.60	2.60	75.15	2.31	2.31	131.68
3 6046	5.50	5 50	7 26	.25	.25	8 28	2.60	2.60	37.50	2.59	2.59	75.29	2.29	2.29	132.84
3.7547	7.05	7.05	7 64	-1.26	-1.26	8.24	2.59	2.59	36.90	2.58	2 58	75.45	2 28	2.28	134.02
3 9049	7.96	7.96	7.84	-2.13	-2.13	8.29	2.58	2 58	36.28	2.57	2 57	75 63	2.26	2 26	135.21
4.0551	8 53	8.53	7.97	-2 65	-2 65	8.32	2 56	2.56	35.63	2.56	2 56	75.83	2 24	2.24	136.40
4.2053	8 81	8 81	8 06	-2.89	-2 89	8.33	2.54	2.54	34.96	2 55	2.55	76.05	2.22	2.22	137.61
4.3555	8 81	8.81	8 10	-2.83	-2 83	8.30	2 52	2 52	34.25	2 54	2.54	76.28	2.20	2 20	138.82
4.5057	8.43	8 43	8.08	-2 39	-2.39	8 17	2.49	2.49	33 51	2.53	2.53	76.53	2.18	2.18	140.04
4.6559	7.39	7.39	7 94	-1.28	-1.28	7.88	2.45	2.45	32.72	2.52	2 52	76.79	2.16	2.16	141.26
4.8061	3.60	3.60	8.83	2.59	2.59	5.72	2.40	2.40	31.85	2.50	2.50	77 06	2 15	2.15	142.49
4.9563	3.42	3.42	12.83	7.44	-1.67	.00	2.32	2.32	30.88	2.49	2.49	77.34	2 13	2 13	143.72
5.1065	3.55	3.55	15.53	9.90	-4.08	.00	2.19	2.19	29.74	2.47	2 47	77 62	2.11	2.11	144.95
5.2566	3.84	3 84	18.28	11.31	-5.46	.00	1.93	1.93	28 27	2.46	2.46	77.92	2.09	2.09	146.18
5.4068	4.95	4.95	21.54	12.28	-6 41	.00	.84	84	26 17	2.45	2.45	78 21	2.07	2.07	147.42
5 5570	7.42	7 42	23 37	12.99	-7.09	00	-1.61	-1.61	25.46	2.43	2.43	78.51	2.05	2.05	148.66
5.7072	9.09	9 09	24.22	13.49	-7.56	.00	-3.25	-3.25	25 71	2.41	2.41	78 81	2.03	2.03	149.89
5.8574	10.28	10.28	24.89	13.83	-7.86	.00	-4.42	-4.42	26.12	2.40	2.40	79.12	2.01	2.01	151.13

APPENDIX E

THE APPROXIMATE METHOD FOR CRITICAL FLOW VELOCITY BASED ON SLENDER BODY THEORY AND COMPARISON WITH THE RESULTS OF THIS THEORY

Considering small lateral motion of the flexible centre-body about its position of rest and assuming that the angle of incidence i and $\partial i/\partial x^*$ are sufficiently small, based on slender body theory the equation of motion of the flexible centre-body immersed in inviscid flow is given by

$$EI \frac{\partial^4 e_o^*}{\partial x^{*4}} + M \left(\frac{\partial}{\partial t^*} + U_o^* \frac{\partial}{\partial x^*}\right)^2 e_o^* + m_s \frac{\partial^2 e_o^*}{\partial t^{*2}} = 0, \qquad (E\text{-}1)$$

as proposed by Lighthill [24]. Here, the virtual mass, M, is equal to $\chi \rho_f A$, where A is the cross-sectional area of the flexible centre-body. For confined flow, based on slender body theory, χ is expressed as follows:

$$\chi = \frac{(a+H^*)^2 + a}{(a+H^*)^2 - a}, \qquad (E\text{-}2)$$

where a is the radius of the flexible centre-body and H^* is the annular gap. Thus, it is clear that χ increases as the annular gap ratio decreases.

At this point, the critical flow velocity corresponding to onset of buckling may be found particularly easily, taking into consideration Euler's method of equilibrium [13]; the mechanism of instability is the same as compared with the clamped-clamped pipe conveying fluid. It is noted that at instability other equilibrium points $e_o^*(x^*)$ exist near the trivial position $e_o^*(x^*)=0$. Lateral displacement of the centre-body axis $e_o^*(x^*)$ must satisfy equation (E-1) with the time-derivatives eliminated. Thus,

$$EI \frac{\partial^4 e_o^*}{\partial x^{*4}} + MU_o^{*2} \frac{\partial^2 e_o^*}{\partial x^{*2}} = 0, \qquad (E\text{-}3)$$

where, $e_o^* = \sum a_\kappa e^{i\alpha x^*}$ (the destabilizing force in this case is proportional to MU_o^{*2}).

As a result, a system with clamped ends loses stability by divergence, approximately, at $(\chi\rho_f A/EI)^{1/2} U_b^* \ell^* = 2\pi$ for inviscid flow; therefore, the nondimensional critical flow velocity may be expressed by

$$U_b = \frac{U_b^*}{U_{refl}} = 2\pi \left(\frac{1}{\chi}\right)^{1/2}, \qquad \text{(E-4)}$$

where U_{refl} is defined in equation (2-3).

These approximate values for U_b are compared with the results U_{bl}, which are obtained by inviscid flow theory in Chapter IV, in Table E for ℓ=20 and 100 for three values of the annular gap. As expected, it is shown that the discrepancy becomes smaller as ℓ increases, i.e., as the slender-body theory becomes more valid.

It is also interesting to note that the two results agree best for the smallest annular gap (h=0.01), where the assumption made by this theory, effectively that $1/(a+h) \simeq 1/a$ becomes more valid.

Table E Values of the nondimensional critical flow velocities, with respect to U_{refl}, for potential flow

length ratio $\ell = \ell^*/a$	annular gap ratio $h = H^*/a$	approximate result U_b	present result U_{bl}	discrepancy $(U_{bl}-U_b)/U_b \times 100$ %
20	0.05	1.39	1.49	7.2
	0.10	1.94	2.13	9.8
	0.15	2.34	2.64	12.8
100	0.01	0.627	0.631	0.7
	0.05	1.387	1.425	2.7